THE PARTIAL CHARACTERISATION OF AN NFKB HOMOLOGUE FROM THE SOUTH AFRICAN ABALONE *HALIOTIS MIDAE* UTILISING *IN VIVO* AND *IN VITRO* TECHNIQUES

BY

Roslyn Michelle Ray

A thesis submitted in partial fulfilment of the requirements for the degree of Master of Science in the Department of Molecular and Cell Biology, Faulty of Science, University of Cape Town, South Africa.

Cape Town

March 2010

Department of Molecular and Cell Biology, University of Cape Town, Private Bag, Rondebosch, 7701, South Africa

TABLE OF CONTENTS

Acknowledgements		I
Abstract		III
Chapter 1	Introduction	1
Chapter 2	Methods and Materials	25
Chapter 3	Results	54
Chapter 4	Discussion	87
References		111
Appendix A	Media and solutions	117
Appendix B	Standard methods and PCR profiles	128
Appendix C	Plasmid maps	136
Appendix D	RNA quality and qPCR profiles	139

ACKNOWLEDGEMENTS

I would firstly like to thank my supervisor, Associate Professor Vernon Coyne. Under his supervision, I have grown to be a more thoughtful scientist. I thoroughly enjoyed being his student and his attitude towards his students was always reflected in the laboratory atmosphere, easy-going and supportive. He has always been encouraging during my moments of crises and managed to allay my fears (difficult!) and point me in the right direction in my studies.

I would also like to thank my co-supervisor, Professor Janet Hapgood, for her support throughout the duration of my studies and her confidence in my abilities as a scientist.

I would also like to thank the National Research Foundation for the Grantholders bursary in my first year of study, and the DoL scarce skills scholarship in my second year of study. I would also like to thank UCT and KW Johnstone for their financial support of my studies. This study would not be possible without their support.

I would like to thank my parents for there support over the years. They are now familiar with terms such as RNA and DNA and even understand the principle of PCR. They have been my greatest fans and have always rooted for me. So, thank you guys for always being there for me and guiding me into the person I have become. I love you both. To Trevor:

thanks for being the best brother ever and thinking that I'm the greatest…next to you of course! To my church family and my friends, you are all awesome and have always been supportive and caring and wonderful. I would be no one without my faith, and so I give God praise.

Lastly, but definitely not least, to my Lab 201 buddies, you guys are awesome! I have made some truly awesome friendships and I cherish them so much! Thanks for always listening to my ideas, my paranoia and enduring my bizarre humour! Lab 201 for life!

ABSTRACT

Haliotis midae is an important marine gastropod that is commercially farmed along the South African coastline. The demand for the edible foot of the abalone far exceeds the supply, as such monitoring the health status of commercially farmed abalone is important if the demand is to be met. In farming conditions, bacterial infections can spread rapidly leading to mass mortalities amongst the abalone population. In order for treatment to be effective, there needs to be an effective monitoring system in place that can assess the health status of the abalone. This study sought to address these issues by identifying a candidate gene that could be an ideal biomarker with respect to a bacterial stress. Nuclear factor κB is a key regulatory gene that is involved in processes such as cell division, apoptosis and the immune response. In invertebrate innate immunity, NFκB homologues regulate the activation of anti-microbial peptides in response to Gram-negative and Gram-positive bacterial, fungal and yeast infections. In this study, two fragments of an NFκB homologue were identified in *H. midae* and found to be closely related to the *H, diversicolor supertexta* NFκB homologue. *H. midae* were exposed to heat killed *Vibrio anguillarum* 5676, and the haemocytes isolated, were assayed for changes in various physiological responses and in changes in transcriptional regulation of NFκB. The number of circulating haemocytes decreased significantly at 12 hours post infection in the infected samples and NFκB relative expression levels were significantly up-regulated at 24 hours post infection in the infected group. It was concluded that NFκB is an ideal candidate as a biomarker of stress and that exposure to heat killed *V. anguillarum* 5676 had an affect on some of the

physiological responses assayed. In this study, haemocytes from *H. midae* were partially characterised and optimised for use in an *in vitro* primary cell line. It was found that the haemocytes could be maintained *in vitro* for five days. The characterisation of the haemocytes revealed that there were two types of haemocytes present, blast-like cells and halinocytes. An *in vitro* challenge trial was performed to assess the response of *in vitro* haemocytes to heat killed FITC labeled *V. anguilarium* 5676. There was a significant increase in phagocytic ability at 1 and 2 hpi in the infected samples compared to time 0. The transcriptional expression studies revealed that NFκB was significantly up-regulated at 1, 2 and 3 hpi compared to the control group. It was concluded that the *in vitro* culture system yielded sensitive and reproducible results that were comparable to the *in vivo* results and was a useful tool to study aspects of the *H. midae* immune response.

CHAPTER 1

INTRODUCTION

CONTENTS

1.1 Abalone and aquaculture 2
1.2 The invertebrate immune system 5
1.3 Haemocytes 8
1.4 Interactions in the immune response and key genes involved 11
1.5 Nuclear Factor kappa B characterisation 15
1.6 Aims of this study 20

1.1 ABALONE AND AQUACULTURE

Abalone are commercially important marine gastropods belonging to the family *Haliotidae* in the phylum *Mollusca* of the class *Gastropoda* (Branch *et al.*, 1994). They exist along ocean coastlines in both temperate and tropical regions (Proudfoot, 2006). *Haliotis midae* are abalone that have characteristic large shells with irregular corrugations along the spire. They exist in shallow reefs with a high proportion of the population existing in kelp (*Ecklonia maxima*) beds (Branch *et al.,* 1994).

In South African abalone aquaculture, *H. midae* is the only abalone species to be commercially cultured. This is because *H. midae* is the largest and most prolific of the 5 endemic species that occur along the South African coastline (Proudfoot, 2006). Interestingly, South Africa is the second largest producer of abalone in the world, with 500 metric tonnes produced in 2003 (Troell *et al*., 2006). The need for abalone aquaculture in South Africa has become more evident in recent years, with the demand for the edible foot of the abalone exceeding the current supply (Reddy-Lopata *et al.,* 2006) and the natural population decreasing due to illegal poaching and over exploitation of natural stocks (Troell *et al.,* 2006). Abalone aquaculture is therefore an economically viable prospect in South Africa with over 12 abalone farms in commercial production (Ten Doeschate and Coyne, 2008). Currently there is a need to optimise the growth rate of abalone in order to shorten the length of time needed to reach harvestable size (Ten Doeschate and Coyne, 2008). In order for the abalone to reach harvestable size they must be healthy at all stages

of growth. As such, monitoring and improving the health system of the abalone within farming conditions is very important (Bacheré, 2003).

In most farming systems abalone are stocked at high densities. This can lead to the rapid spread of disease and potential build up of abiotic factors (such as ammonia) that may lead to increased abalone mortality (Reddy-Lopata *et al.,* 2006). Within commercial farming environments of various molluscs, the susceptibility of an outbreak is based on the presence of pathogens, the environment, as well as the health status of the cultured organism (Martello *et al.,* 2003). Thus monitoring the health status of abalone is necessary as it will indicate the current state of the cultured organism and potentially identify the causative stress.

Reliable diagnostic methods that monitor the health status of a species must be developed that will be able to identify the effects of different stresses exerted on the cultured organism. However, before diagnostic kits can be developed, proper analysis of the health system of the cultured organism, in this case *H. midae* needs to be performed using molecular techniques. This is essential to identify key genes that are involved in pathogenic attack responses and genes regulated in response to environmental changes that may occur within the farming system (Bachére, 2003). These genes will then be potential candidates as biomarkers in diagnostic kits. The identification of molecular stress markers will assist abalone farmers in identifying the cause of the stress, leading to effective and efficient treatment.

Bachére (2003) noted that while there are many bacterial pathogens against molluscs, the most harmful belong to the *Vibrio* genus, infecting molluscs at larval, juvenile and grow-out phases (Bachére, 2003). Several *Vibrio* species have been isolated from sick *H. midae* individuals and were found to be pathogenic (Dr Anna Mouton, personal communication). As such, it is ideal to understand the immune response to infection by Gram-negative bacteria like *Vibrio* and to identify the genes involved as possible biomarker candidates.

Currently, there is very little literature on the immune system of *H. midae*. A more complete understanding of the abalone immune system and the genes involved therein is required to facilitate the development of proper tools for the accurate identification of stress within *H. midae.*

1.2 THE INVERTEBRATE IMMUNE SYSTEM

Vertebrates possess a highly intricate immune system consisting of two components, the innate immune system and the adaptive immune response (Bosch *et al*., 2009). Invertebrates, however, rely solely on the innate immune system for defence against pathogens, lacking the adaptive immune system that consists of memory-based immune components (such as antibodies) and natural killer cells (Loker *et al.*, 2004). *Haliotis midae*, being an invertebrate, thus relies on the innate immune system as a protection mechanism against pathogens. Currently, there is little literature on the abalone innate immune response; consequently information on the innate immune system is derived from bivalves and other invertebrate species like *Drosophila* (Hooper *et al.,* 2007).

Marine invertebrates have developed a highly effective and complex innate immune system to combat pathogen attack (Tincu and Taylor, 2004). The immune system is comprised of two separate modes of action, the humoral immune response and the cellular immune response (Tincu and Taylor, 2004). The humoral response in invertebrates is multi-faceted consisting of the production of anti-microbial peptides, coagulation of haemocytes, melanisation, and the production of reactive oxygen species (ROS) (Marmars and Lampropoulou, 2009), degradative enzymes (Wootton and Pipe, 2003) and opsonins which are usually in the form of agglutinins or lectins (Wootton *et al.*, 2003). Antioxidant enzymes are released alongside the free radical species to minimise damage to the tissue of the animal (Wootton and Pipe, 2003). The cellular response is composed of phagocytosis,

encapsulation and nodulation which are mediated through haemocytes (Marmars and Lampropoulou, 2009).

Molluscs predominately use the cellular defence system as the primary mechanism of defence against pathogen attack, in which haemocytes play a pivotal role (Tincu and Taylor, 2004). The first step in combating pathogen attack is chemotaxis. This is a process whereby haemocytes migrate to the site of infection. This is modulated and controlled by chemotaxins. Chemotaxins are either excreted by host cells or from a foreign agent (Donaghy *et al.*, 2009). Once haemocytes have migrated to the site of infection, one of the main modes of action is phagocytosis, whereby apoptotic cells and invading pathogens are recognised and engulfed by haemocytes (Marmars and Lampropoulou, 2009). In clams, phagocytosis occurs by invagination of the cell membrane followed by pseudopodia formation and particle internalization into an endocytic vacuole, called the primary phagosome. This phagosome then fuses with lysosomal granules, which contain enzymes such as hydrolases, esterases and amidases, which degrade the foreign material (Donaghy *et al.*, 2009).

Encapsulation is a process by which haemocytes bind to large targets to combat parasite infection (Marmars and Lamproulou, 2009). It is used primarily when phagocytosis is not possible (Donaghy *et al.*, 2009). The haemocytes form a capsule around the large target and, using processes such as melanisation and the production of free radicals, destroy the invader (Marmars and Lamproulou, 2009).

Nodulation is another aspect of the cellular immune response and is the action by which haemocytes aggregate and enclose a large amount of bacteria. These nodules can be melanised or non-melanised in response to the type of pathogen. It has been found that the prophenoloxidase enzyme is involved in this process (Marmars and Lampropoulou, 2009). The prophenoloxidase enzyme is also involved in melanisation, an aspect of the humoral immune response. Melanisation is not only used to defend against pathogens but is also part of the wound healing response (Aladaileh *et al.*, 2007). Prophenoloxidase is activated via a cascade pathway that is initiated through pattern recognition proteins (Charoensapsri *et al.*, 2009). The now active phenoloxidase facilitates the formation of melanin which is important in the sequestration of foreign material during encapsulation (Butt and Raftos, 2008).

It has been suggested that cellular immune parameters are sensitive to environmental changes such as temperature, salinity, microbial infection and as such could potentially reflect the health status of bivalves (Donaghy *et al.*, 2009). Thus immune parameter assays that detect cellular changes could be used as effective indicators to determine the relative stress levels of an organism. At present there are well designed assays that can be used to measure phagocytosis (Mortensen and Glette, 1996), phenoloxidase activity (Cheng *et al.*, 2004), number of circulating haemocytes present (a total haemocyte count) and anti-bacterial activity (Ordàs *et al.,* 2000) in invertebrate systems.

1.3 HAEMOCYTES

Haemocytes are blood-like cells (Cao *et al.,* 2007) that mediate and perform various functions in bivalves such as wound repair, shell regeneration (Bettencourt *et al.,* 2009), transport of nutrients and the cellular immune response (Cima *et al.,* 2000). Bivalves contain an open, haemolymphatic circulatory system in which haemocytes are able to circulate and detect changes within the environment (Donaghy *et al.*, 2009). Haemocytes can be divided into various types based on size and granular content. The two most prolific types of haemocytes in bivalves are granulocytes and agranulocytes. Granulocytes are large and contain granules such as neutrophils, acidophils or basophils. Agranulocytes are divided into different subtypes and include halinocytes and blast-like cells. (Cima *et al.,* 2000; Donaghy *et al.,* 2009). The primary function of haemocytes is in the cellular immune response utilising phagocytosis, nodulation and encapsulation as a means of combating pathogenic attack (Bettencourt *et al.,* 2009).

As haemocytes play such a pivotal role in the immune response and are easily sampled, it makes them an attractive candidate for study at an *in vitro* level. Presently, primary haemocyte cultures are being used in investigations, as it has not been possible to immortalise haemocyte cell cultures or determine the way in which haemocytes are able to proliferate (Matozzo *et al.,* 2008). However, Matozzo *et al.* (2008) discovered the appearance of mitotic spindles and microtubules in the haemoblasts (a type of haemocyte) of the clam, *Tapes philippinarum*, indicating that circulating haemocytes are able to

undergo cell division. The authors found that the haemoblasts make up a small percentage of the total population of haemocytes (19%), indicating that the rate of proliferation is low (Matozzo *et al.*, 2008).

Novas *et al*. (2007) developed a primary haemocyte cell culture from *Mytilus galloprovincialis* in order to ascertain the variability of nitric oxide production and its effect on mounting an immune response. By utilising a primary cell culture, the authors were able to stimulate an immune response using lipopolysacharides (LPS) from *Escherichia coli* and various cytokines, including: human TNF-α, recombinant human IL-2, TGF-β1 and PDGF, and were successfully able to assay total nitric oxide production and determine protein expression levels of enzymes involved in nitric oxide production (Novas, *et al.,* 2007).

Iakovleva *et al.* (2006) utilised haemocytes obtained from the periwinkle, *Littorina littorea,* to determine the effects that infection had on mitogen activated protein kinases (MAPKs). LPS from *E. coli*, mannans from *Saccharomyces cerevisiae* and secretory-excretory products (SEPs) from trematodes were used as infecting agents to elicit a response in primary haemocyte cultures. The authors isolated protein from the primary cultures and utilising western blotting, were able to determine whether there was an increase in expression of MAPK proteins with respect to infection. The authors found that LPS activated two MAPKs namely ERK2 and p38 for a prolonged period during the time course of the experiment compared to the control groups. Mannan (from *S. cerevisiae*) was found to increase the level of phosphorylation of p38 during the time course and prolonged the activation of

ERK2, while SEP induced no visible changes in MAPK activity over the course of the experiment (Iakovleva *et al.*, 2006). A similar study was also conducted by Canesi *et al.* (2005) who looked at the effects of *E. coli* and *Vibrio cholerae* strains on MAPKs in *Mytilus galloprovincialis* haemocytes. The authors found that each infecting agent produced distinctive changes in the activation and phosphorylation of various MAPKs involved in the immune response (Canesi *et al.,* 2005). In both of these reports it is evident that the use of primary cultures yields reproducible and sensitive responses with respect to signalling changes in the immune response that occur upon infection.

Parisi *et al.* (2008) recently analysed the involvement of different haemocyte types in combating bacterial infection in the mussel, *M. galloprovincialis*. The authors found that sub-populations of haemocytes were able to distinguish between two *Vibrio* species used in infection challenge trials, *Vibrio splendidus* and *Vibrio anguillarum*. The authors used flow cytometry to distinguish the various haemocyte types and found that three types of haemocytes in *M. galloprovincialis* decreased and increased differently at various time points in response to the *Vibrio* species used in the experiment (Parisi *et al.,* 2008). The authors also found that the total haemocyte population was affected differently at various time points with respect to different bacteria (*Micrococcus lysodeikticus, V. splendidus,* and *V. anguillarum*), including time points at which the infection had been completely cleared within the circulatory system of the mussel *M. galloprovincialis* (Parisi *et al.*, 2008). These results reflect the specificity of the haemocyte response to bacterial infection and the sensitivity the response displays by being able to distinguish the two *Vibrio* species tested.

Cao *et al.* (2007) used a primary cell culture of *M. galloprovincialis* haemocytes to determine seasonal variations in the immune response mounted by haemocytes (Cao *et al.,* 2007). Primary haemocyte cell cultures have been used effectively in other marine molluscs including: the clams *Mercenaria mercenaria* (Buggé *et al.,* 2007) and *Tapes philippinarum* (Matozzo *et al*., 2008 and Cima *et* al., 2000), the shrimp *Penaeus chinensis* (Jiang *et al.*, 2006), the scallop *Pecten maximus* (Mortensen and Glette, 1996) and the abalone *Haliotis tuberculata* (Lebel *et al.*, 1996).

Primary haemocyte cultures have proved an efficient method of analysis in marine invertebrate studies. It is therefore of interest to develop a primary cell culture of haemocytes from the South African abalone *Haliotis midae* as a means of studying its vitally important and interesting immune system.

1.4 INTERACTIONS IN THE IMMUNE RESPONSE AND KEY GENES INVOLVED

There are two pathways in the invertebrate humoral immune response that lead to the regulation of antimicrobial peptides, the toll pathway and the immune deficiency (imd) pathway (Irving *et al.,* 2004). In *Drosophila,* the toll pathway is involved in the up-regulation of antimicrobial peptides that act specifically against Gram-positive bacteria and fungi (Irving *et al.,* 2004). The Toll-like receptors (TLRs) detect pathogen-associated molecular patterns (PAMPs) and initiate the up-regulation of antimicrobial peptides (Bosch

et al., 2009). PAMPs are generally found on the surface of microorganisms, such as peptidoglycan from Gram-positive bacteria and 1-3 β-glucans from fungal cell walls (Nikapitiya *et al.*, 2008). *Drosophila* Toll receptors mediate signalling of various pathogen recognition proteins (PRPs), such as peptidoglycan recognition proteins (PGRPs) (Kurata *et al.*, 2006). Once a PRP recognises a PAMP, the Toll pathway is activated through a Toll receptor via a protein known as Spätzle which subsequently leads to the formation of a receptor-adaptor complex consisting of three proteins, MyD88, Tube and Pelle (Irving *et al.,* 2004). This complex initiates the dissociation of Dif or Dorsal (NFκB homologues) from its inhibitor Cactus (IκB homologue) via a phosphorylation pathway. The Dif or Dorsal protein is then able to translocate to the nucleus and up-regulate anti-microbial peptide genes (Irving *et al.,* 2004). A simplified diagram of the signalling pathway is presented in Figure 1. Interestingly, the Toll pathway is also needed for proper encapsulation to occur (Marmaras and Lampropoulou, 2009) showing that in *Drosophila,* regulation of the humoral and cellular responses is linked in combating microbial infection.

In *Drosophila*, PGRP family members act as PRPs upstream of both the Toll and imd pathways. The imd pathway (Figure 1) leads to the up-regulation of anti-microbial peptides that are specific to Gram-negative and Gram-positive bacteria (Kurata *et al.*, 2006). In the imd pathway the recognition of PAMPs via PGRPs leads to the activation of a signal transduction pathway involving proteins that have not yet been fully elucidated (Khush *et al.*, 2001). This cascade then leads to the activation of Relish (NFκB homologue) via a caspase protein known as Dredd. Relish remains inactive in the cytoplasm via its own

ankyrin repeats which act as inhibitor domains and is endo-proteolytically cleaved once activated (Irving *et al.,* 2004). Relish is then able to translocate to the nucleus and up-regulate anti-microbial peptides (Irving *et al.,* 2004).

Meng *et al*. (1999) isolated *Drosophila* mutants that were Dorsal and Dif deficient in order to investigate the effects of these mutations on antimicrobial synthesis. They found that the mutants challenged with *Escherichia coli* had lower expression levels of antimicrobial peptides compared to healthy flies (Meng *et al.*, 1999). Antimicrobial peptides are important in the defence of invertebrates as they are able to function without high specificity or memory. They are amphiphilic molecules that are able to disrupt cellular membranes in bacteria. These molecules are small and highly effective at preventing bacterial proliferation (Tincu and Taylor, 2004).

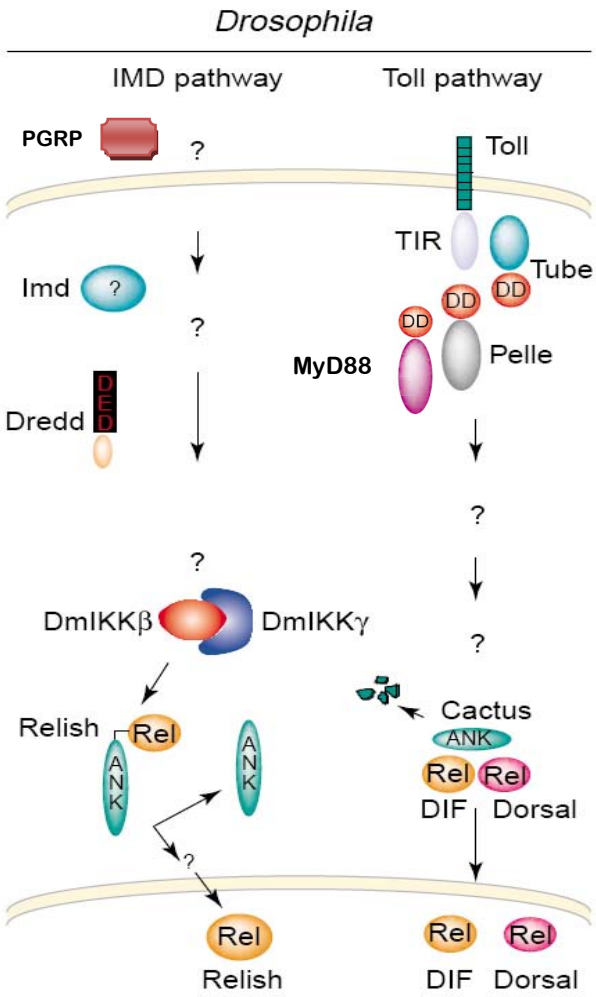

Figure 1: The imd and Toll signalling pathway in *Drosophila melanogaster* taken from Khush *et al.* (2001) with adaptations from Irving *et al.* (2004). In the imd pathway, peptidoglycan recognition proteins (PGRPs) recognise PAMPs and initiate the signalling pathway by unknown proteins and mechanisms. This eventually leads to the activation of Relish by Dredd and possibly IKK (Inhibitor kinase kinase) which leads to the auto-cleavage of the ankyrin repeat domain (ANK) allowing Relish to translocate to the nucleus. In the Toll pathway, once PAMPs are recognised, a signalling pathway is induced that leads to the activation of Tube, MyD88 and Pelle in a complex. This pathway then leads to the activation of Dif or Dorsal via the release of their inhibitor Cactus in a yet unknown phosphorylation pathway.
ANK: Ankyrin repeats, DD: death domain; Rel: REL homology domain; TIR: Toll/IL-1R domain

There is one common factor in all the pathways that lead to the up-regulation of antimicrobial peptides: the regulatory protein NFκB. The various homologues of NFκB, namely Relish, Dif and Dorsal, are responsible for activating genes that combat microbial infection (anti-microbial peptides). This makes NFκB a candidate gene that may be useful in determining the health status of *H. midae* in response to bacterial infection. NFκB factors are important regulators of the innate immune system of vertebrates and invertebrates (Mason *et al.*, 2004). In mammals, NFκB mediates vital components of the innate immune system such as cytokines and chemokines. NFκB interacts with Toll-like receptors (TLRs) and pattern recognition molecules including, bacterial components (LPS), inflammatory cytokines (such as TNFα) and viral products such as RNA (Jiang and Wu, 2007). These interactions lead to different modes of defence as different TLRs have been linked to different kinds of pathogen attack (Caamaño and Hunter, 2002).

1.5 NUCLEAR FACTOR KAPPA B CHARACTERISATION

NFκB belongs to a group of dimeric transcription factors that can be homo- or hetero-dimeric proteins (Bosisio *et al.,* 2006). This family of transcription factors is involved in the regulation of inflammation, the immune response, apoptosis, cell proliferation and differentiation (Jiang and Wu, 2007). All NFκB subunits contain a Rel homology domain, which is a 300 amino acid sequence in the N-terminal region that is indicative of the NFκB group (Caamaño and Hunter, 2002). This domain is involved in processes such as

dimerisation and site specific interactions, and contains a nuclear localisation signal (NLS) to which its inhibitor binds. NFκB proteins can be distinguished into two different classes, namely class I and class II. Class I NFκB proteins contain ankyrin repeat domains, such as p100, p105 and Relish and require proteolytic processing in order to become active (Bosisio *et al.*, 2006). Class II includes NFκB proteins that have a transactivation domain in the C-terminal region (Jiang and Wu, 2007) and transcriptional activation domains (Perkins, 2000). Class II NFκB proteins do not require proteolytic processing in order to generate active forms (Perkins, 2000). Figure 2 illustrates the different subunits in the NFκB family of transcription factors.

An NFκB homologue has not been identified from the abalone *H. midae*. It is therefore important to amplify the gene from the organism of interest if it is to be studied. To date, mainly class II NFκB transcription factors have been isolated from marine invertebrates and have been found to be regulated by various bacterial stimuli. Jiang and Wu (2007) characterised a class II NFκB homologue in *Haliotis diversicolor supertexta.* The authors isolated the homologue by designing degenerate primers to the rel homology domain. The homologue, Ab-rel, was found to have a role in the immune response of *H diversicolor supertexta*. The authors showed that Ab-Rel was activated by *E. coli* LPS through a pattern recognition receptor that is a component of the TLR family. The authors also found that the homologue was ubiquitously expressed in different tissues, namely the foot muscle, mantle margin, gills, digestive gland and haemocytes. The authors suggest that ubiquitous expression of Ab-Rel in *H. diversicolor supertexta* is due to the fact that NFκB is pleotropic,

and therefore involved in other important biological processes. Ab-Rel was shown to have a strong evolutionary relationship with the *Drosophila* (Dif and Dorsal) and *Crassostrea gigas* NFκB homologues, clustering together on a phylogenetic tree (Jiang and Wu, 2007). Interestingly activation of Ab-rel by *E. coli* LPS suggests that the *H. diversicolor supertexta* NFκB homologue responds to all microbial infections, as opposed to the *Drosophila* NFκB which responds solely to Gram-positive bacteria and fungi.

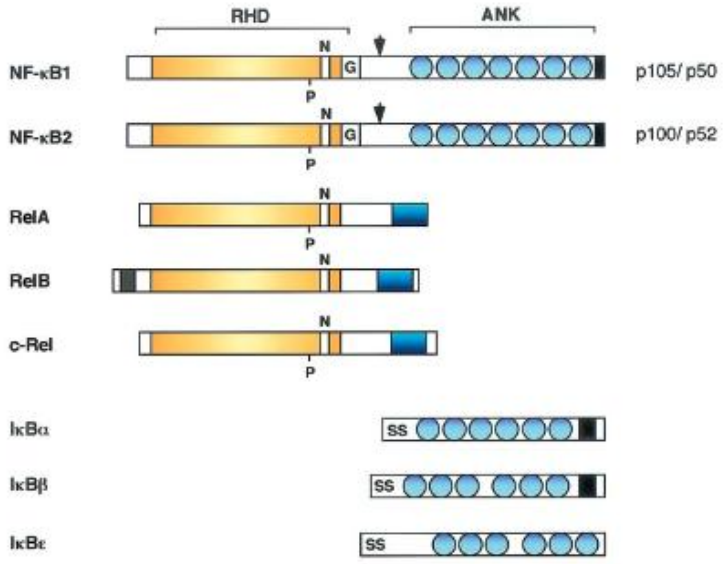

Figure 2: The different subunits in the NFκB family of transcription factors. The arrows indicate the endoproteolytic cleavage sites of p105 and p100 which give rise to p50 and p52, respectively. RHD, Rel homology domain; ANK, ankyrin repeat; SS, signal-induced phosphorylation sites (Caamaño and Hunter, 2002).

A Dorsal (LvDorsal) homologue was isolated from the shrimp, *Litopenaeus vannamei,* by Huang *et al.* (2009). LvDorsal was isolated from *L. vannamei* using degenerate primers to the rel homology domain and was found to be a class II NFκB homologue. Huang *et al.* (2009) transfected the full length LvDorsal homologue into *Drosophila* S2 cells and found

that it up-regulated the anti-microbial peptide penaeidin-4. Interestingly, this peptide is specific for Gram-negative bacteria, which suggests that it should be a component of the imd pathway that is regulated by Relish. The authors propose that there could be cross-talk between the imd pathway and the Toll pathway (Huang *et al*., 2009). A recent study on the NFκB binding sites (κB motifs) in *Drosophila* found that while there are specific motifs which bind either Relish or Dif, a subset of κB motifs exist that bind both Dif and Relish homologues (Busse *et al.*, 2007). In their studies, the authors found that some genes (AttA and AttD) were up-regulated to a greater extent if both Dif and Relish were present. The authors suggest that there could be a greater interplay between the imd and Toll pathways leading to a more diverse and sensitive immune response pathway (Busse *et al.*, 2007).

Gueguen *et al.* (2003) performed a large scale study of immune genes that are up-regulated upon infection of the oyster *C. gigas* with a bacterial mix (*Vibrio anguillarum, Vibrio metshnikovii, Vibrio tubiashii and Vibrio* S322), by generating a library of expressed sequence tags isolated from haemocytes following infection. The authors found a myriad of genes involved in the immune response including several genes belonging to the NFκB signalling pathway. The authors isolated genes encoding proteins with homology to Vav proteins. Vav proteins participate in transmitting signals to the NFκB signal cascade. These include MyD88, TRAF, ECSIT, which are downstream proteins regulated in the NFκB cascade and Cactus (the IκB homologue found in *Drosophila*). This is the first study that has isolated several genes involved in the NFκB cascade from an invertebrate species other

than *Diptera,* and suggests that a strong evolutionary conservation of this pathway may exist amongst species (Gueguen, *et al.,* 2003).

Jiang and Wu (2007) and Huang *et al.* (2009) have shown that it is possible to isolate an NFκB homologue from an invertebrate species utilising degenerate primers designed to the conserved rel homology domain. These studies further indicate that NFκB is an important immune response gene in invertebrates that can be stimulated by a wide range of bacterial stressors.

1.6 AIMS OF THIS STUDY

H. midae is a commercially important species that it susceptible to bacterial pathogens in the farming environment. It is thus imperative to monitor the health status of the cultured organism, to ensure harvestable yields. In South Africa, the abalone aquaculture is expanding rapidly, and consequently, it is of importance to analyse key genes that could be used to detect stress responses. In invertebrates, NFκB has been identified as a central regulator of the innate immune response. Class II NFκB homologues were identified as being upregulated in response to Gram-negative bacterial species in *H. diversicolor supertexta, M. gallinoprovincialis* and *P. monodon*. The central objective of this study is to investigate NFκB as a candidate biomarker of bacterial stress.

The first aim of this project was to isolate and characterise an NFκB homologue from *H. midae* by obtaining sequence information of the gene. For this study both degenerate and gene specific primers were used to amplify the NFκB homologue from complementary DNA (cDNA). Sequence information is useful as it identifies sequence conservation amongst species (homology), the type of NFκB subunit isolated and active domains present.

The second aim of this project was to gain insight into some of the physiological responses that occur within *H. midae* upon a bacterial challenge, and to identify the suitability of NFκB as a biomarker.

For this study, *H. midae* were challenged with Gram-negative heat killed *V. anguillarum* 5676. Haemocytes isolated from *H. midae* were assayed for various physiological responses that may have occurred upon exposure to the heat killed pathogen, such as phagocytosis, the activity of anti-microbial-peptides, the production of phenoloxidase and the number of circulating haemocytes present in the stressed organism.

Phagocytosis is the primary mode of action in invertebrate immunity. It is a process whereby haemocytes engulf and degrade foreign particles. Phagocytosis is assayed using a simple technique, whereby labelled bacteria are added to haemocytes and are visualised under a flourescent microscope. The number of haemocytes able to phagocytose are counted and the percentage of phagocytosis is calculated. This assay was used to determine whether exposure to the heat killed pathogen elicited a change in the phagocytic activity of *H. midae.*

The serum anti-bacterial assay measures the ability of the cell-free haemolymph to decrease or inhibit the growth of *E. coli.* An anti-bacterial index (BI) is calculated which measures the level of inhibition of growth and thereby determines anti-microbial activity in the cell-free haemolymph. This assay investigated whether there was a difference in the activity of anti-microbial peptides in *H. midae* haemolymph upon exposure to the heat killed pathogen.

The phenoloxidase assay quantitates phenoloxidase enzyme activity. Phenoloxidase facilitates the formation of melanin, which is important in the sequestration of free radicals produced during phagocytosis and encapsulation. Phenoloxidase converts dopamine into dopachrome and eventually melanin. In this study, the assay was used to detect whether there was a change in phenoloxidase activity in abalone exposed to heat killed *V. anguillarum* 5676.

Quantitative real time PCR is a sensitive method for detecting changes in the expression levels of mRNA, utilising cDNA as template in the amplification steps. This technique was used to determine the regulation of the NFκB homologue in *H. midae* in response to a bacterial stress. The mRNA expression levels of NFκB will determine its relevance as a biomarker of stress in farmed *H. midae*.

Many published studies have used immune parameter assays to describe the physiological state of a marine invertebrate in response to a bacterial stressor. This study will therefore provide relevant insight into the physiological responses that occur in *H. midae.* Taken together, this data will expand upon what is known regarding abalone immunity by identifying physiological changes that occur when *H. midae* is exposed to a heat killed pathogen and determining whether NFκB is upregulated upon exposure to the pathogen and is thus a suitable biomarker of stress. Regulation of the NFκB homologue will also provide insight into the regulatory pathway of the innate immune response in *H. midae*.

Haemocytes were identified as ideal candidates to study the invertebrate innate immune system as they are the primary effectors in eliciting cellular immune responses. The next aim of this study was to determine the usefulness of an *in vitro* system as a means of characterising abalone haemocytes in terms of their role in innate immunity.

The maintenance of haemocytes *in vitro* has been described in several studies. In this study, viability assays (phagocytosis and the trypan blue viability assay) were used to determine the sustainability of primary *H. midae* haemocyte cultures *in vitro.* Haemocytes were also observed using light microscopy to identify their characteristics in an *in vitro* system. *H. midae* haemocytes have not been described in the literature; as such staining techniques using histochemical techniques were employed to determine morphological features of *H. midae* haemocytes.

The last aim of this study was to determine the relevance of an *in vitro* system as a useful tool to study aspects of the *H. midae* immune response. This was achieved by performing an *in vitro* challenge trial. Labelled heat killed *V. anguillarum* 5676 was used to elicit a response in primary *H. midae* cultures. Using the same techniques described in the *in vivo* challenge trial, the primary haemocyte culture was assessed for its relevance as a tool to study biological responses in *H. midae* haemocytes.

Currently, literature on invertebrate innate immunity is largely based on bivalves and *Drosophila.* In-depth knowledge of *H. midae* innate immunity will serve to manage disease in the abalone farming industry by identifying useful biomarkers of stress, and consequently, establishing effective treatment plans. This study aims to enrich the current knowledge regarding *H. midae* innate immunity by identifying some of the physiological responses that occur upon exposure to a bacterial stressor and investigating the suitability of NFκB as a biomarker of stress. This study will also provide insight into the usefulness of a primary haemocyte system as a tool to study the innate immune response of *H. midae.*

CHAPTER 2

METHODS AND MATERIALS

CONTENTS

2.1 Cloning and sequencing of *H. midae* NFκB homologue 27

2.1.1 RNA isolation 27

2.1.2 cDNA synthesis 30

2.1.3 Amplification of *H. midae* NFκB 30

2.1.3.1 Primer design 30

2.1.3.2. PCR 33

2.1.3.3. Nested PCR 34

2.1.4 Cloning and transformation 35

2.1.5. Bioinformatic analysis 36

2.2 Physiological response and NFκB expression of *V. anguillarum* 5676 challenged *H. midae* 38

2.2.1 Challenge Bacteria 38

2.2.2 Challenge tRials 39

2.2.3 Total Haemocyte Counts: 40

2.2.4 Serum anti-bacterial activity 41

2.2.5 Phenoloxidase Assay 42

2.2.6 Phagocytosis Assay 43

2.2.6.1 PREPARATION of labelled bacteria for phagocytosis assay 43

2.2.6.2 Assay 44

2.2.7 Real Time quantitative PCR 45

2.3 Haemocyte Tissue Culture 46

2.3.1 Viability 47

2.3.1.1. TRypan blue assay 47

2.3.1.2 Phagocytosis assay 48

2.3.2. Haemocyte staining 48

2.3.2.1. Giemsa Dye 48

2.3.2.2. Neutral Red Dye 49

2.3.2.3. Acridine Orange staining 49
2.3.3 *In Vitro* Challenge Trial 50
2.3.3.1 RNA isolation and cDNA conversion 51
2.3.3.2 Quantitative real time PCR 52
2.4 Statistical Analysis 53

2.1 CLONING AND SEQUENCING OF *H. MIDAE* NFKB HOMOLOGUE

2.1.1 RNA ISOLATION

Haemolymph was sampled from the pedal sinus of abalone using a 21G X 1½″ sterile hypodermic needle (Uniqiao, Wupro Tech.) attached to a sterile 2.5 ml syringe. Five hundred microlitres to one mililitre of haemolymph was isolated per medium sized abalone (6.9 cm ± 3.2). The haemolymph was aliquoted into 1 ml volumes and haemocytes were collected by centrifugation at 8 000 X *g* for 10 minutes. The serum was removed and the concentrated haemocytes were flash frozen with liquid nitrogen and stored at -80°C.

Total RNA was extracted from haemocytes in an adapted version of the single step RNA isolation by Acid Guanidium thiocyanate-Phenol-Chloroform extraction from Chomczynski *et al.* (1987). Briefly, concentrated haemocytes were resuspended in 750 µl RNA lysis buffer (Appendix A 3.2). Seventy five microlitres of 2 M sodium Citrate pH 4 (Appendix A 3.3) was added and the solution was mixed by inversion. Seven hundred and fifty microlitres of phenol (pH 4) was added to the solution, mixed by inversion after which 150 µl of chloroform:isoamyl (49:1) was added. The solution was mixed by vortexing for 10 seconds, incubated on ice for 10 minutes and subsequently centrifuged for 20 minutes at 13 000 X *g* at 4°C. The aqueous phase was removed and dispensed into fresh 1.5 ml microfuge tubes. One volume of isopropanol was added to each sample, mixed by inversion and incubated for approximately 16 hours at -70°C. The samples were centrifuged for 10

minutes at 13 000 X *g* at 4°C and the supernatant removed. The RNA pellet was resuspended in 150 µl RNA lysis buffer and 1 volume of isopropanol was added. The RNA was allowed to precipitate for 1 hour at -20°C. The RNA was concentrated by centrifugation for 10 minutes at 13 000 X *g* at 4°C, and washed with 96% ethanol followed by a 70% ethanol wash. The RNA was air dried for 5 minutes to remove excess ethanol and resuspended in Diethylpyrocarbonate (DEPC) water (Appendix A 3.1). RNA was quantitated spectrophotometrically (NanoDrop® ND-1000 Spectrophotometer, NanoDrop 1000 software version 3.7.1) by measuring the absorbance at 260 nm. A DNase treatment was included to remove residual genomic DNA. One unit of RNase free DNase I (Fermentas) was added per microgram of RNA in a 50 µl reaction and incubated at 37°C for 1 hour according to the manufacturer's instructions. Fifty microlitres of phenol (pH 4):chloroform:isoamyl (25:24:1) was added to the samples and mixed by inversion. The samples were centrifuged for 10 minutes at 13 000 X *g* at 4°C. The aqueous phase was recovered and mixed with 5 µl of 3 M Na-acetate (pH 5.2, Appendix A 3.5) and 150 µl of 100% ethanol. The samples were centrifuged for 10 minutes at 13 000 X *g* at 4°C to concentrate the RNA. RNA was air dried for 5 minutes and resuspended in 25 µl DEPC treated sterile water. RNA was quantitated spectrophotometrically as described above.

RNA integrity was determined by visualisation on a RNA formaldehyde agarose 1.2 % (*w/v*) gel (Sambrook *et al.,* 1989, Appendix D1.1). Briefly, one microgram total RNA was denatured for 15 minutes at 65°C in RNA sample application buffer (Appendix A.3.7) in a ratio of 1:2 of RNA: sample application buffer. The samples were electrophoresed at 80 V in

1 X 3-(N-morpholino)propanesulfonic acid (MOPS) buffer (Sambrook *et al.,* 1989, Appendix A 3.6) and visualised under a short wave UV light box (Biorad GelDoc EQ-system™, Biorad Laboratories). Genomic DNA contamination (Appendix D 1.2 and D 1.3) of the RNA was verified by amplifying the ribosomal factor L28 gene using 1 µl RNA as template (Appendix B 3.1 and B2.1).

RNA quality and quantity was also analysed using RNA lab-on-a-chip® technology (Appendix D 1.1). Each RNA lab-on-a-chip® was set up according to the manufacturer's instructions (RNA Nano Lab Chip Kit, Agilent Technologies) and 1 µl of RNA isolated from *H. midae* haemocytes was added to each well. The resultant chip was visualised on the bioanalyser (Agilent 2100 Bioanalyser, Agilent Technologies) using Expert software (2100 Expert Software, version 1, Agilent Technologies) which detects both RNA quality and genomic DNA contamination (Appendix D 1.1).

The 18S rRNA and 28S rRNA isolated from *H. midae* migrates closely together through the RNA lab-on-a-chip acrylamide gel, and consequently, the algorithm used to infer an RNA integrity number (RIN) was unable to calculate a RIN value for any of the samples due to the apparent discrepancy of the migration pattern. The electropheregrams and resultant digital gel photos of each RNA sample were used to deduce RNA quality (Appendix D 1.1).

2.1.2 CDNA SYNTHESIS

cDNA was synthesised using 2 µg of total RNA isolated from haemocytes. Conversion reactions were performed in a total volume of 40 µl according to the manufacturer's instructions (Promega ImProm-II™ Reverse Transcription System). The priming strategy involved adding a combination of random hexamers (Promega) and oligo dTs (Promega) to the cDNA synthesis at a ratio of 1:1 to ensure a better quality and quantity of cDNA produced. The cDNA reactions were incubated at 42°C for 16 hours in a water bath placed in a hybridisation incubator (Amersham Biosciences). The reactions were heat inactivated for 15 minutes at 75°C and subsequently aliquoted into 10 µl volumes and stored at -80°C. One cDNA synthesis was performed per sample per biological repeat.

2.1.3 AMPLIFICATION OF *H. MIDAE* NFKB

2.1.3.1 PRIMER DESIGN

Primers *Nf* and *Nr* described in Jiang and Wu (2007) were used to amplify the 3' end of the *H. midae* NFκB homologue using PCR. To obtain further sequence information, 5' RACE (SMART Clontech RACE kit, Takara Bio) was attempted. PCR primers with an annealing temperature of 68°C or greater are necessary for RACE to be successful. Unfortunately, 5' RACE proved unsuccessful since the AT rich content of the *H. midae* sequence obtained

prevented primers with the appropriate annealing temperatures from being designed. Consequently, degenerate primers (Drelf and Drelr) were designed to the Rel homology domain of NFκB (class II), located at the 5' end of the gene, in an attempt to obtain additional sequence information regarding the *H. midae* NFκB homologue. Protein sequences obtained from the National Centre for Biotechnology Information (NCBI) database (www.ncbi.nlm.nih.gov) (Table 1) were used to form multiple sequence alignments in BioeEdit (BioEdit version 7.0.0© 1997-2004, Tom Hall). A codon usage table for *H. midae* was constructed using 148 coding sequences obtained from a microarray study (Bronwyn Arendze, unpublished data) with the program JEMBOSS using the cusp algorithm (version 1.5, European Molecular Biology Open Software Suite), as sequence conservation between the cDNA fragments was poor. The aligned protein sequences, together with the *H. midae* codon usage table, were used to design degenerate primers (Drelf and Drelr, Table 2) to conserved regions of the NFκB Rel homology domain. In addition, gene specific primers (GSRf and GSRr, Table 2) to the Rel homology domain were designed from the *H. diversicolor supertexta* ab-rel sequence (accession number: AY700781) since a similar approach using the gene specific primers N*f* and N*r* proved successful for amplification of the non-conserved 3' portion of the *H. midae* NFκB homologue. The locations of the primers used in this study with respect to the *H. midae* NFκB homologue are observed in Figure 3.

Table 1: NFκB sequences used to design degenerate primers

Name	Accession number
Haliotis diversicolor supertexta	AY700781
Crassostrea gigas	AY039648.1
Pinctada fucata	EF121959.1
Venerupis decussatus	DQ673624.1
Mytilus galloprovincialis	DQ673623.1
Mercenana mercenaria	DQ673622.1
Bathymodilous azorizus	DQ673621.1
Tubifex tubifex Dorsal	AB192889.1
Euprymna scalopes	AY956819.1
Allomyrina dichotoma	AB125691.1
Gallus gallus	AF000241.1

Table 2: Primer Names and Sequence information.

Name	Primer Sequence		Tm (˚C)	Reference
Nf	5′ GAACTTGAGGATCGACCACAC	3′	64	Jiang and Wu (2007)
Nr	5′ TGTGGCAGCAAATCAACCAG	3′	60	Jiang and Wu (2007)
Drelf	5' GAMGATCTGCWGGNAGTATTCCKGGA	3'	55 - 60	This study
Drelr	5' TRGCACACTGAATKCCNAGATGWGG	3'	53 - 58	This study
GSRf	5' CGAGTGTGAGGGACGATGTGC	3'	58	This study
GSRr	5' GCATCAGGCAGGAAGACTTGGA	3'	57	This study
RTF1	5' TCCTTGTGCATCCTGGAGATAGGCG	3'	63	This study
RTR1	5' TTGACAGCTCGGTTGTACAGAACCAGC	3'	65	This study
818F	5′ GAAGGATTGACAGATTGAAAGC	3′	62	Bronwyn Arendze (unpublished data)
818R	5′ CAGGCTAGAGTCTCGTTCG	3′	64	Bronwyn Arendze (unpublished data)
18sF	5′ TGGACTCACCGTCAGCACG	3′	64	Bronwyn Arendze (unpublished data)
18sR	5′ TTCTGGTGACCAAGACAACGCC	3′	65	Bronwyn Arendze (unpublished data)
RfillF	5′ GAGATGAGGAAATGTTATCG	3′	46.2	This study
RfillR	5′ GAGCTGTCAATTACATTCCC	3′	48.2	This study

Figure 3: Representation of the *H. midae* NFκB homologue allocating the different primer pairs used in this study. The blue (Drelf and Drelr) and the red (GSRf and GSRr) arrows indicate the nested PCR primers used to amplify the rel homology domain (RHD). The orange arrows (N*f* and N*r*) indicate the primers described in Jiang and Wu (2007) used to amplify the initial 3' region of the gene. The pink arrows (RTF1 and RTR1) indicate the quantitative real time primers used in this study, and the green arrows indicate the primers designed (RfillF and RfillR) to amplify the bridging sequence.

N*r* (Table 2) using the XP thermocycler (Bioer). Twenty microlitre reactions were performed using 0.5 units (U) of Supertherm Taq polymerase (Southern Cross Biotechnology), 2 µl 10 X Taq polymerase buffer, 3 mM $MgCl_2^{2+}$ and equal amounts of all four dNTPs (0.25 µM each). The template was amplified using the following cycle profile: initial denaturation 94˚C for 4 minutes, 35 cycles of denaturation at 94˚C for 30 seconds, annealing at 53˚C for 30 seconds and elongation at 72˚C for 40 seconds, and a final elongation step at 72˚C for 10 minutes.

The PCR products were analysed on a 1.2% (*w/v*) agarose gel in 1X Tris Acetate EDTA (TAE) buffer containing ethidium bromide (0.4 µg/ml, appendix A 2.8), after electrophoresis at 100V in 1 X TAE buffer (Sambrook *et al.,* 1989). The products were visualised using a long wavelength UV light box (Biorad GelDoc EQ-system™, Biorad Laboratories). The correct size band was excised from the gel and extracted using the Biospin Gel Extraction kit (Bioer Technology Co., LTD) according to the manufacturer's

instruction. The purified product was used in a subsequent ligation reaction (see section 2.1.4).

2.1.3.3. NESTED PCR

One microlitre of cDNA or 150 ng of genomic DNA (Appendix B 1.1) was amplified with 0.3 µM of primers GSRf and GSRr (Table 2) using the XP thermocycler (Bioer). Twenty microlitre reactions were performed using 0.5 units (U) of Supertherm Taq polymerase (Southern Cross Biotechnology), 2 µl 10 X Taq polymerase buffer, 3 mM $MgCl_2^{2+}$ and equal amounts of all four dNTPs (0.25 µM each). The template was amplified using the following cycle profile: initial denaturation 95˚C for 5 minutes, 40 cycles of denaturation at 95˚C for 30 seconds, annealing at 55˚C for 30 seconds and elongation at 72˚C for 40 seconds, and a final elongation step at 72˚C for 5 minutes.

One microlitre of the amplified product was used as template in an amplification reaction using 0.3 µM of primers Drelf and Drelr (Table 2). The amplification reaction was the same as described for the amplification above with the exception that 5 mM $MgCl_2^{2+}$ was used. The template was amplified using the following cycle profile: initial denaturation 95˚C for 5 minutes, 40 cycles of denaturation at 95˚C for 30 seconds, annealing at 53˚C for 30 seconds and elongation at 72˚C for 40 seconds, and a final elongation step at 72˚C for 5 minutes.

The PCR products were analysed on a 1.2% (*w/v*) agarose gel in 1 X Tris Acetate EDTA (TAE) buffer containing ethidium bromide (0.4 µg/ml, appendix A 2.8), after electrophoresis at 100V in 1 X TAE buffer (Sambrook *et al.,* 1989). The products were visualised using a long wavelength UV light box (Biorad GelDoc EQ-system™, Biorad Laboratories). The correct size band was excised from the gel and extracted using the Biospin Gel Extraction kit (Bioer Technology Co., LTD) according to the manufacturer's instruction. The purified product was used in a subsequent ligation reaction (see section 2.1.4).

2.1.4 CLONING AND TRANSFORMATION

Fermentas InsTAclone™ PCR cloning Kit (Fermentas) was used for cloning. Both the PCR and the nested PCR amplification products were ligated into the pTZ57R/T vector (Appendix C) at 15°C overnight according to the manufacturer's instruction. Ten microlitres of each ligation reaction was used to transform *Escherichia coli* DH5α competent cells using a standard heat shock method (Sambrook *et al.,* 1989). The transformation reactions were inoculated onto Luria agar (LA) solid media supplemented with 0.2 % X-gal (*w/v*) and 100 µg/ml Ampicillin (Amp) (Appendix A.1.5). Transformants (white colonies) were selected and inoculated onto LA-Amp (100 µg/ml) solid media. Plasmid DNA (Appendix B 1.1) was isolated according to Sambrook *et al.,* (1989), and digested using the restriction enzymes *Pst*I (Fermentas) and *Eco*RI (Fermentas) to confirm the presence of the insert. M13 forward and reverse primers were used to amplify the inserts to confirm the restriction enzyme digest results (Appendix B 3.1 and B.3.2).

Plasmids containing the correct size insert (200 bp and 250 bp respectively) were sequenced (Macrogen, Korea) using the M13 forward and reverse primers. Sequences were edited and analysed using the software Chromas version 2.1 (Technelysium PTY, Ltd).

2.1.5. BIOINFORMATIC ANALYSIS

BioEdit Sequence Alignment Editor © (Version 7.0.5.2) was used to perform all multiple sequence alignments using the Clustal*W* multiple sequence alignment algorithm. The BLASTx algorithm was used to determine the identity of the sequences obtained by aligning it with other protein sequences from the National Centre for Biotechnology Information (NCBI) online database (www.ncbi.nlm.nih.gov/blast). The conserved domains and open reading frame were found using the conserved domain finder and the ORF-finder features on the NCBI website (www.ncbi.nlm.nih.gov). Sequences available on the NCBI database (see Table 3) were used to construct a neighbour joining evolutionary tree with bootstrapping (1000 replicates) using the MEGA software (MEGA version 3.1, Tamura *et al.,* 2007).

Table 3: Sequences used in the construction of a phylogenetic tree

Sequence Name	Accession Number
Haliotis diversicolor supertexta	AY700781
Euprymna scolopes	AY956819.1
Pinctada fucata	EF121959.1
Crassostrea gigas	AY039648.1
Biomphalaria glabrata	FJ711166.1
Tubifex tubifex (Dorsal)	AB192889.1
Bathymodiolus azoricus	DQ673621.1
Venerupis decussatus	DQ673624.1
Mercenaria mercenaria	DQ673622.1
Helobdella stagnalis	AF410863.1
Helobdella robusta	AF410862.1
Aedes aegypti (Dorsal 1-B)	AY748244.1
Litopenaeus vannamei Dorsal	FJ998202.1
Apis mellifera **dorsal protein splice variant B**	AY268031.1
Drosophila simulans **Dorsal**	AY354439.1
Halocynthia roretzi **Rel1**	AB051857.1
Drosophila melanogaster **Dorsal isoform A**	NM 165217.2
Apis mellifera **dorsal protein**	NM 001011577.1
Drosophila melanogaster **relish, transcript variant A**	NP 477094.1
Bombyx mori **relish homologue Bmrelish1**	NP 001095935.1
Carcinoscorpius rotundicauda **Relish**	ABC75034.1
Aedes aegypti **relish R7 isoform**	AAM97896.1
Homo sapiens **nuclear factor of kappa light polypeptide gene enhancer in B-cells 1 (NFKB1), transcript variant 2**	NP_001158884.1

2.2 PHYSIOLOGICAL RESPONSE AND NFKB EXPRESSION OF *V. ANGUILLARUM* 5676 CHALLENGED *H. MIDAE*

2.2.1 CHALLENGE BACTERIA

Vibrio anguillarum 5676 was isolated from infected abalone samples by Dr Anna Mouton (personal communication). *V. anguillarum* 5676 was inoculated onto Tryptone Soy Agar (TSA) with 2.5% (*w/v*) NaCl (appendix A 1.7), and incubated for approximately 16 hours at room temperature. The bacteria were subsequently inoculated into 5 ml Tryptone Soy Broth (TSB) with 2.5% (*w/v*) NaCl (Appendix A.1.2) and cultured for approximately 16 hours at room temperature with shaking. The 5 ml culture was used to inoculate 100 ml TSB-2.5% (*w/v*) NaCl and incubated for approximately 16 hours at room temperature with shaking. The 100 ml culture was heat inactivated by heating the culture to 65°C for 10 minutes in a water bath (Labotec ®). Cells were harvested by centrifugation at 13 000 X *g* for 10 minutes at 4°C. Cells were washed twice with 1 X phosphate buffered saline (PBS, Appendix A 1.4.), and resuspended in 15 ml of sterile sea salts. The concentration of the bacterial suspension was determined by counting the bacteria on a haemocytometer at 1000 X magnification under a microscope (Olympus CX21), using an eight block count. Cells were calculated using the following equation:

cells/ml = [(no. of cells/0.1) / 0.32] x 1000 x dilution factor.

The bacterial suspension was stored at -20°C in 2 ml aliquots at a concentration of 1 X 10^9cells/ml.

Heat killed *V. anguillarum* 5676 was chosen for the challenge trials to elicit an immune response without inducing mortality of *H. midae.*

2.2.2 CHALLENGE TRIALS

Three large polyethylene tanks containing 98 *l* of aerated and continuously flowing (330 *l* h^{-1}) natural seawater at 15 – 18 °C were used in the challenge trials. Seventy two medium sized (6.9 cm ± 3.2) abalone were randomly placed into each of the three tanks; untouched control (24 abalone), the mock infected control (24 abalone) and the infected group (24 abalone). Three challenge trials, serving as biological repeats, were performed, with a total of 216 abalone used. The untouched group served as a control by which the mock infected and infected group could be compared in order to deduce whether there was a response induced in the trial. The mock infected group was included to ensure that the response shown by the infected group was due to the inclusion of the pathogen *V. anguillarum* 5676, and not a general wound response induced by injecting the abalone with sterile sea salts. Animals were fed *Ecklonia maxima* (kelp) twice a week and the tanks were thoroughly cleaned once a week. Abalone were acclimatised for three days prior to the experiment.

After acclimatisation, a 25 X G 5/8″ sterile hypodermic needle (Tae-Chang Industrial Co.) attached to a 1 ml syringe was used to inject 100 µl of heat killed *V. anguillarum* 5676 (1 X 10^9 cells/ml) into the anterior right side of the foot of the abalone in one tank (infected group). The same procedure was used to inject the second group (mock infected) with 100

µl sterile sea salts (Appendix A 1.3). The third group was left unchallenged (the untouched control group). Five hundred to eight hundred microlitres of haemolymph was sampled and pooled from the pedal sinus of six abalone from each group at 0, 6, 12 and 24 hours post infection using a 21G X 1½″ sterile hypodermic needle (Uniqiao, Wupro Tech.) attached to a sterile 2.5 ml syringe. One hundred microlitres of haemolymph was placed into separate 1.5 ml microfuge tubes for subsequent cell counts. The remainder of the haemolymph was aliquoted into 1 ml volumes and haemocytes were collected by centrifugation at 8000 X *g* for 10 minutes. The serum was removed and transferred to a fresh 1.5 ml microfuge tube to be used in the subsequent physiological assays. The concentrated haemocytes were immediately frozen in liquid nitrogen and stored at -80˚C.

2.2.3 TOTAL HAEMOCYTE COUNTS:

One volume of haemolymph from each sample point was added to 2 volumes of Alsevers Solution (Appendix A.2.5). Ten microlitres of the mixture was placed on a haemocytometer (Neubauer Improved Brightline Haemocytometer, Superior) and counted under a light microscope (Olympus CX21) at 40 X magnification. Each sample was counted four times, using an eight block count on the haemocytometer to determine the number of cells per millilitre. Circulating haemocyte concentration was determined using the following equation:

Blood Count (cells/ml) = [(no. of cells/0.1) / A] x 1000 x 3

Where A is 0.32 for an eight block cell count and 0.16 for a four block cell count.

2.2.4 SERUM ANTI-BACTERIAL ACTIVITY

The serum anti-bacterial assay was used to determine the anti-bacterial response of the serum during the time course of the challenge trial and was modified from the method described in Ordas *et al.* (2000). *E. coli* DH5α was inoculated into 5 ml Luria broth (LB) and cultured for approximately 16 hours at 37°C. The OD was measured at 600 nm on a spectrophotometer (Beckman DU530) and the cultures were subsequently diluted to an OD of 0.5 with LB.

Twenty five microlitres of serum was added to 75 µl of *E. coli* DH5α (OD 0.5) in 1.5 ml microfuge tubes and incubated for three hours at 37°C with occasional mixing of the tubes. One hundred microlitres of 1 mg/ml (*w/v*) 3-(4, 5-Dimethylthiazol-2-yl) -2, 5-diphenyl-tetrazolium bromide (MTT, Sigma®) in 1 X PBS (appendix A 2.23) was added to each tube and incubated for 15 minutes at 37°C with mixing every five minutes. One hundred microlitres of dimethyl sulfoxide (DMSO, Merck) was added to stop conversion of MTT to a purple formazan. Distilled water was added to a final volume of 1 ml and the OD of the resultant mixture was measured at 600nm on a spectrophotometer (Beckman DU530). A negative control was included in the assay, 25 µl of LB was added to 75 µl *E. coli* DH5α (OD

0.5) and the same procedure was followed as described above. Reactions were calibrated against 100 µl LB subjected to the same treatment as the samples. The results were recorded as an anti-bacterial index (BI) calculated as follows: OD of experiment/OD negative control. A high BI indicates less anti-bacterial activity.

2.2.5 PHENOLOXIDASE ASSAY

The phenoloxidase assay was adapted from the method by Cheng *et al*. (2004). Briefly, 100 µl of haemolymph was centrifuged in a 1.5 ml microfuge tube at 1600 X *g* for 5 minutes at 4°C and the supernatant removed into a separate microfuge tube. One hundred microlitres of 0.5 mg/ml sodium alginate (appendix A 2.2) was added and incubated for 30 minutes at 26°C. Fifty microlitres of 3 mg/ml L-β-3, 4 Dihydoxy-phenylalanine (L-DOPA, Sigma®) in1 X PBS (appendix A 2.1) was added and incubated for 15 minutes at 26°C. The OD was determined at 490 nm to deduce melanin formation on a spectrophotometer (NanoDrop® ND-1000 Spectrophotometer, NanoDrop 1000 software version 3.7.1). The blank for the experiment contained one hundred microlitres 0.5 mg/ml sodium alginate and fifty microlitres 3 mg/ml in L-DOPA in 1 X PBS, which experienced the same conditions as the experimental samples. The supernatant followed the same protocol as mentioned above.

2.2.6 PHAGOCYTOSIS ASSAY

2.2.6.1 PREPARATION OF LABELLED BACTERIA FOR PHAGOCYTOSIS ASSAY

Vibrio anguillarum 1989 was fluorescently labelled according to Mortensen and Glette (1996). *V. anguillarum* 1989 was incubated for approximately 16 hours on TSA with 2.5% (*w/v*) NaCl at room temperature. Single colonies were inoculated into 5 ml TSB, 2.5% (*w/v*) NaCl and incubated for approximately 16 hours at room temperature with shaking, and subsequently used to inoculate 100 ml TSB, 2.5% (*w/v*) NaCl which was incubated for approximately 16 hours at room temperature with shaking. After the addition of formaldehyde to a final concentration of 8% (*v/v*), the culture was incubated at room temperature for 30 minutes with shaking to kill the bacteria. The formaldehyde treated cells were harvested by centrifugation at 13 000 X *g* for 10 minutes at 4°C. The cells were washed twice with 1 X PBS and resuspended in 0.1 M $NaHCO_3$ pH 9 (Appendix A 2.6.1) containing 0.1 mg/ml fluorescin 5-isothiocyanate (FITC) Isomer 1 (Sigma ®) (Appendix A 2.6.2). Cells were incubated in the dark with shaking at 25°C for approximately 16 hours, centrifuged at 13 000 X *g* for 10 minutes at 4°C and resuspended in 10 ml 1 X PBS. The concentration of bacteria was determined using a 4 block cell count on a haemocytometer and calculated as follows:

cells/ml = [(no. of cells/0.1) / 0.16] x 1000 x dilution factor

2.2.6.2 ASSAY

Haemolymph at a concentration of 1 X 10^6 cells/ml was placed onto acid-washed glass slides within a ring of silicon ($1cm^2$) for 30 minutes in a dark, moist chamber and allowed to adhere to the glass surface. The haemocytes were washed once with ice cold modified Hanks buffered saline solution (MHBSS, Appendix A 2.7) and 100 µl of FITC isomer 1-labelled *Vibrio anguillarum* 1989 (1 X 10^8 cells/ml) was added to the slide. The slide was incubated for a further 20 minutes after which they were washed once with ice cold MHBSS. One hundred and fifty microlitres of methanol was added to fix the cells to the slide. The methanol was removed by washing with ice cold MHBSS. One hundred microlitres of ethidium bromide (100µg/ml, Appendix A 2.8) was added to the slides and incubated for one minute. Excess ethidium bromide was removed by washing with ice cold MHBSS. Glass cover slips were placed over the silicon rings and the number of phagocytic haemocytes was determined using an inverse fluorescent microscope (Nikon Inverted Microscope DIAPHOT-TMD containing a Nikon EPI-Fluorescent attachment TMD-EF) at 400 X magnification using a 510 nm excitation filter. Images were captured using an AxioCam (Zeiss) camera with its corresponding software AxioVision AC version 4.4. Haemocytes that contained more than three FITC-labelled *V. anguillarum* 1989 were considered as phagocytic cells. The percentage of phagocytosing haemocytes was determined from a total of 200 haemocytes and calculated as follows:

% phagocytosis = (phagocytosing haemocytes/total haemocytes counted) X 100

Each sample was assayed in duplicate and each duplicate was counted twice.

2.2.7 REAL TIME QUANTITATIVE PCR

Real time quantitative PCR (qPCR) primers were designed using Beacon designer design software and FastPCR, with primers designed to the 3' end of the NFκB gene product previously isolated (Table 2, RTR1 and RTF1) with a product length of 132 bp. The reference gene, ribosomal factor L28, was selected from a microarray of *H. midae* haemocytes (Bronwyn Arendze, unpublished data) and primers were designed (Table 2, 818F and 818R) with a product length of 134 bp. Primer pairs for both the gene of interest and the reference gene were optimised for use in amplification reactions containing 3 mM magnesium chloride at an annealing temperature of 60°C. Oligo dT Sybr green Sensi mix kit (Quantace) was used for real time quantitative PCR (qPCR) analysis to determine the mRNA levels of the NFκB gene with respect to infection. The reactions were performed according to the manufacturer's instructions using quarter reaction volumes of 12.5 µl per sample in 0.1 ml Strip tubes (Qiagen). Primer concentrations were used at a final concentration of 200 µM per primer, with 1 µl cDNA added to each reaction. For each biological repeat, a 10 fold dilution series of pooled cDNA consisting of every sample from all treatment groups was utilised as template in the construction of a standard curve for each gene. All time points and standard curve points were performed in triplicate reactions for technical efficiency. The qPCR was performed using a Rotor-Gene™ 6000 (Corbett Research), and analysed with the respective software (Rotor-Gene™ Series Software version 1.7) See Appendix D 1.1, 1.2 and 2.1 for RNA quality, genomic DNA contamination assessment and qPCR data for the *in vivo* trial. The qPCR profile was set up as follows: initial denaturation of 94°C for 5 minutes, followed by 45 cycles of 94°C for 10 seconds,

60°C for 15 seconds and 72°C for 20 seconds, with a final extension period of 5 minutes at 72°C.

The Pfaffl method (Pfaffl, 2001) was used to calculate the fold change expression values of the qPCR data for each biological repeat, taking into account the efficiencies of the reactions. Time 0 was used as the calibration point in each treatment group in all biological repeats.

The equation used was as follows:

$$Fold\ change\ expression\ =\ Efficiency_{GOI}^{(Calibrator-sample)} \div\ Efficiency_{RG}^{(Calibrator-sample)}$$

where GOI is the gene of interest and RG is the reference gene.

2.3 HAEMOCYTE TISSUE CULTURE

Haemolymph was isolated from *H. midae* via the pedal sinus using a 21G X 1½″ sterile hypodermic needle (Uniqiao, Wupro Tech.) attached to a sterile 2.5 ml syringe, and stored on ice. Once the concentration of haemocytes was determined per millilitre of haemolymph using a haemocytometer, specific concentrations were seeded onto 35 X 10 mm tissue culture dishes (Nunclon™ Delta Surface, Nunc™) and the haemocytes allowed to adhere for 30 minutes in a dark, moist chamber under a laminar flow hood (Labotec®). The excess haemolymph was removed and the haemocytes were washed once with MHBSS to remove

haemocytes that had not adhered as well as other possible contaminants. One millilitre of 1 x Hanks M-199 media (Gibco, Appendix A 4.2 and A 4.4) modified with the addition of a supplementary salt solution (Suja and Dharmaraj, 2005, Appendix A 4.1), 100 µg/ml Streptomycin G (Invitrogen), 100 U/ml Penicillin G (Invitrogen) and 10 µg/ml Amphotericin B (Sigma ®) was added to each culture dish, and the cultures subsequently incubated in a dark moist chamber at 19°C. Media was replaced every second day.

2.3.1 VIABILITY

2.3.1.1. TRYPAN BLUE ASSAY

Haemocytes were removed from the tissue culture plates by sloughing the surface of the plates with a cell scraper and suspended in 100 µl of 1 X PBS. One volume of 0.2% (*w/v*) Trypan blue (Appendix A 2.4.3.1) was added to the haemocyte suspension and allowed to react for 5 minutes. Haemocytes were viewed under a light microscope at 100 X magnification (Olympus CX21) and the number of transparent cells (live) and blue cells (dead) were counted. Viable cells were calculated as follows: % Viable Cells = (Viable cells/total cells) X 100.

2.3.1.2 PHAGOCYTOSIS ASSAY

Phagocytosis assays were performed in the culture dishes. Haemocytes were seeded at a concentration of 1 X 10^6 cells/ml. The assay was performed as described in section 2.2.6 with the exception of the first 30 minute incubation step which was omitted as the cells were already adhered to the surface of the culture dish.

2.3.2. HAEMOCYTE STAINING

Haemocytes were seeded onto acid washed 75 X 25 mm glass slides at a concentration of 1 X 10^6 cells per slide and allowed to adhere for 30 minutes in a dark moist chamber at room temperature. The following staining techniques were used once haemocytes were adhered to glass slides.

2.3.2.1. GIEMSA DYE

Giemsa aqueous solution (10 % (*v/v)* in 1 X PBS, Gurr) was added to the haemocytes and incubated for 10 minutes at room temperature. Giemsa stains nuclei blue and cytoplasm light blue. The images were captured with a Nikon DS Camera Control Unit DS-U2 and DS-5M Camera head Nikon on a Eclipse 50i Compound Microscope at 1000 X magnification with its' respective software NIS Elements Documentation and Digital 3D Imaging.

2.3.2.2. NEUTRAL RED DYE

Neutral Red (8 mg/l in 1X PBS, Sigma) was added to the haemocytes and incubated for 30 minutes. The images were captured with a Nikon DS Camera Control Unit DS-U2 and DS-5M Camera head Nikon on a Eclipse 50i Compound Microscope at 1000 X magnification with its' respective software NIS Elements Documentation and Digital 3D Imaging. The dye specifically stains lysosomes orange.

2.3.2.3. ACRIDINE ORANGE STAINING

Acridine Orange (0.1 mg/ml in 1 X PBS, Sigma) was added to the haemocytes and allowed to incubate for 90 seconds at room temperature. Slides were washed with MHBSS and visualised under a fluorescence microscope (Nikon Inverted Microscope DIAPHOT-TMD containing a Nikon EPI-Fluorescent attachment TMD-EF) at 400 X and 1000 X (oil) magnification using a 510 nm filter. Images were captured using an AxioCam (Zeiss) camera with its corresponding software AxioVision AC version 4.4. The red dye confers fluorescence on acid cell components.

2.3.3 *IN VITRO* CHALLENGE TRIAL

Phenoloxidase activity, phagocytic activity, total haemocyte counts and NFκB expression were evaluated in an *in vitro* challenge trial. Monolayers of haemocytes were seeded at a concentration of 1 X 10^6 cells/ml as described in section 2.3. The media containing antibiotics was removed from the monolayers and the monolayers were washed with ice cold MHBSS to remove excess media. Media containing antibiotics was removed from the cultures and replaced with media containing no antibiotics. Haemocytes were incubated overnight at 19°C in a dark, moist chamber. One hundred microlitres of 1 X PBS was added to half the cultured haemocytes (control group) and 100 µl of 1 X 10^8 cell/ml heat killed FITC isomer 1 labelled *V. anguillarum* 5676 was added to the remaining haemocyte cultures (infected group). All procedures were performed under the laminar flow hood in order to eliminate other possible contaminants due to the lack of antibiotics in the media. Each group was assayed at 0, 1, 2, 3 and 6 hours post infection. Three biological repeats were performed for the *in vitro* challenge trial.

For the phenoloxidase assay, smaller volumes were used to accommodate the decreased concentration of starting haemocytes. Briefly, 25 µl of serum (media from culture dishes) and 25 µl of cells collected by scraping from monolayers in 100 µl 1 X PBS was centrifuged at 5 000 X *g* for 5 minutes at 4°C. The assays were performed in triplicate and the same procedure was followed as described in section 2.2.5. The scraping of cells from the monolayers did not affect cell morphology or activity.

The phagocytosis assay was performed in duplicate as described in section 2.3.1.2 with heat-killed FITC labelled *V. anguillarum* 5676. The serum anti-bacterial assay was performed as described in section 2.2.3.

Total haemocyte numbers and the percentage of viable cells were calculated in triplicate using the trypan blue assay. One hundred microlitres of haemocytes isolated from monolayers was added to 200 µl 0.2% (*w/v*) trypan blue and left to incubate for 5 minutes. Ten microlitres of the solution was added to a haemocytometer and the cells were counted (Neubauer Improved Brightline Haemocytometer, Superior) under a microscope (Olympus CX21) at 100 X magnification. Each count was repeated 4 times. The percentage of viable cells was calculated using the following equation:

% Viability = (Viable cells/ml / Total cells/ml) x 100

2.3.3.1 RNA ISOLATION AND CDNA CONVERSION

RNA was isolated from three pooled samples of *in vitro* haemocytes for each treatment group at each time point and converted to cDNA using the Cells-to-cDNA kit (Ambion), in a one step process according to the manufacturer's instruction. Briefly, 100 µl 1 X PBS was added to 2 culture dishes containing 1 X 10^6 cells. Cells were removed from the surfaces

and the resultant suspensions pooled, vortexed and centrifuged briefly. One hundred microlitres of the pooled suspension was removed and centrifuged for 10 minutes at 4°C at 2500 X *g*. Cells were resuspended in 100 µl of the Lysis buffer II (Ambion) and allowed to incubate for 10 minutes at 75°C. The RNA sample was subsequently cooled on ice for 1 minute before the addition of DNase I (10 U/µl), and incubation for 15 minutes at 37°C. The RNA sample was subsequently used in the cDNA conversion reaction included in the cells-to-cDNA kit. Oligo dT was used in subsequent conversion reactions in order to prevent reverse transcription of bacterial RNA (*V. anguillarum* 5676). Cell counts ensured that equal numbers of cells were used in each reaction for all biological repeats. The presence of genomic DNA contamination was determined by amplification of the 18s rRNA gene (Appendix B 3.1 and B 3.2.3, Appendix D 1.3).

2.3.3.2 QUANTITATIVE REAL TIME PCR

The qPCR reactions were performed as previously described in section 2.2.7. The qPCR was performed using a Rotor-Gene™ 6000 (Corbett Research) and analysed with the respective software (Rotor-Gene™ Series Software version 1.7) (See Appendix D 2.2). The standard curve for each gene and biological repeat was comprised of plasmid DNA containing either the NFκB insert (PTZ57R/T, Fermentas) at a starting concentration of 0.01 ng/µl or the Ribosomal Factor L28 insert (pDNR-Lib, Clonetech-SMART cDNA Library construction kit Appendix C, Bronwyn Arendze) with a starting concentration of 0.1 ng/µl. The qPCR profile was set up as follows: 94°C for 5 minutes, followed by 45 cycles of 94°C for 10 seconds,

60°C for 15 seconds and 72°C for 20 seconds, with a final extension period of 5 minutes at 72°C. The Pfaffl method (Pfaffl, 2001) was used to analyse the qPCR data for biological repeats as in the *in vivo* challenge trial analysis (Section 2.2.7).

2.4 STATISTICAL ANALYSIS

All statistical analysis was performed using SigmaStat version 3.1 (Systat Software™ Inc. GmbH, 2004). A two way ANOVA was performed for the *in vitro* and *in vivo* physiological assays with an Ad hoc Tukey test performed on each data set. For count data such as phagocytosis, trypan blue viability and cell number, data was transformed by square rooting the values for more sensitive statistical analyses. A two-way ANOVA on ranks was performed on transformed (log_{10}) qPCR data from the *in vitro* challenge trial, with the addition of an Ad hoc Tukey test. $P<0.05$ was used in all statistical analyses to determine significance.

A one-way ANOVA was used to determine statistical significance of data that contained a single variable. Microsoft Excel (Microsoft Office 2003, Microsoft Corporation) was used to determine the descriptive statistics (mean, standard deviation and standard error) for all data acquired.

CHAPTER 3

RESULTS

CONTENTS

3.1 NFκB gene sequence 55

3.2 *In vivo* challenge trial 63

3.2.1. Physiological tests 64

3.2.2. Quantitative real time PCR 69

3.3 Haemocytes 71

3.3.1. Viability 71

3.3.2. Haemocyte staining 76

3.4 *In vitro* challenge trial 80

3.4.1 Physiological tests 80

3.4.2 Quantitative real time PCR 85

3.1 NFKB GENE SEQUENCE

In order to determine the eligibility of NFκB as a suitable biomarker, the homologue first needed to be amplified and characterised from *H. midae.* Primers *Nf* and *Nr* described in Jiang and Wu (2007) specific to the 3' end of Ab-rel in the abalone *Haliotis diversicolor supertexta* were used in a PCR amplification, yielding a single band of the expected size of 280 bp (Figure 5, lanes 2, 3, 4 and 5). The product was cloned and three positive clones were sequenced, the concensus sequence aligned (Figure 6 A and B) and subsequently identified as an NFκB homologue. The concensus sequence aligned only to the *H. diversicolor supertexta* Ab-rel sequence (AY700781) upon BLASTx analysis (NCBI) with an e value of 1e-15. The sequence aligned to the 3' end of the *H. diversicolor supertexta* ab-rel sequence (Figure 7).

Since 5' RACE, attempted to obtain additional sequence information regarding the *H. midae* NFκB homologue, was unsuccessful, a nested PCR strategy was developed. The amplification strategy and products isolated are described in Figure 4. Degenerate primers (Drelf and Drelr) were designed to the rel homology domain using aligned protein sequences from class II invertebrate NFκB homologues. However, the degenerate primers were unsuccessful in amplifying a product from *H. midae* cDNA (Figure 8, lane 4). The next strategy was to use gene specific primers (GSRf and GSRr) designed to the rel homology domain of *H. diversicolor supertexta* (AY700781)*;* however this was also unsuccessful (Figure 8, lane 1 and 2). Lastly, nested PCR was attempted utilising both degenerate and

gene specific primers to the rel homology domain to amplify genomic DNA and cDNA templates from *H. midae* (Figure 8). Amplification of genomic DNA with either the specific (Figure 8, lane 1) or degenerate (Figure 8, lane 3) primers yielded an array of products; however nested PCR on genomic DNA yielded no products. The predominant 400 bp product obtained using the degenerate primers was sequenced and found to have no sequence homology to any sequences available in the NCBI database. cDNA yielded no discernable products upon amplification with either degenerate or specific primers (lane 2 and 4) but yielded an expected 250 bp product upon nested PCR amplification with both primer sets (lane 5). The product was sequenced (Figure 9 A) and subsequently identified as an NFκB homologue when performing a BLASTx search of the NCBI database. It was found that the sequence contained the conserved rel homology domain (RHD) (Figure 9 B). The RHD sequence was found to be most similar to *H. diversicolor supertexta* and shared sequence similarity with other marine invertebrate species (Table 4).

A phylogenetic tree (Figure 10) was constructed to determine the relationship between the NFκB rel homology domain (RHD) sequence from *H. midae* and NFκB RHDs from other species. It was found that the *H. midae* NFκB RHD clustered with other class II homologues. *H. midae* and *H. diversicolor supertexta* clustered together with a very strong bootstrap value of 100%, indicating a strong evolutionary relationship between the NFκB RHDs from these abalone. Interestingly the *H. midae* and *H. diversicolor supertexta* NFκB RHDs did not group with the snail, *B. glabrata*, the only other gastropod in the evolutionary tree. Instead *B. glabrata* grouped with bivalve species (*B. azoricus, M. mercenaria*, *V. decussates, P. fucata*

and *C. gigas*) and annelids (*H. stagnalis* and *H. robusta)*. The squid *E. scolopes* and *H. rorezti* (a sponge) NFκB homologues formed independent branches within the class II NFκB sub-tree.

Primers (RfillF and RfillR) were designed to both the 5' and the 3' end of the *H. midae* NFκB gene sequence (Figure 3) to obtain sequence data spanning the gap between the two sequenced portions of the *H. midae* NFκB gene. Amplification of this portion of the *H. midae* NFκB gene was not successful, and consequently, it remains unclear whether the two sequenced portions of the *H. midae* NFκB are two different classes of NFκB or the ends of the same homologue. All data obtained from the NFκB expression studies were obtained using primers designed to the 3' end of the *H. midae* NFκB.

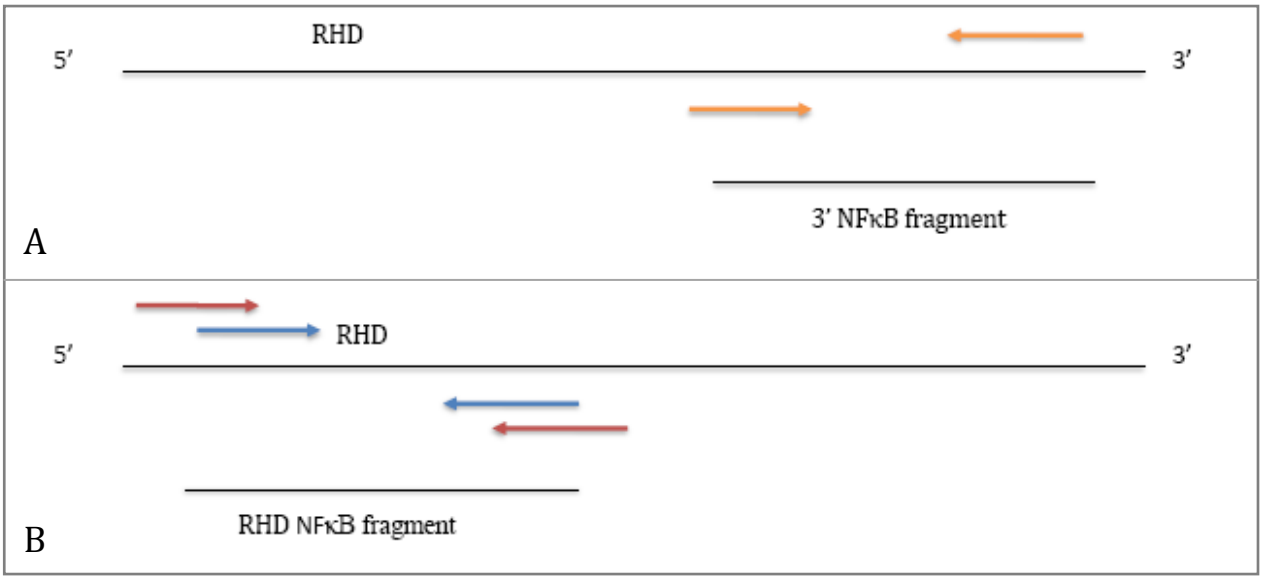

Figure 4: NFκB amplification strategy. (A) Represents the 3' NFκB fragment amplified using the gene specific primers described in Jiang and Wu (2007). (B) Represents the RHD fragment isolated using gene specific primers designed to the rel homology domain of *H. diversicolor supertexta* (red) and degenerate primers designed to the rel homology domain from several invertebrate class II NFκB homologues (blue arrows).

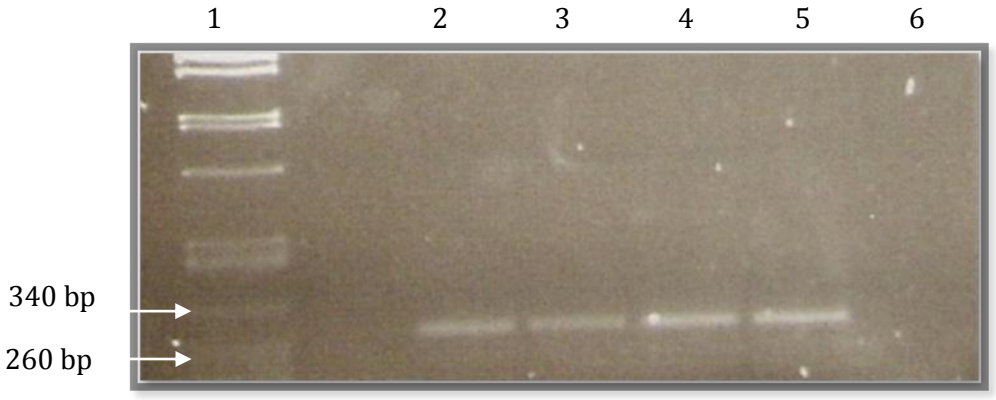

Figure 5: PCR amplification of the Rel homolog in *H. midae*. Lane 1: lambda *Pst*I molecular weight marker White arrows indicate marker sizes. Lanes 2, 3, 4 and 5 are 280bp products amplified from cDNA using primers N*f* and N*r*. Lane 6: no template control

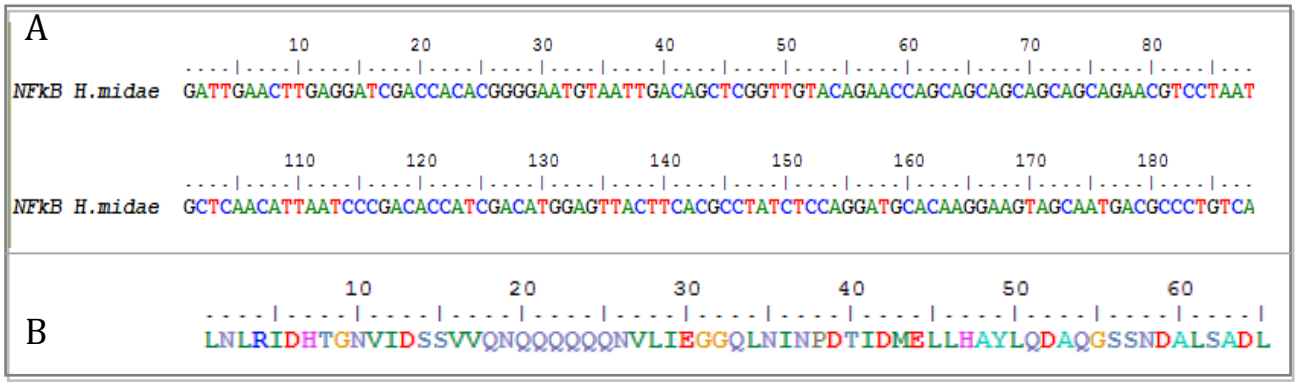

Figure 6: 3' end of the *H. midae* (A) 198 bp edited NFκB nucleotide sequence and (B) the corresponding protein sequence (B).

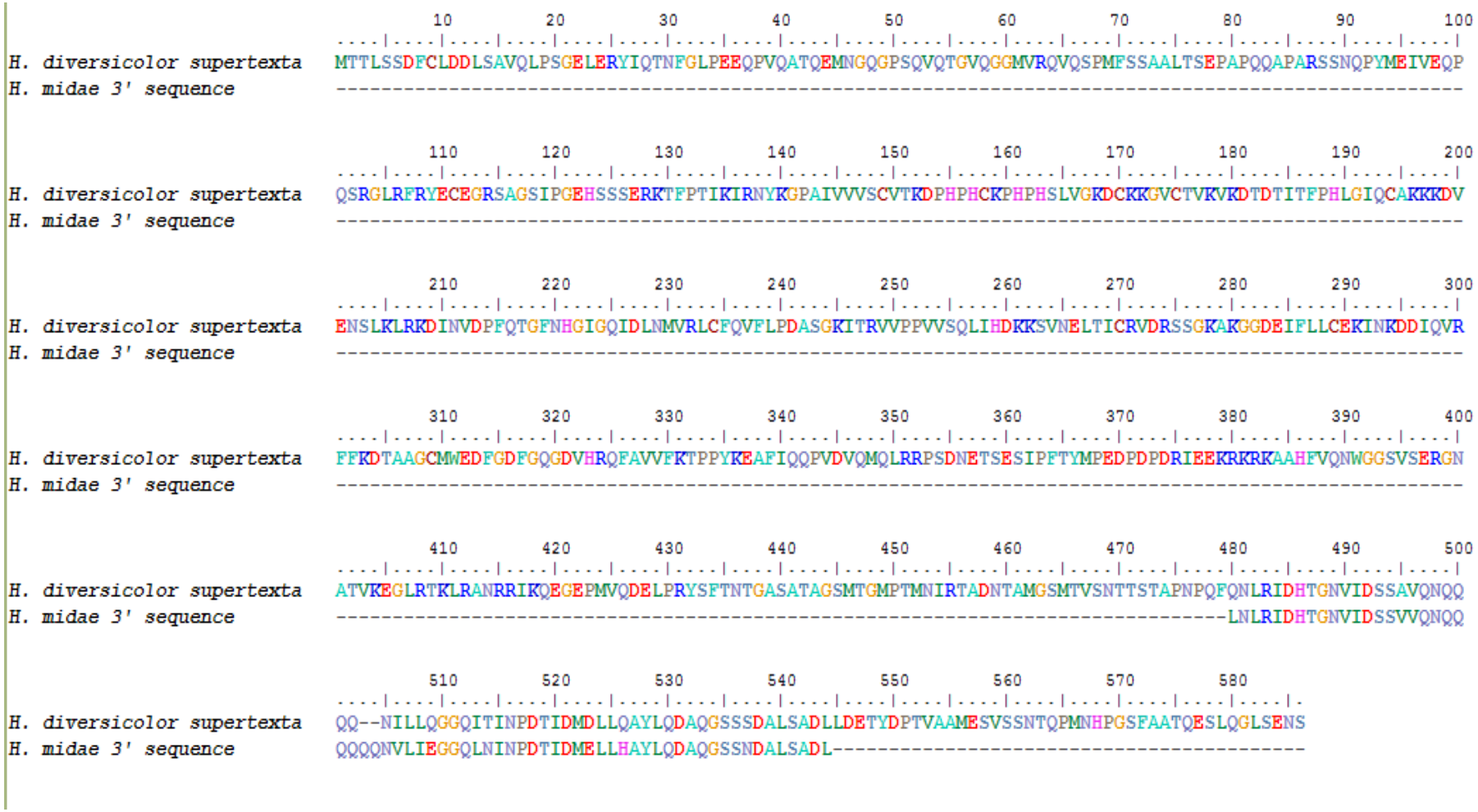

Figure 7: Protein sequence alignment of *H. midae* 3' NFκB sequence with the full length NFκB sequence of *H. diversicolor supertexta* (AY700781).

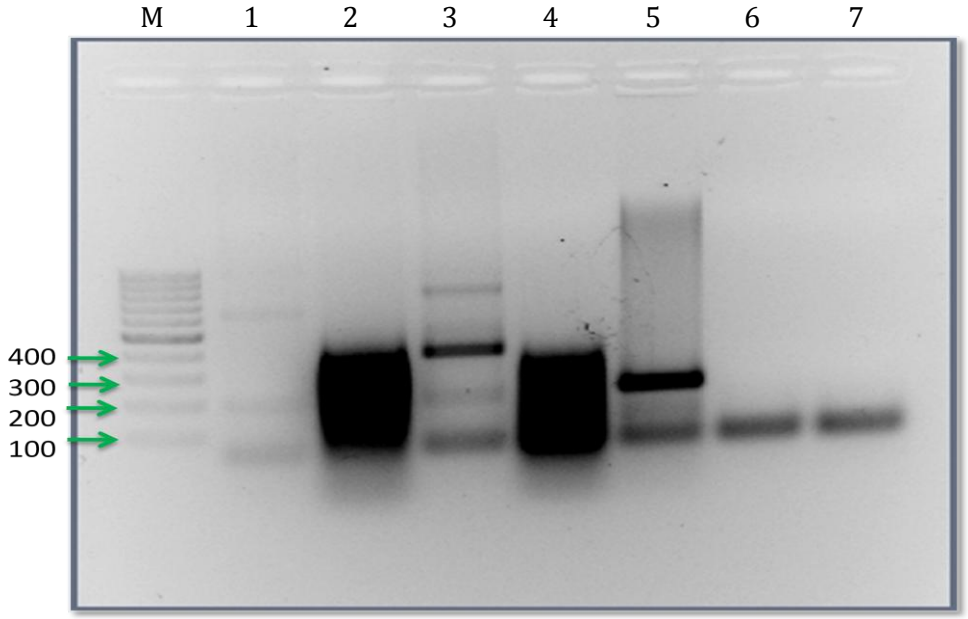

Figure 8: A 1.2% agarose gel indicating PCR products obtained utilising nested PCR with specific and degenerate primers on both cDNA and genomic DNA. M: Fermentas 100 bp plus Ladder with marker sizes in base pairs (green arrows). Lane 1: genomic DNA with specific primers only, Lane 2: cDNA with specific primers only, Lane 3 genomic DNA with degenerate primers only, Lane 4: cDNA with degenerate primers only, Lane 5: Nested PCR amplification with specific and degenerate primer sets using cDNA as template, Lane 6: Nested PCR amplification with specific and degenerate primer sets using genomic DNA as template Lane 7: No template control for nested PCR reaction

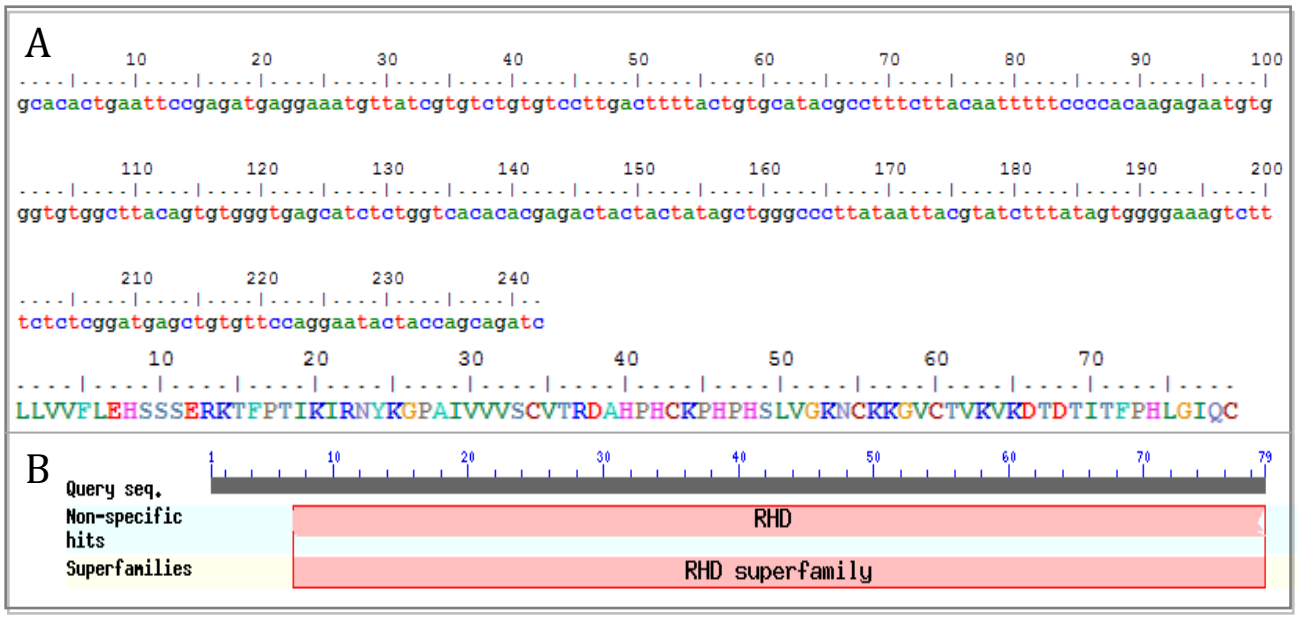

Figure 9: *H. midae* RHD sequence (A) is the consensus nucleotide sequence (from 3 clonal sequences) of NFκB *H. midae* (242 bp) and the deduced protein sequence (B) suggests that the nucleotide sequence encodes part of the rel homology domain (BLASTx).

Table 4: Top ten alignments to NFκB *H. midae* RHD sequence from BLASTx

Accession number	Protein Name	Species Name	Score (bits)	E value
AY700781	Transcription factor NFκB	*Haliotis diversicolor supertexta*	129	$1e^{-28}$
ABL63469.1	NFκB	*Pinctada fuctata*	118	$3e^{-25}$
AAK72691.1	Transcription factor Rel 2	*Crassostrea gigas*	115	$2e^{-14}$
AAK72690.1	Transcription factor Rel 1	*Crassostrea gigas*	115	$2e^{-14}$
ACN73461.1	NFκB	*Biomphalaria glabrata*	110	$4e^{-23}$
AAY27981.1	REL/NFκB	*Euprymna scolopes*	109	$7e^{-23}$
ABG73423.1	RHD protein	*Mytilus galloprovincialis*	104	$3e^{-21}$
ABG73422.1	RHD protein	*Mercenaria mercenaria*	103	$4e^{-21}$
ABG73424.1	RHD protein	*Venerupis (Ruditapes) decussates*	103	$4e^{-21}$
ABG73421.1	RHD protein	*Bathymodiolus azoricus*	103	$4e^{-21}$

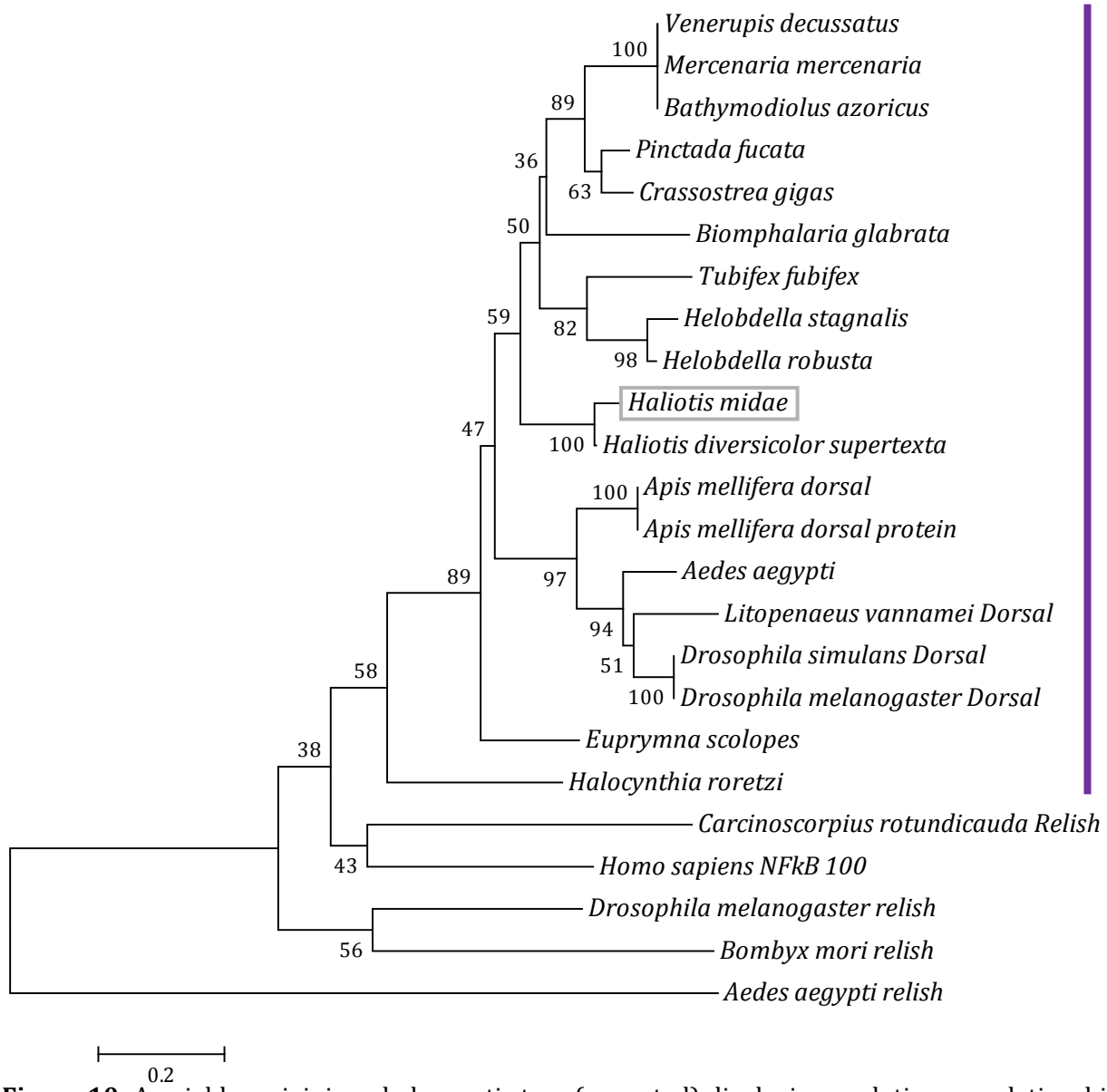

Figure 10: A neighbour joining phylogenetic tree (unrooted) displaying evolutionary relationships between the *H. midae* NFκB RHD sequence (□) and NFκB sequences from invertebrate and vertebrate species. The percentage of replicate trees in which the associated taxa clustered together in the bootstrap test (1000 replicates) is shown next to the branches of the tree. Two distinct groupings can be seen in the phylogenetic tree, the purple line indicates the first group consisting of class II NFκB homologues. This group is comprised of sequences from mussels (*B. azoricus* DQ673621.1, *M. mercenaria* DQ673622.1 and *V. decussates* DQ673624.1), oysters (*P. fucata* EF121959.1 and *C. gigas* AY039648.1), a snail (*B. glabrata* FJ711166.1), a worm (*T. tubifex* AB192889.1), leeches (*H. stagnalis* AF410863.1 *and H. robusta* AF410862.1), abalone (*H. diversicolor supertexta* AY700781 and *H. midae*), the honey bee (*A. mellifera* AY268031.1), mosquito (*A. aegypti* AY748244.1), white shrimp (*L. vannamei* FJ998202.1), fruit fly (*D. melanogaster* NM 165217.2), squid (*E. scolopes* AY956819.1) and a sponge (*H. rorezti* AB051857.1). The second group (green line) consists of class I NFκB homologues. This group contains sequences from the horseshoe crab (*C. rotundicauda* ABC75034.1), humans (*H. sapiens* NP_001158884.1), the fruit fly (*D. melanogaster* NP 477094.1), the silk worm (*B. mori* NP 001095935.1) and the mosquito (*A. egypti* AAM97896.1).

3.2 *IN VIVO* CHALLENGE TRIAL

H. midae were separated into three groups for the challenge trial. The first group consisted of abalone that had been injected with a heat killed pathogen, *V. anguillarum* 5676*.* The second group contained abalone that had been injected with sea salts and served as a mock infected control. The third group contained abalone that remained untouched for the duration of the challenge trial. These controls were included to ensure that the biological changes were in response to the infection and not due to natural biological variation (unchallenged) or due to a wound response (mock infected control).

The immune parameter assays were utilised to determine whether certain physiological responses occurred in response to a heat killed bacterial challenge. Immune factors assayed included phagocytosis, phenoloxidase production and the concentration of the total haemocyte population in the circulating haemolymph of *H. midae.*

Quantitative real time PCR was utilised to determine the extent of NFκB regulation in response to a bacterial challenge. This would provide insight into whether NFκB is a good candidate gene as a biomarker of stress in farmed *H. midae*.

The total haemocyte count was significantly lower in abalone infected with heat killed *V. anguillarum* 5676 (infected) at 12 hours post infection (hpi) (2.8 X 10^6 cells/ml) compared to abalone that had not been challenged (untouched) (6.5 X 10^6 cells/ml) at the same time point (Figure 11). Overall, the total haemocyte counts in abalone infected with heat killed *V. anguillarum* 5676 were significantly different to that of the untouched group ($p<0.05$). Although no statistical significance was established, a trend observed at time points 6, 12 and 24 hpi, where abalone infected with heat killed *V. anguillarum* 5676 had less circulating haemocytes per millilitre than mock infected abalone, which had less circulating haemocytes per millilitre than the untouched control group of abalone. The concentration of circulating haemocytes in the infected group decreased at 6 hpi (3.8 X 10^6 cells/ml) and 12 hpi (2.8 X 10^6 cells/ml) compared to time zero (5.1 X 10^6 cells/ml) and increased back to basal levels at 24 hpi (5.6 X 10^6 cells/ml). No significant changes in haemocyte concentrations were observed in abalone injected with sea salts (mock infected) or the untouched control group of abalone. Interestingly, an increase in haemocyte concentration at 24 hpi was observed in all treatment groups compared to the other time points. The data suggest that the number of circulating haemocytes is affected by exposure to heat killed *V. anguillarum* 5676.

No detectable changes in anti-bacterial activity (BI) were observed between treatment groups or across time within treatment groups (Figure 12). It is interesting to note that

there was no change in BI in abalone infected with heat killed *V. anguillarum* 5676 compared to the control groups (unchallenged and mock infected abalone).

Phenoloxidase activity was detected in both the cell-free haemolymph and the haemocytes. No observable differences in dopachrome formation were evident across time in the cell-free haemolymph (Figure 13 A). Although there was an increase in activity at 12 hpi, it was not significant ($p>0.05$). The data was affected by one biological repeat, in which high readings were detected for all three treatment groups at 12 hpi; as such, the reliability of the data at this time point is uncertain. The cell-free haemolymph phenoloxidase activity (Figure 13 B) was greater compared to the cellular component, suggesting that phenoloxidase activity was greater extracellulary than intracellularly.

No significant differences were observed in the phagocytic activity of haemocytes sampled at each time point and from each treatment group (Figure 14). There was a minimal decrease in phagocytic activity at 6 hpi for all treatment groups, after which phagocytic activity stabilised. The phagocytic ability of haemocytes isolated from abalone infected with heat killed *V. anguillarum* 5676 decreased at 6 hpi (19%) and 12 hpi (17%) compared to 0 hpi (29%) and returned to near basal levels at 24 hpi (22%). The mock infected and the untouched control groups displayed similar trends.

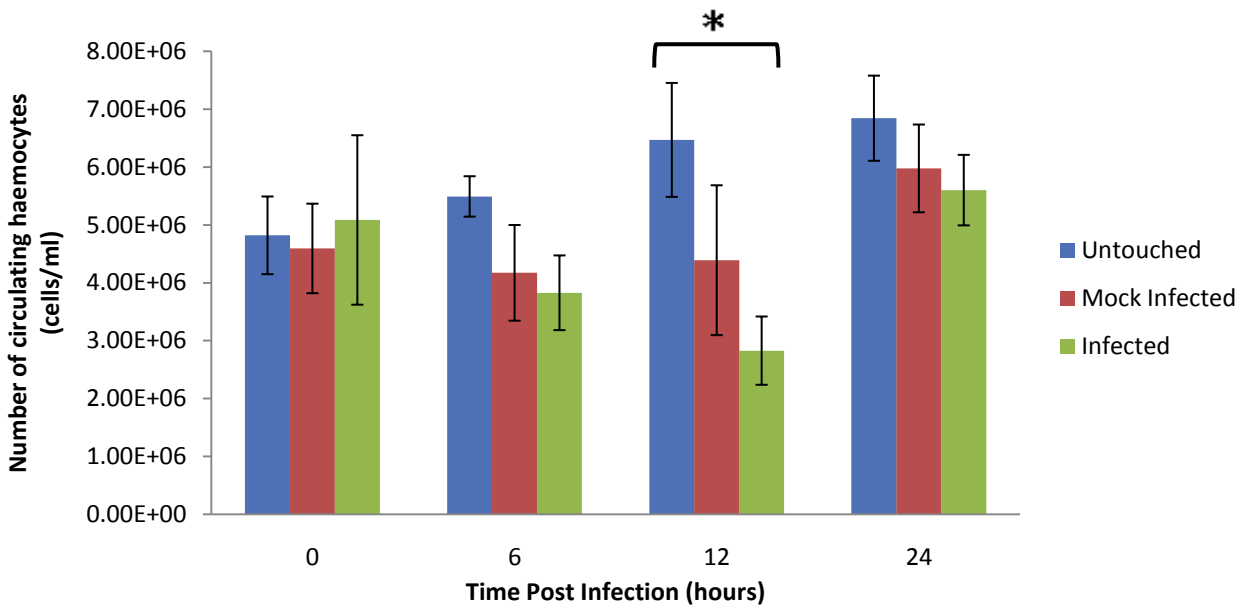

Figure 11: Total haemocyte counts. Bars represent total number of haemocytes/ml of haemolymph. Error bars represent the standard error of the means for three biological repeats. A two way ANOVA was performed with the addition of a Tukey test to compare data between groups. The asterisk (*) indicates significant difference ($p<0.05$) compared to the untouched control group. The haemocyte count of the infected group was significantly different overall to the untouched group but not to the mock infected group.

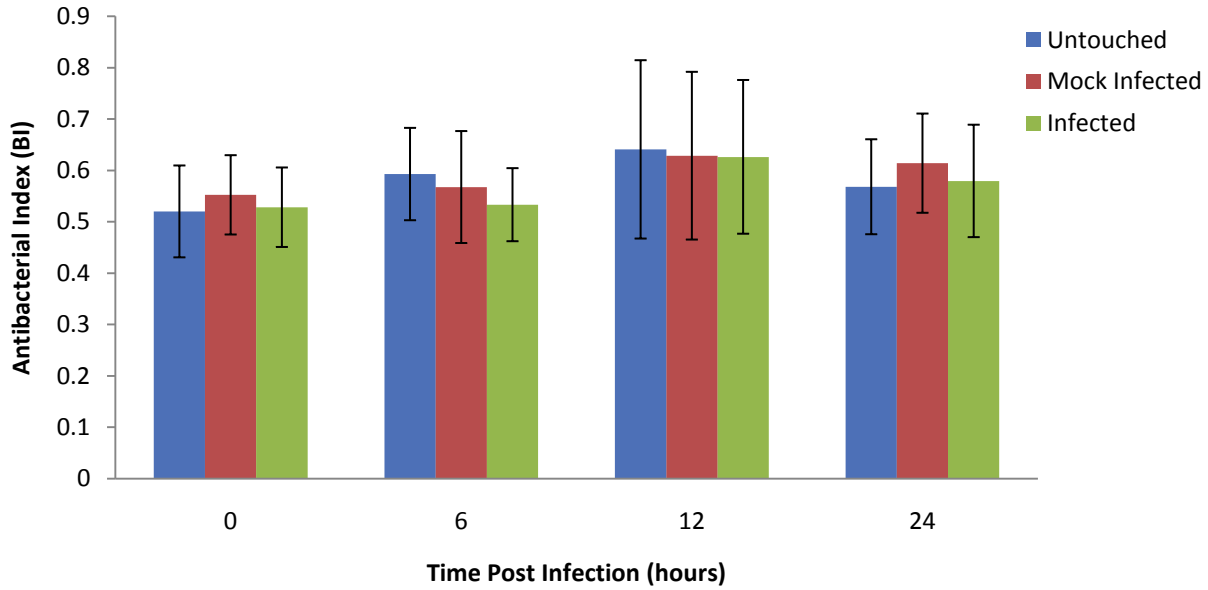

Figure 12: Serum-antibacterial activity in the cell-free haemolymph extracted from the untouched, mock infected and control groups. Bars represent the mean anti-bacterial index of the serum. Error bars represent standard error of the means calculated from 3 biological repeats.

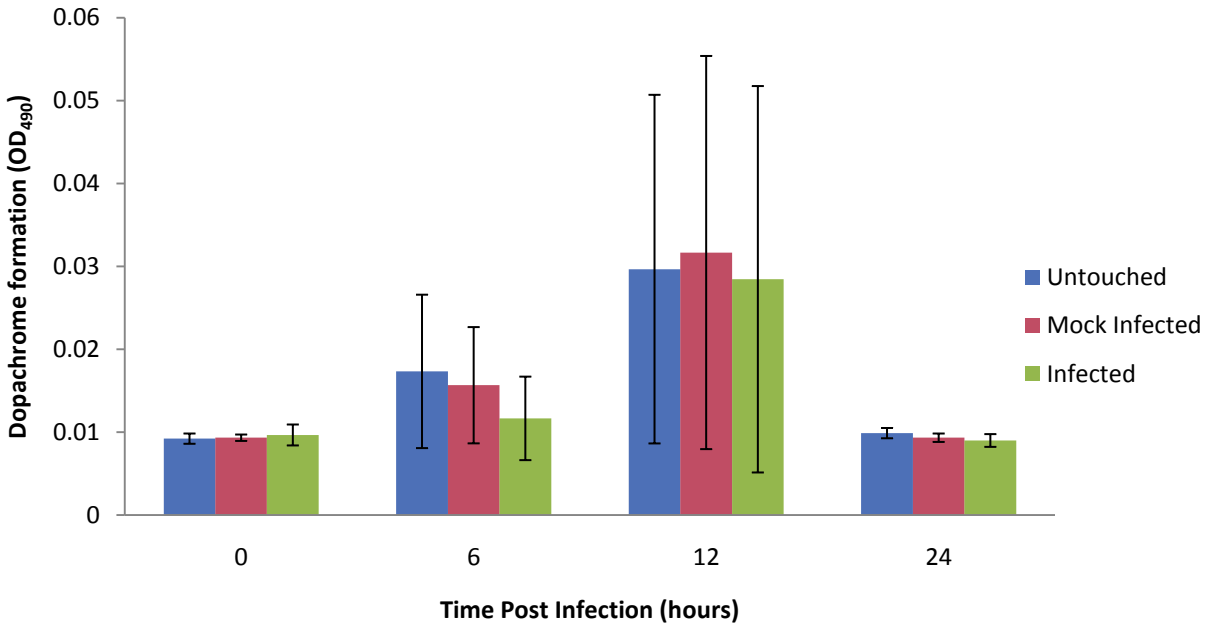

A

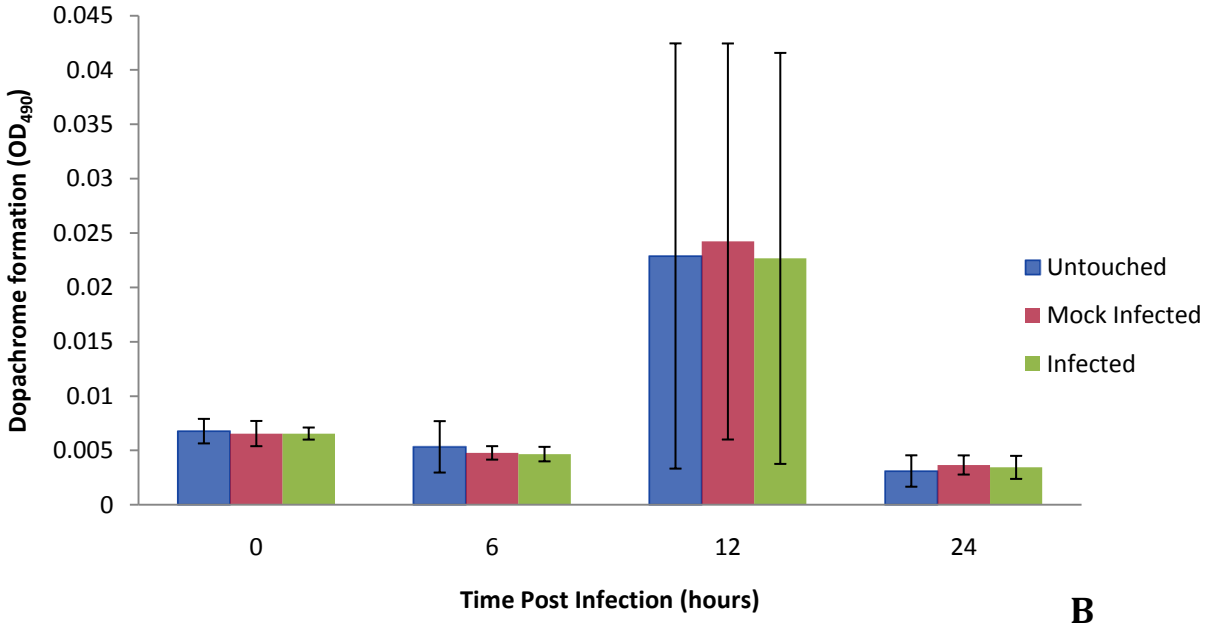

B

Figure 13: Phenoloxidase activity from both the cell-free haemolymph (serum) and the haemocytes isolated from untouched, mock infected and infected *H. midae.* Bars represent the mean dopachrome formation at OD_{490}. Error bars represent standard error of the means calculated from three biological repeats. (A) Phenoloxidase activity present in the serum of the haemolymph and (B) represents phenoloxidase activity in the haemocytes. No significant difference ($p>0.05$) occurred between treatment groups or across time.

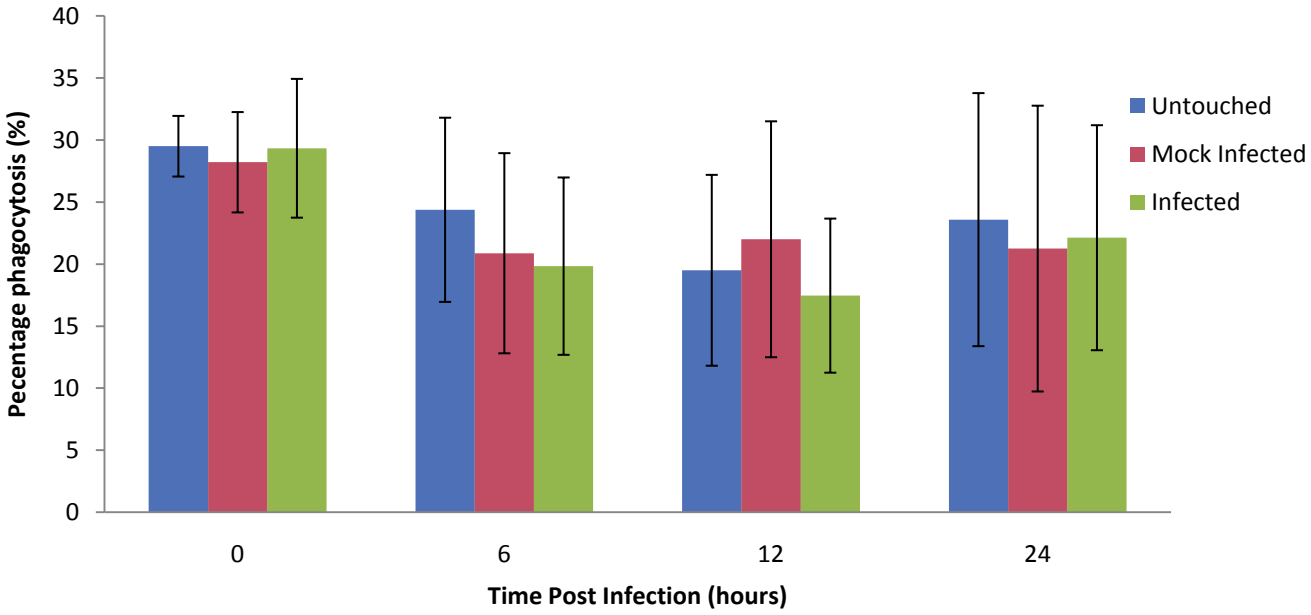

Figure 14: Phagocytic activity of haemocytes isolated from untouched, mock infected and infected *H. midae.* Bars represent the mean percentage phagocytosis for the different treatment groups. Error bars represent standard error calculated from three biological repeat experiments.

3.2.2. QUANTITATIVE REAL TIME PCR

The quantitative real time PCR (qPCR) data indicated that the NFκB homologue in *H. midae* was differentially expressed in response to infection with heat killed *V. anguillarum* 5676 over the time course of the experiment (Figure 15). The relative mRNA expression of NFκB was significantly different in abalone infected with heat killed *V. anguillarum* 5676 compared to abalone infected with sea salts (mock infected) and abalone that were unchallenged (untouched). The large error observed in this analysis, was due to the inherent biological variation that exists between abalone and due to the difficulties associated with obtaining good quality RNA for each time point.

The NFκB relative expression observed in abalone infected with heat killed *V. anguillarum* 5676 increased at 6 hpi (2.9 fold) and at 12 hpi (3.7 fold) compared to time point 0 (1 fold). NFκB expression subsequently decreased at 24 hpi by 1.1 fold to 2.6 fold compared to 12 hpi. At 24 hpi the fold change expression was significantly different to the unchallenged control group.

The relative NFκB expression levels observed in abalone infected with sea salts increased at 6 hpi (1.8 fold) compared to time 0 (1 fold). The relative expression increased at 12 hpi (2 fold) and subsequently decreased by 0.4 fold at 24 hpi (1.6 fold). NFκB expression levels in the untouched abalone were similar to the fold change pattern observed in the mock infected control group. At 6 hpi the relative NFκB expression increased to 1.4 fold

compared to time 0 (1 fold) and increased further at 12 hpi to 2.1 fold. The expression levels subsequently decreased at 24 hpi to 1.6 fold.

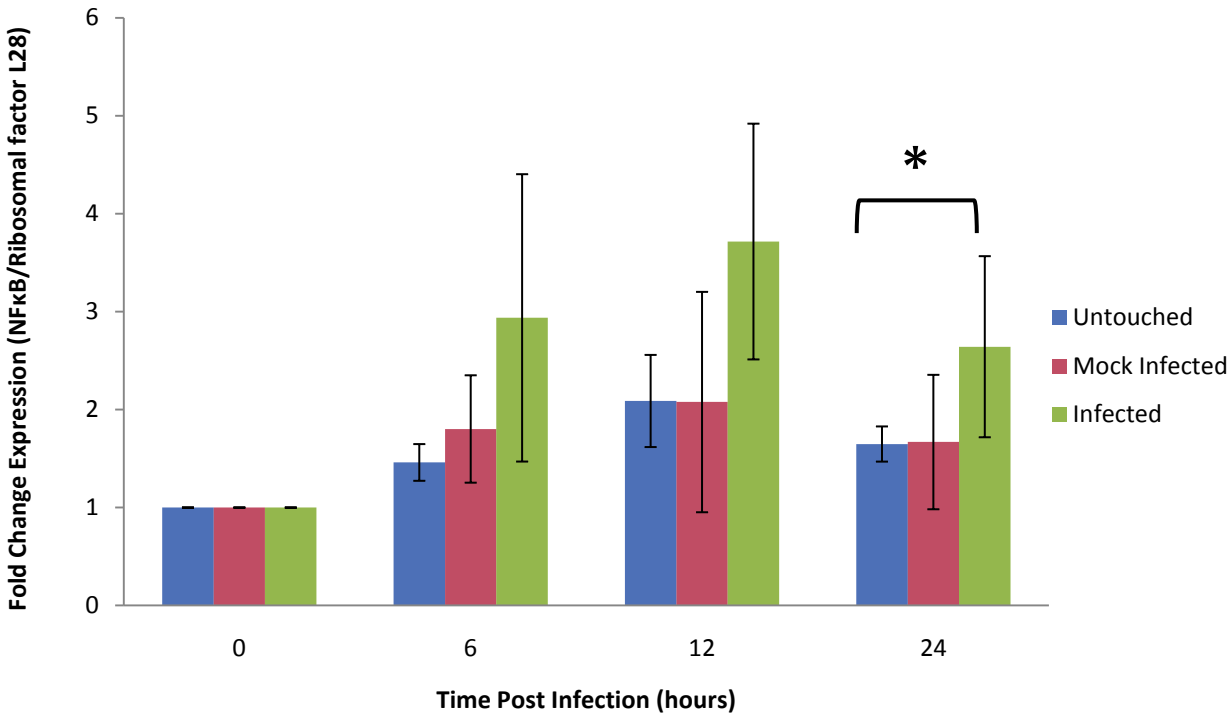

Figure 15: Quantitative real time PCR (qPCR). The bars represent the mean fold change of NFκB expression compared to the reference gene ribosomal factor L 28 from the untouched, mock infected and infected cDNA samples isolated from *H. midae.* Error bars represent the standard error calculated from 3 biological repeats. The asterisk (*) indicates significant difference ($p<0.05$) compared to the untouched group. The infected group was significantly different overall to the unchallenged group. Two way ANOVA was performed ($p<0.05$) using a Tukey ad hoc test to compare data between groups.

3.3 HAEMOCYTES

Haemocytes are the primary elicitors of the cellular immune response in invertebrates. As such, primary haemocyte cultures may be a useful tool to study aspects of the innate immune response of *H. midae*. Haemocytes isolated from *H. midae* were maintained *in vitro,* assayed for viability and partially characterised to determine their appearance and behaviour in the *in vitro* environment.

3.3.1. VIABILITY

Haemocytes aggregated and formed long, smooth pseudopodia from day 1 post seeding (Figure 16 A and B) at 19°C to 3 days post seeding (Figure 16 E). After 2 days post seeding, an increase in the presence of unattached haemocytes was observed under the microscope (Figure 16 C). Thinner and longer pseudopodia were detected on day 2 compared to the first day post seeding (Figure 16 D). Debris or possible contamination was observed in some of the cultures at day 3 post seeding (Figure 16 F). The debris was more evident at day 5 post seeding (Figure 16 H and I), with no haemocytes visible at day 6. Haemocyte appearance changed notably after 4 days post seeding. The haemocytes that formed pseudopodia appeared grainy and irregular (figure 16 G) compared to the smooth characteristics observed over the first 3 days. At 5 days post seeding there were less haemocytes detected per field of view. There were no pseudopodia visible and the haemocytes appeared to be unattached and irregular in shape (Figure 16 H and I).

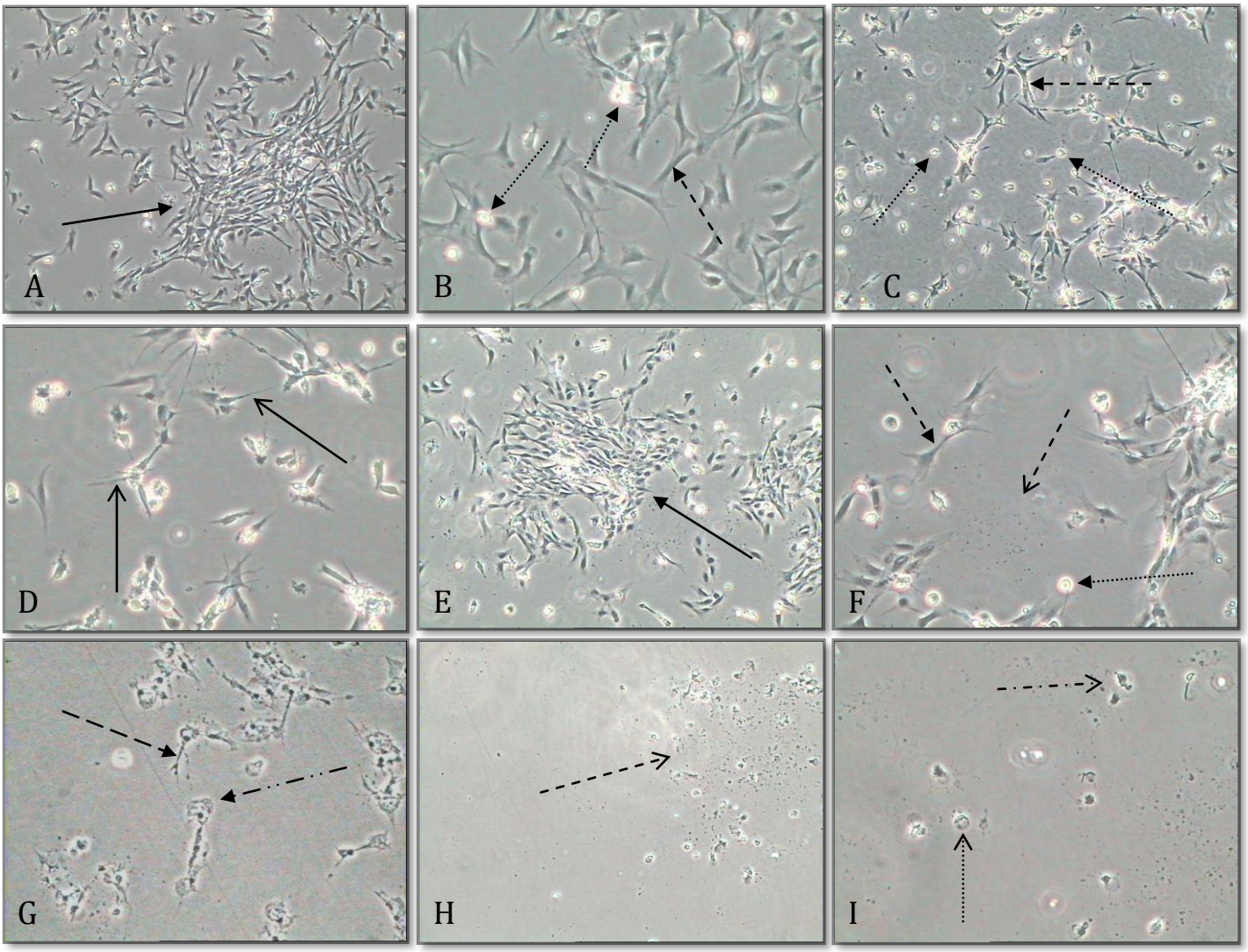

Figure 16: Haemocyte monolayer formation post seeding. (A)Haemocytes at day 1 form pseudopodia upon contact with the surface and are most often found to aggregate. Black arrow indicates a large group of haemocytes at 100 X magnification. (B) Haemocytes (day 1) are flat and elongated upon pseudopodia formation (indicated by black dashed arrows), while unattached round cells are indicated by dotted arrows (image at 200 X magnification). (C) Haemocytes at day 2 exhibit distinct pseudopodia formation (dashed arrows) and unattached cells are also present (dotted arrows) (100 X magnification). (D) Haemocytes at day 2 with narrow, long pseudopodia (thin arrow head) (200 X magnification). (E) Aggregating haemocytes at day 3 post seeding (solid arrow) (100 X magnification). (F) Debris (dashed arrow with thin arrow head), attached cells with pseudopodia (dashed arrow) and unattached cells (dotted arrow) at day 3 (200 X magnification). (G) Haemocytes at day 4 post seeding showing changes in pseudopodia. Haemocytes appear irregular and grainy (long and short dashed arrows) and pseudopodia appear disjointed (long dashed arrows) (200 X magnification). (H) Haemocytes at day 5 post seeding no longer possess pseudopodia. There is an increase in cellular debris (thin dashed arrow) (100 X magnification). (I) Some haemocytes at day 5 are round in appearance (thin, dotted arrow) and others have irregular shapes (thin dashed and dotted arrow) (200 X magnification).

Total haemocyte counts were performed daily throughout the duration of the viability study. A decrease in haemocyte number was observed over time (Figure 17). Haemocytes were seeded at an initial concentration of 1 X 10^6 cells/ml. At day 1 post seeding, haemocytes were at an average concentration of 1.17 X 10^6 cells/ml and decreased by 1.2 fold at day 2 (9.25 X 10^5 cells/ml). At day 3 post seeding, a further decrease by 1.2 fold (7.38 X 10^5 cells/ml) was detected which was significantly different to haemocyte numbers on days 1 and 2. At day 4 post seeding, a further 2.5 fold decrease in haemocyte concentration was observed (2.92 X 10^5 cells/ml) which was significantly different to haemocyte numbers at all the other time points. At day 5 post seeding the haemocyte concentration decreased further to 1.5 X 10^5 cells/ml. It was no longer possible to perform haemocyte counts at day 6 post seeding. Overall, there was a 7.7 fold decrease in haemocyte concentration between days 1 to day 5 post seeding.

The trypan blue viability assay was performed daily over the time course of the experiment. The trypan blue count is an effective viability assay that is able to distinguish between live and dead cells. Dead cells appear blue under a light microscope while live cells remain clear. There were no detectable changes in haemocyte viability (Figure 18); however the error of the counts increased at each time point. The error incurred was due to the decreased haemocyte concentrations on day 4 and 5 post seeding (Figure 17). The decrease in total haemocyte concentration affected the viability calculation, thus increasing the error.

Phagocytosis was another measure of cell viability as it measured the ability of *in vitro* haemocytes to phagocytose bacteria. The highest phagocytic activities were detected at day 1 (29 %) and 2 (22 %) post seeding (Figure 19). At day 3 post seeding, there was a decrease of phagocytic ability (4.5 %). At day 4 post seeding, phagocytic activity of the *in vitro* haemocytes was low. Phagocytic activity was not detected at day 5.

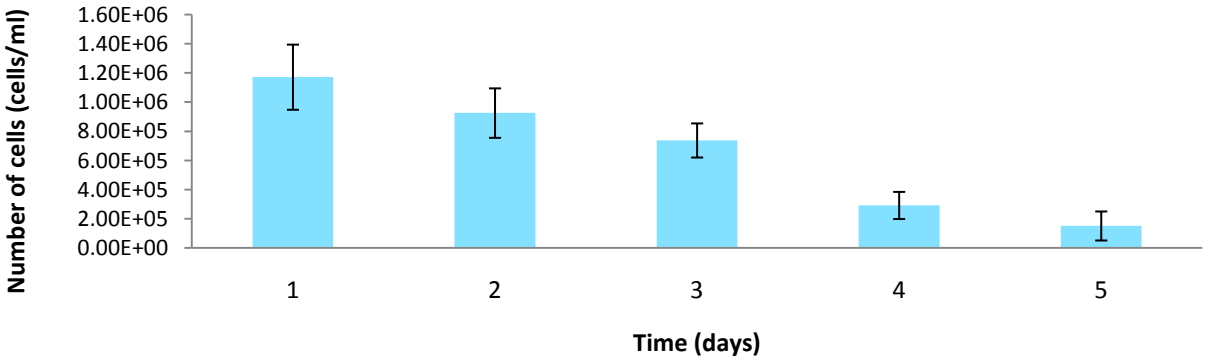

Figure 17: Total haemocyte count during viability study. The bars represent the mean haemocyte count of the *in vitro* haemocytes. The error bars represent the standard deviation of the means for three technical repeats.

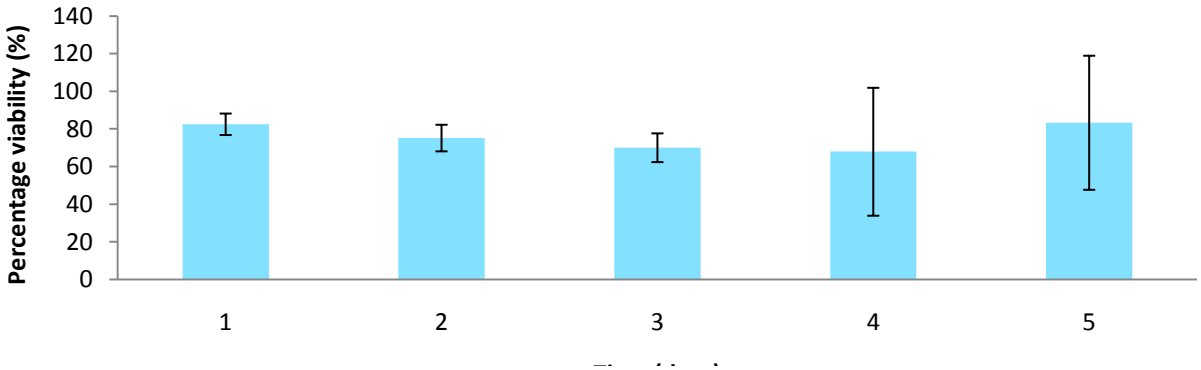

Figure 18: Trypan blue viability count during the viability study. The bars represent the mean percentage viability of the *in vitro* haemocytes. The error bars represent standard deviation of the means for three technical repeats. There were no statistically significant differences in viability over time ($p>0.05$).

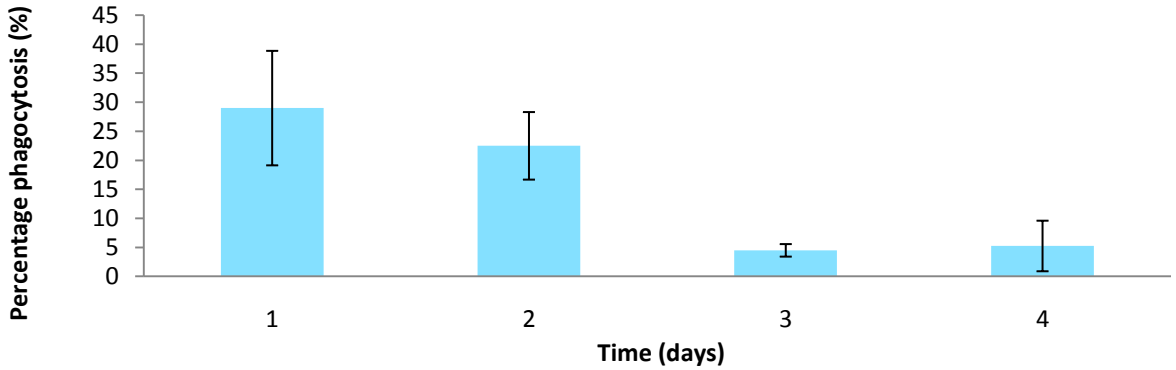

Figure 19: Phagocytic activity of haemocytes post seeding. The bars represent the mean percentage phagocytic activity of *in vitro* haemocytes. The error bars represent the standard deviation of the means for three technical repeats.

3.3.2. HAEMOCYTE STAINING

Staining techniques provided an insight into the basic features of haemocytes from *H. midae*. The giemsa stain revealed different nuclei structures present in the haemocytes. The stain indicated that there was one nucleus per haemocyte which is located either at the centre or to the side of the cell (Figure 20 A). A few of the haemocytes were observed to possess bi-lobulated nuclei. Both small, thin pseudopodia and large pseudopodia development were observed around the cells (Figure 20 B). There were dark purple, blue and orange stained components (Fig. 20 A and B) which could not be identified. Two types of haemocytes were observed, halinocytes and blast-like cells. Halinocytes possess a large cytoplasmic area, while the blast-like cells have a small cytoplasmic area (Figure 20 A). The acridine orange stain revealed that a large proportion of haemocytes contained acid vesicles of varying sizes (Figure 21 A). The acridine stain also identified two types of haemocytes, blast-like cells and halinocytes and clearly revealed the nucleus, cytoplasm and the bright red acid vesicles (Figure 21 B). The neutral red stain indicated that most haemocytes contained multiple lysosomes of various sizes (Figure 22). The lysosomes were most often located at the outer edges of the cell and occurred in groups.

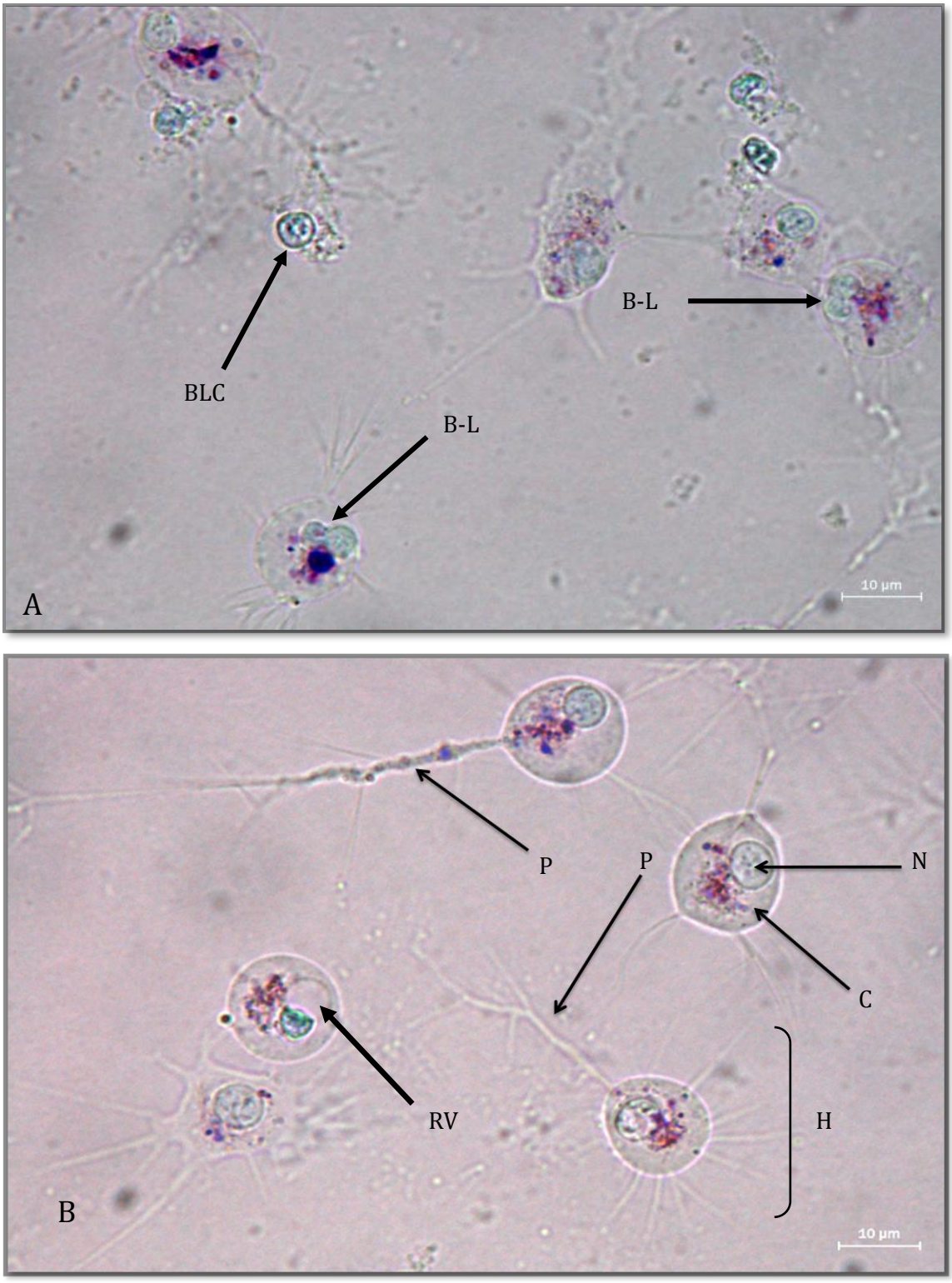

Figure 20: Giemsa dye of haemocytes, nuclei appear blue while the cytoplasm appears light blue. (A) Bi-lobulated nuclei present in two haemocytes at 1000X magnification. (B) Haemocytes containing one nucleus per cell were observed, with the nucleus located either in the centre or to the side of the cell (1000 X magnification). Long, narrow pseudopodia were observed around the edges of the cell. Abbreviations: B-L: Bi-lobulated nucleus; N: Nucleus; C: Cytoplasm, P: Pseudopodia, RV: Refringent vacuole, H: halinocyte and BLC: Blast-like cell

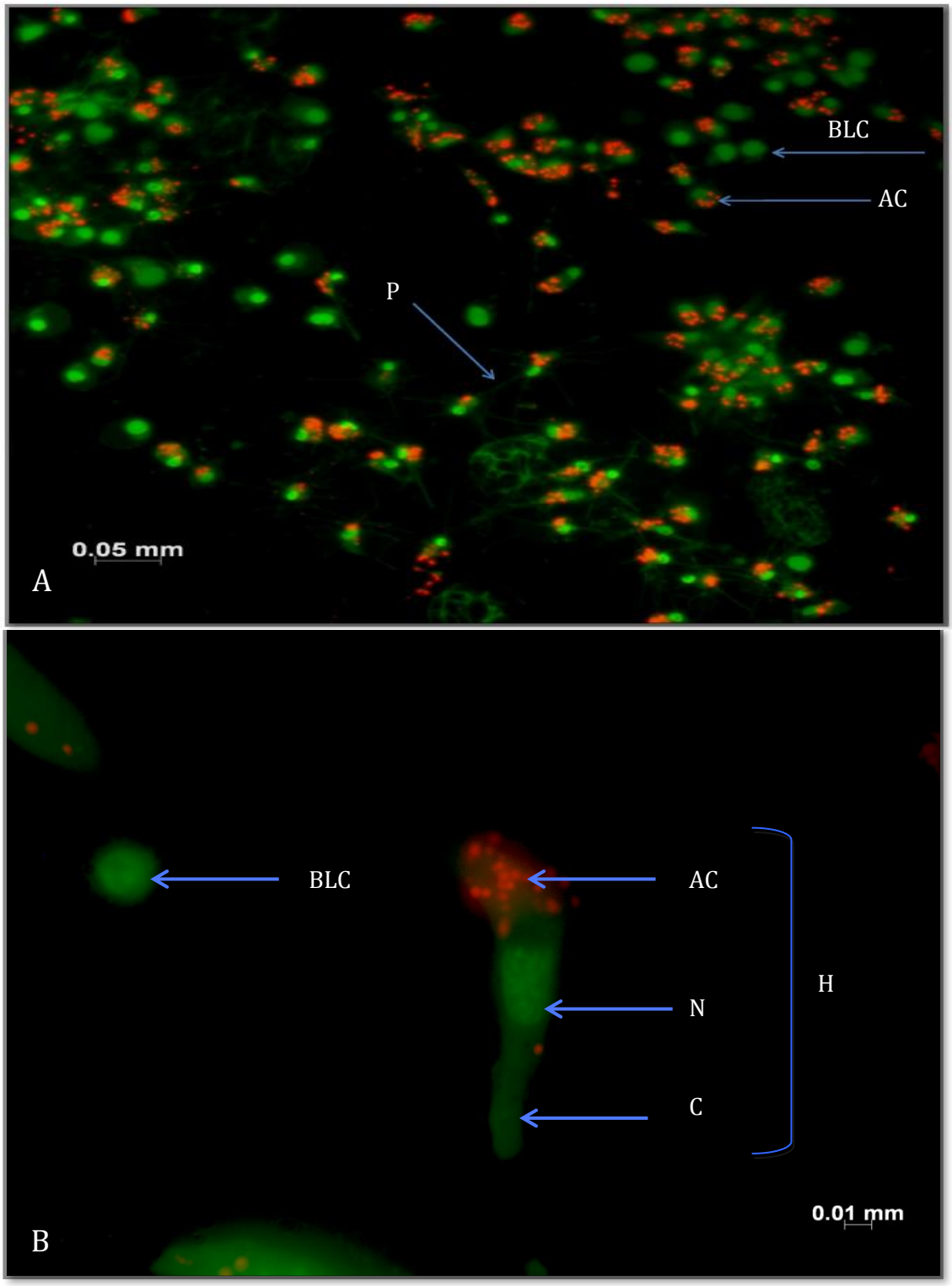

Figure 21: Acridine orange stained haemocytes. Acid cell components fluoresce red and haemocyte structures (nucleus and cytoplasm) fluoresce green. (A) Reveals that the majority of the haemocytes contain acid cell components while a small proportion do not (400 X magnification). (B) Fluorescence of one cell at 1000 X magnification. Distinct nucleus, cytoplasmic regions and acid cell vesicles were observed. Abbreviations: AC: Acid cell vesicle; BLC: blast like cell with no acid cell components; P: pseudopodia; N: nucleus; H: halinocyte and C: cytoplasm

Figure 22: Neutral Red staining indicates the presence of lysosomes in haemocytes and are a distinctive orange colour. Haemocytes often contained more than one lysosome of different sizes (1000 X magnification). Abbreviations: P: Pseudopodia, SL: Small lysosome and LL: Large lysosome

3.4 *IN VITRO* CHALLENGE TRIAL

Haemocytes from *H. midae* maintained *in vitro* were separated into two groups for the challenge trial; FITC-labelled heat killed *V. anguilarium* 5676 treated haemocytes and PBS treated haemocytes (which served as the control). FITC-labelled heat killed *V. anguilarium* 5676 was used in the experiment to quantitate phagocytic activity of the *in vitro* haemocytes over time. The two treatment groups were assayed to determine whether physiological responses (phagocytic activity, phenoloxidase activity, total haemocyte counts and viability) occur *in vitro* and whether the *H. midae* NFκB homologue was regulated in response to treatment with FITC-labelled heat killed *V. anguilarium* 5676.

3.4.1 PHYSIOLOGICAL TESTS

The total haemocyte counts revealed that no significant changes occurred in the haemocyte population over the duration of the challenge trial in both the PBS and FITC-labelled heat killed *V. anguilarium* 5676 treated haemocytes (Figure 23). The trypan blue viability assay indicated that there was no significant difference between the treatment groups at each time point or over the duration of the challenge trial (Figure 24). Although haemocyte viability (50%) in the FITC-labelled heat killed *V. anguilarium* 5676 treated group at 3 hpi had decreased by 20% in comparison to time 0 (70%), the change was not significant. This difference could have been due to biological variation in the samples as haemocyte viability

in the FITC-labelled heat killed *V. anguilarium* 5676 treated group at 6 hpi was 65%. The PBS treated haemocytes exhibited a similar trend, with 60% cellular viability at 3 hpi compared to 77 % at time 0, whereas haemocyte viability was 69% at 6 hpi. The haemocyte and viability counts suggest that any differences observed between the haemocyte groups with the remaining physiological tests (see below) could not be due to changes in cell viability or number as these remained constant over the course of the challenge trial.

Phenoloxidase activity in both the cells (Figure 25) and the serum (Figure 26) showed no significant difference between the treatment groups over time. The data concur with the *in vivo* challenge trial where no significant changes were observed in either the cellular or serum phenoloxidase activities. The cellular phenoloxidase activity in the PBS-treated haemocytes remained constant over the duration of the challenge trial, while the infected group exhibited an erratic up-down trend which was not statistically significant (Figure 25). The serum phenoloxidase activity (Figure 26) appeared higher in the infected haemocytes but the difference in phenoloxidase activity between the two treatment groups was not significant. It was unexpected that there would be a difference in activity at time 0. The variation at time 0 may be due to biological variation between the three biological repeats and in part due to the sensitivity of the assay.

There was a significant increase in percentage phagocytic activity in the FITC-labelled heat killed *V. anguilarium* 5676 treated haemocytes compared to the PBS treated haemocytes (Figure 27). The haemocytes treated with FITC-labelled heat killed *V. anguilarium* 5676

displayed a significant increase in the number of phagocytosing cells at 2, 3 and 6 hpi compared to time zero. The percentage phagocytic activity increased from 7.7% at time 0 to 31.7% at 2 hpi. The phagocytic activity remained constant from 2 hpi to 24 hpi. At 3 hpi and 6 hpi, the percentage of phagocytosing cells in the FITC-labelled heat killed *V. anguilarium* 5676 treated group was significantly higher than the PBS treated group. The difference in phagocytosis at time zero between the treatment groups was due to the incubation times of the samples, i.e. the FITC-labelled heat killed *V. anguilarium* 5676 treated group indicated a true progression of infection, while the control group used the standard phagocytosis assay procedure, where the haemocytes were incubated for 20 minutes with flourescent bacteria.

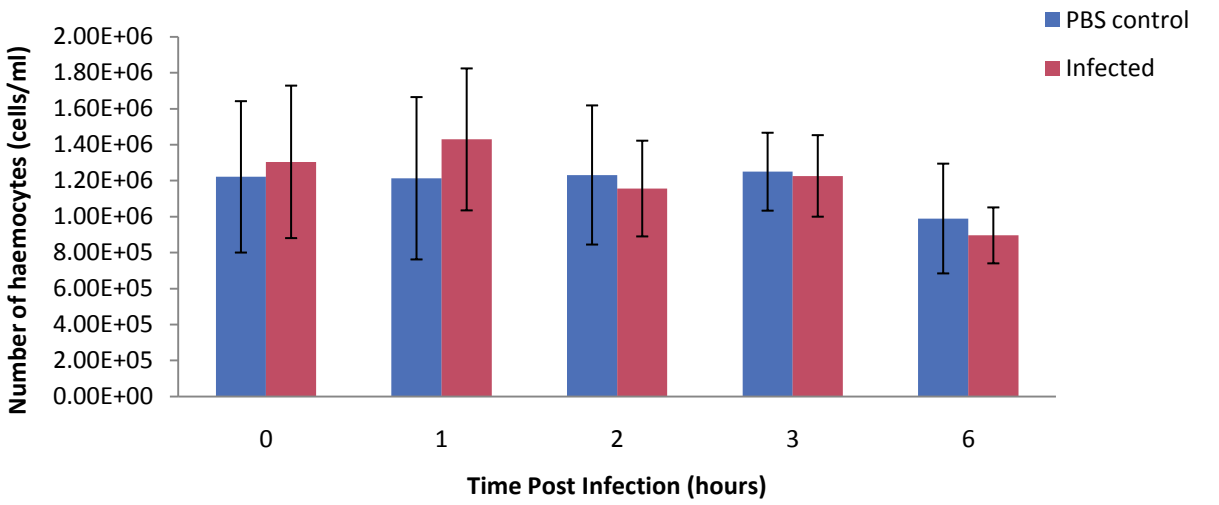

Figure 23: Total haemocyte count. The bars represent the mean number of haemocytes/ml in the FITC-labelled heat killed *V. anguilarium* 5676 treated (infected) and PBS treated haemocytes. The error bars represent the standard error of the means for three biological repeats. There was no significant difference ($p>0.05$) between control and infected haemocyte groups.

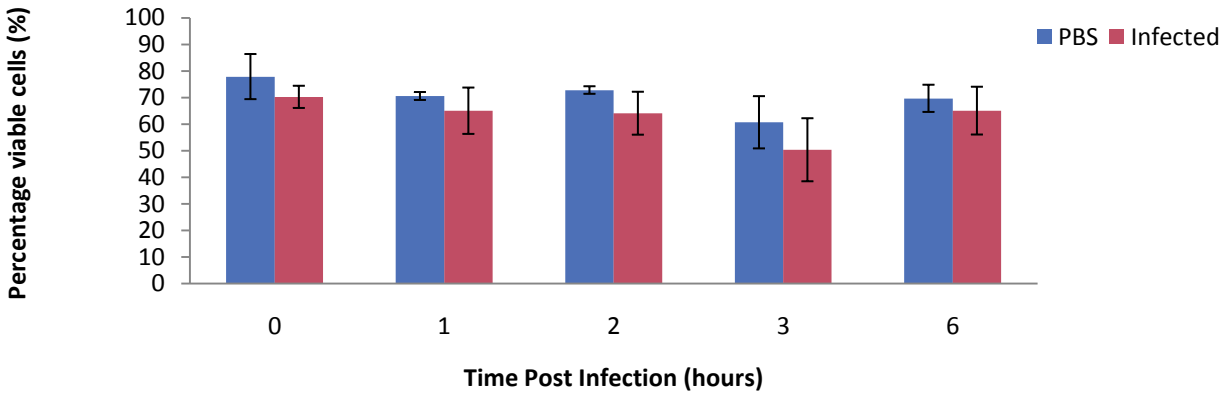

Figure 24: Trypan blue viability assay. The bars represent the mean percentage viability for FITC-labelled heat killed *V. anguilarium* 5676 treated (infected) and PBS treated haemocytes. The error bars represent the standard error of the means for three biological repeats. Statistical analysis revealed no significant difference ($p>0.05$) between time points and treatments groups.

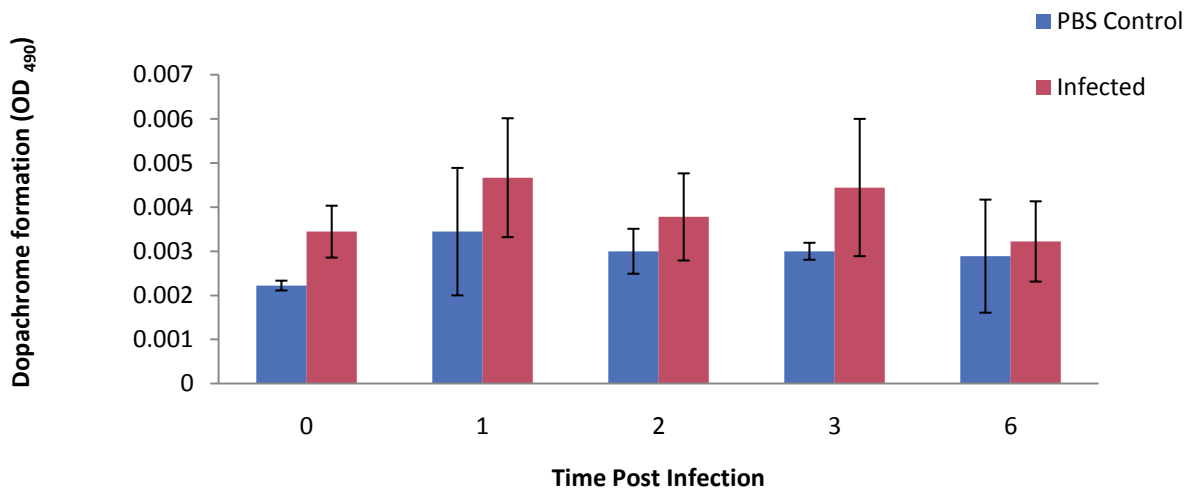

Figure 25: Phenoloxidase activity in haemocytes. The bars are indicative of the mean dopachrome formation at OD_{490} for FITC-labelled heat killed *V. anguilarium* 5676 treated (infected) and PBS-treated control haemocytes. The error bars represent the standard error of the means for three biological repeats. Statistical analysis displayed no significant difference ($p>0.05$) between treatments and over time.

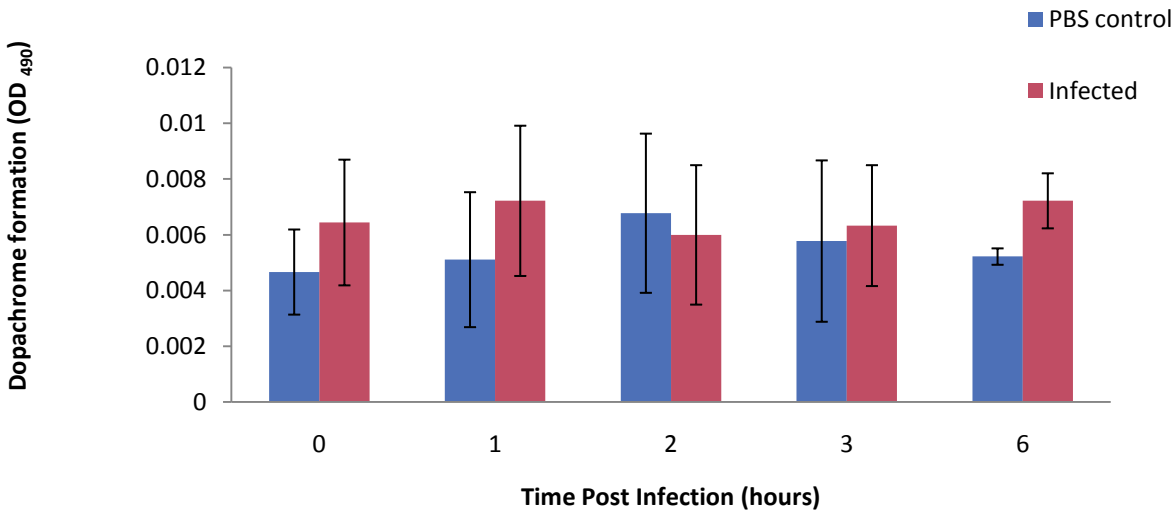

Figure 26: Phenoloxidase activity in the cell-free serum. Bars represent the mean do dopachrome formation at OD_{490} for FITC-labelled heat killed *V. anguilarium* 5676 treated (infected) and PBS treated haemocytes. Error bars represent the standard error of the means for three biological repeats. Statistical analysis revealed no significant difference ($p>0.05$) between treatment groups and over time.

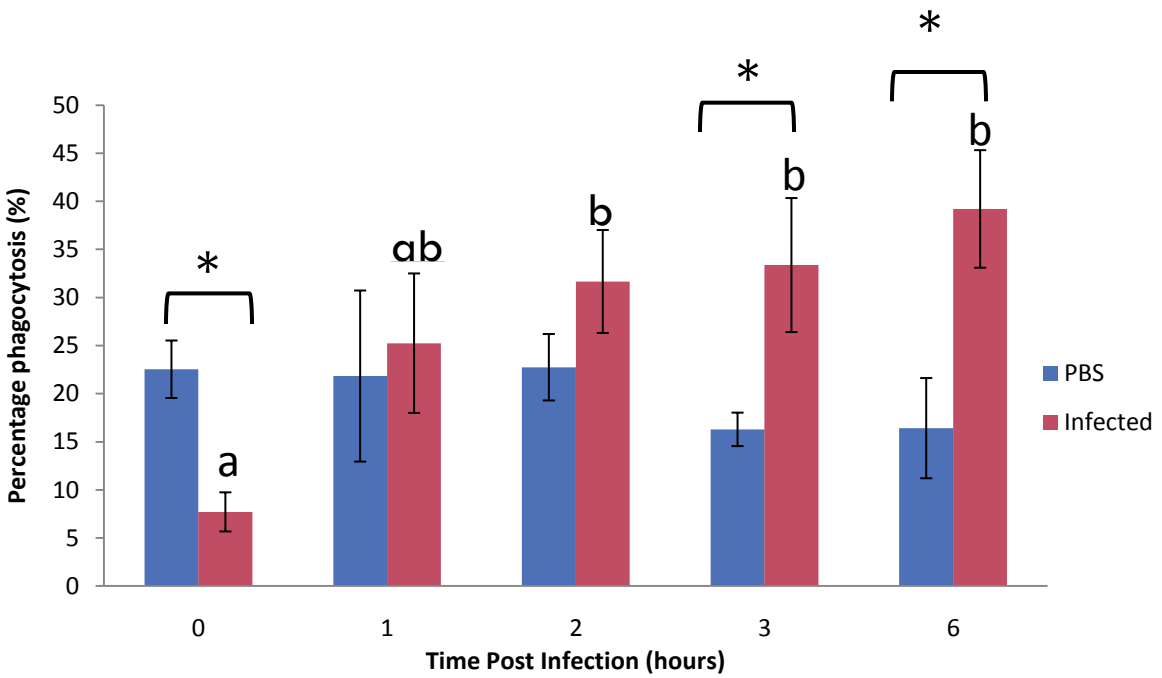

Figure 27: Phagocytosis activity of haemocytes during the *in vitro* challenge trial. The bars represent the mean percentage phagocytosis in FITC-labelled heat killed *V. anguilarium* 5676 treated (infected) and PBS-treated control haemocytes. Error bars represent the standard error of the mean for three biological repeats. A two way ANOVA with a post-hoc Tukey test revealed that there were statistical differences within the infected group and between treatment groups. An asterisk (*) indicates a significant difference ($p<0.05$) between the two treatment groups at 0, 3 and 6 hpi. Different letters above the bars indicate significant differences ($p<0.05$) within the infected group at different times post-infection.

3.4.2 QUANTITATIVE REAL TIME PCR

NFκB expression was significantly different at 1, 2 and 3 hpi in the heat killed FITC labelled *V. anguillarum* 5676 treated haemocytes compared to the PBS treated haemocytes (Figure 28). At 1, 2 and 3 hpi the relative expression was 5.2, 26.2 and 18.7 fold respectively in the heat killed FITC labelled *V. anguillarum* 5676 treated haemocytes. In comparison, NFκB relative expression in the PBS treated haemocytes was 1, 0.6 and 1.4 fold at 1, 2, and 3 hpi, respectively. These significant changes in NFκB gene expression in the FITC-labelled heat-

killed *V. anguilarium* 5676 treated haemocytes indicated that NFκB is regulated in cultured haemocytes following exposure to FITC-labelled heat killed *V. anguillarum* 5676. The large error detected at 2 hpi in the FITC-labelled heat killed *V. anguilarium* 5676 treated group occurred due to a discrepancy in the relative expression calculated in one of the three biological repeats. This discrepancy occurred as the cycle number (Ct value) for the gene of interest (NFκB) was much lower than the other biological repeats. This value is an indication of the prevalence of the transcript, and directly affects the calculation; as a result the relative expression level was higher.

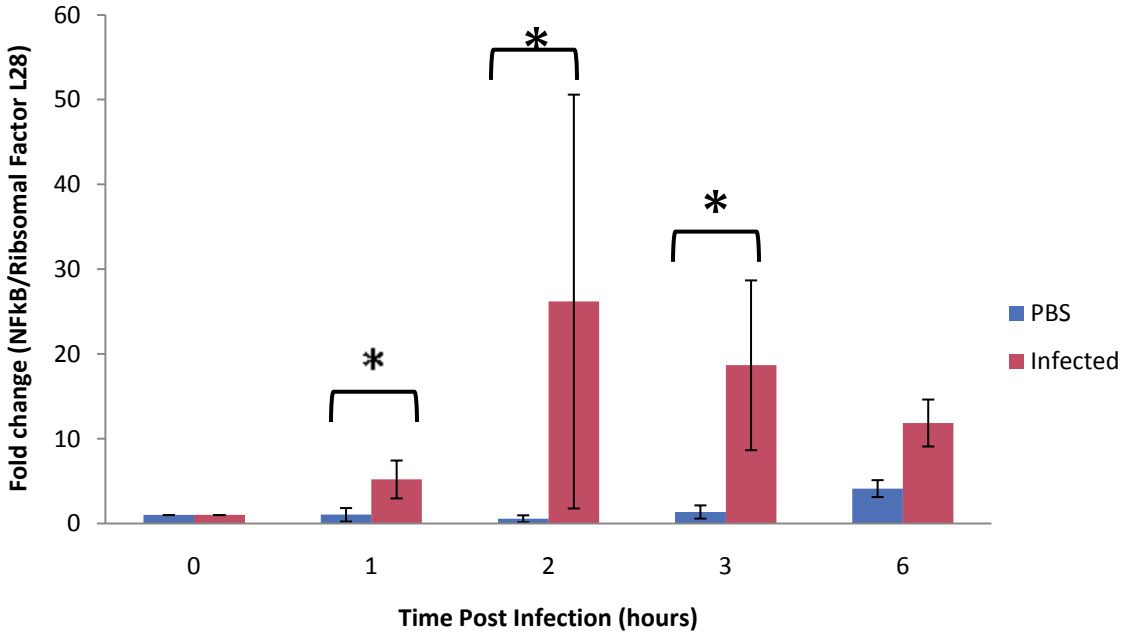

Figure 28: qPCR analysis of the relative fold change of NFκB expression compared to the reference gene ribosomal factor L28. The bars represent the mean fold change expression of NFκB in FITC-labelled heat killed *V. anguilarium* 5676 treated (infected) and PBS-treated haemocytes *in vitro*. Error bars represent the standard error of the means for three biological repeats. A two ANOVA (ranks) with a post-hoc Tukey test was performed. The asterisk (*) indicates a significant difference ($p<0.05$) between the treatment groups.

CHAPTER 4

DISCUSSION

CONTENTS

4.1. NFκB gene sequence 88

4.2. *In vivo* challenge trial 90

4.3 Haemocytes 97

4.4. *In vitro* challenge trial 101

4.6 Conclusion and future work 107

4.1. NFκB GENE SEQUENCE

NFκB was identified in this study as a candidate gene that could be a biomarker of stress in *H. midae.* In order to address this objective, it was necessary to amplify and identify a homologue of NFκB in the organism. In this study, two sequenced cDNA fragments from *H. midae*, a 3' fragment and the RHD fragment, were identified as being homologous to NFκB.

Gene specific primers to *H. diversicolor supertexta* described in Jiang and Wu (2007) successfully amplified a 280 bp product from *H. midae* cDNA. Upon BLASTx analysis, it was revealed that the fragment was similar to the NFκB *H. diversicolor supertexta* homologue. Upon alignment, the fragment was found to align to the 3' end of the *H. diversicolor supertexta* NFκB homologue, and was thus named the 3' fragment.

Various amplification strategies were employed to acquire more sequence information for the *H. midae* NFκB homologue. Of these strategies, nested PCR using primers designed to the rel homology domain (upstream of the 3' fragment) was successful. The rel homology domain (RHD) is a conserved domain present in all NFκB homologues and is found near the 5' end of the gene encoding NFκB (Caamaño and Hunter, 2002).

The RHD fragment was amplified from *H. midae* cDNA and upon BLASTx analysis was found to be homologous to NFκB from invertebrate species and contained the rel homology

domain. It was observed that the RHD fragment of the NFκB homologue from *H. midae* clustered with class II NFκB transcription factor homologues from a variety of organisms in a phylogenetic evolutionary tree

The evolutionary tree revealed that the RHD fragment from *H. midae* paired strongly with *H. diversicolor supertexta* (100 %) but did not group with either gastropod (*B. glabrata*) or bivalve species. This is contrary to the evolutionary tree observed in Jiang and Wu (2007), where ab-rel from *H. diversicolor supertexta* was found to pair strongly (100 % bootstrap value) with Cg-rel from *C. gigas,* a bivalve species (Jiang and Wu, 2007). The tree constructed in this study compared the rel homology domain only, while Jiang and Wu (2007) utilised full NFκB sequences from various species. This may directly influence the similarities observed in the phylogenetic tree and account for the different groupings. The evolutionary tree presented in this study also contained more NFκB homologues from marine invertebrate species (oysters, clams, sponge, squid and abalone) than the Jiang and Wu (2007) study, providing a meaningful and relevant evolutionary tree of the rel homology domain from NFκB homologues.

Both the 3' fragment and the RHD fragment isolated in this study shared homology with *H. diversicolor supertexta* ab-rel. The 3' fragment shared homology with *H. diversicolor supertexta* ab-rel, contained no obvious domain information, and belongs to the class II family. The RHD fragment was also identified as a class II homologue.

Since both fragments isolated in this study were identified as class II NFκB homologues, it is most likely that these fragments are part of the same *H. midae* NFκB homologue. However, there are two class II NFκB homologues in *Drosophila*, namely *Dif* and *Dorsal.* Although it cannot be ruled out that the RHD fragment and the 3' fragment are portions of two different class II NFκB homologues in *H. midae*, *Dif* did not appear in any of the alignment tables obtained following BLASTx searches of the GENBANK database using the *H. midae* NFκB sequences. It thus stands to reason that the 3' fragment and the RHD fragment belong to the same *H. midae* class II NFκB homologue.

4.2. *IN VIVO* CHALLENGE TRIAL

In order to identify the relevance of NFκB as a biomarker of stress, *H. midae* were subjected to infection with a heat killed pathogen *V. anguillarum* 5676. The haemolymph extracted from the challenged abalone was used in various immune parameter assays that would characterise the physiological responses that occur upon infection (such as phagocytosis and phenoloxidase production) and RNA isolated from haemocytes extracted from the haemolymph was used to investigate mRNA expression levels of the NFκB homologue of *H. midae*.

Immune parameter assays have been utilised in various studies as the tests provide an insight into the stress status of the animal. Malham *et al.* (2003) used a phagocytosis assay

and total haemocyte count to determine the relationship between stress (mechanical) and immunity in *H. tuberculata* (Malham *et al.*, 2003). Wootton and Pipe (2003) used a phagocytosis assay, a total haemocyte count and a serum anti-bacterial assay to characterise the immune capabilities of *Scrobicularia plana* haemocytes (Wootton and Pipe, 2003). Lastly, Costa *et al*. (2009) used a phagocytosis assay, a total haemocyte count, a serum anti-bacterial assay and a phenoloxidase assay to characterise the stress response in *Penaeus vannamei* (shrimp) in response to an infectious myonecrosis virus infection (Costa *et al.*, 2009).

In this study, a total haemocyte count, serum anti-bacterial assay, phenoloxidase assay and a phagocytosis assay were utilised in an attempt to gain further insight into the immune mechanisms that occur in *H. midae* in response to stress.

Total haemocyte counts are often performed to identify the current health state of the organism (Malham *et al.,* 2003; Costa *et al.,* 2009). In *H. midae* it was evident that there was a general decrease in the concentration of circulating haemocytes in the group of abalone infected with heat killed *V. anguillarum* 5676, with a significant decrease at 12 hpi compared to the untouched control abalone group, but not in the mock infected group. The decrease in haemocyte population may be due to haemocytes migrating to the site of injection via a process known as chemotaxis (Gopalakrishnan *et al.,* 2009). Parisi *et al.* (2008) observed a decrease in circulating haemocytes at 3 to 12 hpi when the oyster *M. gallinoprovincialis* was infected with heat killed *V. anguillarum* (Parisi *et al.,* 2008) which is

similar to the decrease in haemocyte concentration between 6 and 12 hpi that occurred in the challenge trial conducted in this study.

The serum anti-bacterial assay quantitates anti-bacterial activity in the cell-free haemolymph. An anti-bacterial index is determined which indicates the degree of antibacterial peptide inhibition of bacterial growth. In this study, no significant differences in the anti-bacterial index were detected between the control abalone groups (untouched and mock-infected) and the heat killed *V. anguillarum* 5676 infected group of abalone. This was an interesting observation as it was expected that exposure to heat killed *V. anguillarum* 5676 may increase the amount of anti-microbial peptides produced in the haemolymph. Gram-negative pathogens are recognised as PAMPS due to the presence of cell wall lipopolysaccharide (LPS) chains, and consequently, trigger a cascade event which activates NFκB. This leads to translocation of NFκB into the nucleus and up-regulates expression of anti-microbial peptide genes (Bosch *et al.,* 2009). It was therefore expected that there would be an increase in the amount of anti-microbial peptides produced and thus a lower anti-bacterial index observed in abalone infected with heat killed *V. anguillarum* 5676 compared to abalone that were mock infected with sea salts or unchallenged. Camino Ordás *et al.* (2000) detected a higher anti-bacterial index in uninfected clams in comparison to those that were infected with the parasite *Perkinsus atlanticus.* However, the authors noted that there was a high variability between individuals and uncontrolled changes in abiotic conditions (ammonia and dissolved oxygen levels) could have masked any significant differences in the anti-bacterial index of the two

treatment groups (Camino Ordás *et al,* 2000). A similar explanation may apply to this study where a high variability occurred between the biological repeats and factors such as ammonia and dissolved oxygen levels were uncontrolled.

The prophenoloxidase pathway is an important process in invertebrate immune responses (Aladaileh *et al.,* 2007). Phenoloxidase is involved in reducing the levels of cellular free radicals generated during phagocytosis and other proteolytic processes (Chen *et al.,* 2005). It does this by converting tyrosine to L-DOPA, which then undergoes a series of non-enzymatic changes to form melanin. Melanin is able to bind and sequester reactive oxygen species (Aladaileh *et al.,* 2007). Melanisation has also been shown to be involved in wound healing, nodulation and encapsulation (Aladaileh *et al.,* 2007). It was thus unexpected that no change in phenoloxidase activity was observed in abalone infected with heat killed *V. anguillarum* 5676. Cheng *et al.* (2004) reported increased haemocyte phenoloxidase activity at 24, 48 and 72 hpi when *H. diversicolor supertexta* was infected with *V. parahaemolyticus* at 20°C. However, the increase in activity observed over time was not significant (Cheng *et al.,* 2004). In another study, Aladaileh *et al.* (2007) detected a significant increase in phenoloxidase activity in both the cell-free haemolymph (serum) and haemocytes of Sydney rock oysters (*Saccostrea glomerata)* treated with LPS at 24, 48 and 96 hpi. The authors observed that both the cell-free haemolymph and haemocyte phenoloxidase activities were similar and that there were no significant differences between the two components (Aladaileh *et al.,* 2007). These studies suggest that an increase in phenoloxidase activity may only occur after the initial 24 hours post infection.

Therefore, if this study were to be repeated, phenoloxidase activity should be monitored over a longer period following infection (96 rather than 24 hpi).

Phagocytosis is one of the primary defence mechanisms in response to infection (Cheng *et al.,* 2004). Haemocytes recognise and engulf invading pathogens, which are subsequently degraded (Marmars and Lampropoulou, 2009). Phagocytic activity generally decreased between 6 and 12 hpi in abalone infected with heat killed *V. anguillarum* 5676 and abalone infected with sea salts (mock infected) compared to time 0 and the unchallenged group of abalone. Cheng *et al.* (2004) observed the opposite trend when *H. diversicolor supertexta* was infected with *V. parahaemolyticus.* Phagocytic activity increased significantly at 24, 72 and 120 hpi at 20°C. A possibly important difference between the two experiments is that Cheng and co-workers infected *H. diversicolor supertexta* with 20 µl of live *V. parahaemolyticus* at a concentration of 8 x 10^6 cfu/ml (Cheng *et al.,* 2004). Live bacteria may elicit a more vigorous immune response than a heat killed pathogen which cannot replicate within the host system. This may lead to more dramatic physiological changes in the immune response. In fact, Parisi *et al.* (2008) found that changes in haemocyte populations occurred in the oyster *M. gallinoprovincialis* when challenged with live bacteria compared to their heat killed counterparts. The authors reported that halinocyte and large granulocyte populations increased from 12 hpi with live *V. anguillarum* and remained elevated, whereas these granulocytes remained at a constant lower level in *M. gallinoprovincialis* infected with heat killed *V. anguillarum* (Parisi *et al.,* 2008). Therefore, changes in haemocyte populations upon infection with either live or heat killed pathogens

should be monitored concurrently in order to correlate haemocyte changes with changes in phagocytic activity.

Taken together, the immune parameter data provided insights into some of the physiological responses that occur in *H. midae* upon exposure to a heat killed pathogen. The total haemocyte count suggested that heat killed *V. anguillarum* 5676 does affect the population of circulating haemocytes during the first 24 hours post infection, while the other indicators such as phagocytosis, phenoloxidase activity and anti-bacterial activity suggest that exposure to the heat killed pathogen does not elicit strong physiological responses in *H. midae.*

NFκB expression in *H. midae* haemocytes was measured utilising quantitative real time PCR. There was a significant increase in fold change expression of NFκB at 24 hpi in abalone infected with heat killed *V. anguillarum* 5676 in comparison to the unchallenged group of abalone. There was an increase in NFκB relative expression at 6 and 12 hpi in abalone infected with heat killed *V. anguillarum* 5676, compared to the mock infected and unchallenged abalone groups. This increase however, was not statistically significant. Interestingly, no significant difference was observed when comparing NFκB expression in mock infected abalone with that of unchallenged or infected abalone. This may be due to the larger error that occurred between the biological repeats for the mock infected group and the difficultly of isolating good quality total RNA from all the samples obtained from the challenge trial. The error observed may have masked statistical significance when

comparing the mock infected group to the unchallenged and the heat killed *V. anguillarum* 5676 infected group of abalone. It is also possible that a wound response occurred concurrently and therefore affected the results obtained in the mock infected and the heat-killed *V. anguillarum* 5676 infected group of abalone.

Jiang and Wu (2007) used both qPCR and northern blot analysis to demonstrate a decrease in fold change expression of NFκB at 3 and 6 hpi compared to time 0 in both LPS infected and saline injected *H. diversicolor supertexta*. An increase in fold expression was observed at 9 hpi in the infected group compared to the control group and time point 0 (Jiang and Wu, 2007). Wang *et al.* (2008) detected an increase in NFκB fold change expression when *H. diversicolor* was infected with a cocktail of live bacteria (*Staphylococcus aureus*, *Micrococcus lysodeikticus*, *Staphylococcus epidermidis*, *Escherichia coli* and *Vibrio parahaemeolyticus*). An increase in the expression of NFκB at 36 hpi was also observed in the saline injected control group of abalone (Wang, *et al.*, 2008), indicating that a wound response may play a role in NFκB regulation. However, this was not observed in the study by Jiang and Wu (2007) and may suggest that regulation of NFκB expression is different in different species of abalone. Indeed, Montagnani *et al.* (2004) showed that *cg-rel* from *C. gigas* displayed no increase in mRNA expression levels in response to four different *Vibrio* species (Montagnani *et al.,* 2004).

This study, as well as studies by Jiang and Wu (2007) and Wang *et al.* (2008), indicate that increased expression of a type II NFκB homologue is elicited by Gram-negative bacteria (*V.*

anguillarum 5676, E. coli and *V. parahaemeolyticus*) or cell wall components (LPS). This observation is different to the *Drosophila* immune system where Dif and Dorsal (type II NFκB homologues) are activated by Gram-positive bacterial or fungal PAMPs (see Figure 1). The abovementioned studies lend support to Gueguen *et al.* (2003) who suggest that there may be greater interplay between immune pathways that lead to up-regulation of antimicrobial peptides.

The expression data obtained in this study constitutes the first step in developing a system for detecting stress in farmed *H. midae*. The fact that there was an increase in NFκB mRNA expression in response to the heat-killed Gram-negative bacterium, *V. anguillarum* 5676, suggests that NFκB may be useful in detecting bacterial stress, and thus, is a potential biomarker.

4.3 HAEMOCYTES

Haemocytes are the primary elicitors of the cellular immune response in invertebrates. *In vitro* methodologies utilising primary haemocyte cultures may help provide insight into the immune response pathways (Mortensen and Glette, 1996), and have been utilised in various studies with success. In this study, haemocytes isolated from *H. midae* were maintained *in vitro* and partially characterised using staining techniques.

H. midae haemocytes formed pseudopodia *in vitro* and were observed to preferentially aggregate. Pseudopodia formation was also noted in *H. tuberculata* haemocytes which were predominantly elongated and thin (Travers *et al.,* 2008). In this study, *in vitro* haemocytes maintained viability, cell number and the ability to phagocytose for 2 days post seeding, after which all three indicators decreased. Haemocytes remained viable *in vitro* for eight days (data not shown). Lebel *et al.* (1996) maintained *in vitro H. tuberculata* haemocytes for 6 days with no loss in cell viability; however, the authors did not indicate whether the cell concentration remained the same throughout their time course study (Lebel *et al.*, 1996). The loss in *H. midae* haemocyte cell number and phagocytic ability was affected by contaminants that occurred in the cultures at days 3 and 5. Although the culture media was replaced every second day (with the addition of antibiotics), contamination remained. It may be essential to have exclusive culture chambers for maintaining haemocyte cultures in order to reduce the risk of contamination; unfortunately this was not possible for this study.

H. midae haemocytes were partially characterised using standard staining techniques that stain specific components within the cell, allowing visualisation of morphological characteristics. It was observed that all the haemocytes contained a single nucleus, with a few cells containing bi-lobulated nuclei. Travers *et al.* (2008) also detected haemocytes with bi-lobulated nuclei in *H. tuberculata*. The authors also noted that the nuclei were often located in the centre of the cell (Travers *et al.,* 2008).

Distinctions between haemocyte types were observed using the Giemsa stain. Studies by Cima *et al.* (2000) and Travers *et al.* (2008) used this method to differentiate between cell types based on the nucleus to cytoplasm ratio. Similar distinctions were observed in this study where some *H. midae* haemocytes consisted of a nucleus within a large cytoplasm, while others had a nucleus within a small area of cytoplasm. Travers *et al.* (2008) state that these differences may be indicative of blast-like cells (small cytoplasmic area in comparison to the nucleus) and halinocytes (large cytoplasm). It was observed in this study and by Travers *et al.* (2008) that there were more halinocytes than blast-like cells.

The neutral red dye specifically stains lysosomes which are acidic organelles employed in intracellular degradation of foreign material. During phagocytosis, lysosomes fuse with the primary phagosome (containing the engulfed foreign material) and release hydrolayses, esterases, amidases and oxidative enzymes that break up and destroy the foreign material (Donaghy *et al.,* 2009). It was observed that the majority of *H. midae* haemocytes contained several lysosomes, while few contained no lysosomes. The unequal distribution of lysosomes may be indicative of different functions within the haemocyte population, as it was reported that not all haemocytes are able to phagocytose (Cima *et al.,* 2000; Travers *et al.,* 2008). Travers *et al* (2008) also observed that *H. tuberculata* haemocytes often contained several lysosomes per haemocyte (Travers *et al.,* 2008).

The acridine orange stain revealed acid vesicles in the majority of *H. midae* haemocytes. Travers *et al.* (2008) identified these vesicles in *H. turberculata* and noted that acid vesicles

are composed of lysosomes and late endosomes (Travers *et al.,* 2008). The acridine orange stain also provided details of haemocyte structure. It was apparent that some haemocytes displayed blast-like cell characteristics while others displayed halinocyte characteristics. It was observed that the majority of the halinocyte population contain acid vesicles while only the minority of the blast-like cells appear to contain acid vesicles.

The histochemical study of *H. midae* haemocytes revealed that they are not a uniform population. Some haemocytes contain lysosomes, while some do not. A few haemocytes contain bi-lobulated nuclei while the majority contain a single nucleus. A few of the haemocytes possessed large vacuoles and while many haemocytes contained several acid cell vesicles, some haemocytes contained none. This preliminary investigation indicated that there may be at least two different types of haemocytes within *H. midae*; namely blast-like cells and halinocytes.

Cell types may be further characterised using staining techniques that differentiate granules found in haemocytes, and indicate the presence of granulocytes. The May-Grünewald stain detects acidophilic and basophilic granules (Cima *et al.,* 2000), allowing one to differentiate between different types of granulocytes and halinocytes (Travers *et al.,* 2008). Since the May-Grünewald stain caused the *H. midae* haemocytes to lyse, the procedure will require optimisation before it can be used to differentiate *H. midae* haemocytes.

4.4. THE *IN VITRO* CHALLENGE TRIAL

H. midae haemocytes maintained *in vitro* were treated with FITC-labelled heat killed *V. anguilarium* 5676 and examined for changes in physiological responses (phagocytic activity, phenoloxidase activity, total haemocyte counts and viability) and transcriptional regulation of NFκB over time.

Total haemocyte counts and the trypan blue viability assay were used to assess the effect FITC labelled heat killed *V. anguillarum* 5676 had on haemocytes over the duration of the *in vitro* challenge trial. No significant differences were observed between cell number and viability of the FITC-labelled heat killed *V. anguilarium* 5676 treated haemocytes and the PBS treated haemocytes (control group). These data suggest that FITC labelled heat killed *V. anguillarum* 5676 does not significantly damage haemocytes or affect their viability, and similarly, that changes observed in physiological responses and NFκB expression could not be due to changes in haemocyte concentration or viability.

As previously stated, the prophenoloxidase pathway is activated upon the build up of free radical species during phagocytosis. The phenoloxidase enzyme is involved in the production of melanin which binds to free radicals (Aladaileh *et al.,* 2007). It was expected that since there was a noticeable increase in phagocytic activity in haemocytes treated with heat killed FITC labelled *V. anguillarum* 5676, there would be a corresponding increase in

phenoloxidase activity over the duration of the challenge trial. However, this was not detected in either extracellular (cell-free haemolymph) or cellular (haemocytes) phenoloxidase enzyme assays. These results corroborate the data obtained from the *in vivo* challenge trial. Gagnaire *et al.* (2004) performed an *in vitro* challenge trial utilising *C. gigas* haemocytes treated with different concentrations of the heavy metal, mercury. The authors found that phenoloxidase activity was significantly lower in haemolymph following exposure to mercury compared to the control (Gagnaire *et al.,* 2004). While this challenge trial was not performed using a pathogen, the serum phenoloxidase activity reported in the control group was similar to that found in this study. No other studies were found that investigate phenoloxidase activity in *in vitro* primary haemocytes challenged with a microbial pathogen.

Phagocytosis is an important mechanism utilised by haemocytes to eliminate invading pathogens in invertebrates (Marmars and Lampropoulou, 2009). The *in vitro* phagocytosis assay detected a significant difference in phagocytic activity between heat killed FITC labelled *V. anguillarum* 5676 treated haemocytes and PBS treated haemocytes. The heat killed FITC labelled *V. anguillarum* 5676 treated haemocytes displayed a significant increase in phagocytic activity at 2 hpi compared to time 0. This was also observed in a study by Mortensen and Glette (1996) where *in vitro* phagocytic ability of *Pecten maximus* (scallop) haemocytes increased over a time course of 1, 2, 3 and 4 hours. This increase agrees with the findings of this study where there was a significant increase in phagocytic activity at 1, 3 and 6 hpi in the heat killed FITC labelled *V. anguillarum* 5676 treated

haemocytes compared to the PBS treated group. Travers *et al.* (2008) observed that *H. tuberculata* haemocytes incubated with zymozam particles increased in phagocytosis ability over time (0, 0.5, 1, 2 and 3 hours), with a dramatic increase occurring at 1 hour compared to time point 0 (Travers *et al.,* 2008).

The results obtained in this study suggest that there was an increase in phagocytic activity in *H. midae* haemocytes upon exposure to heat killed FITC labelled *V. anguillarum* 5676. The phenoloxidase assay mirrored that of the *in vivo* challenge trial in that no trend or significant difference was observed between the treatment groups. The stability of the haemocyte counts and viability, suggests that any changes detected in a physiological response or in mRNA expression levels of a gene is due to the pathogen (in this case heat-killed FITC labelled *V. anguillarum* 5676) and not due to other biological responses that may influence NFκB transcription such as apoptosis. This is important as NFκB is known to be regulated in the apoptosis pathway (Schröder, 2008). In light of this data, *H. midae* haemocytes maintained *in vitro* may be a useful system in which to analyse the immune response to bacterial infection.

The NFκB transcriptional expression studies using qPCR indicated that there was a significant increase in NFκB expression between the treatment groups in the *in vitro* challenge trial. The fold change expression was significantly higher in haemocytes treated with heat killed FITC labelled *V. anguillarum* 5676 compared to PBS treated haemocytes at 1, 2 and 3 hpi. The results suggest that the *H. midae* NFκB homolog is regulated *in vitro*

upon treatment with heat killed FITC labelled *V. anguillarum* 5676. The data also corroborates the *in vivo* results that also detected an increase in NFκB transcription levels; although the increased NFκB expression in the *in vitro* trial occurred at an earlier time point compared to the *in vivo* challenge trial. The earlier response of NFκB *in vitro* may be due to the absence of additional defence strategies that occur *in vivo.* This includes the humoral response, which involves opsonins and agglutinins present in the haemolymph, which combats microbial infection. The haemolymph is removed and replaced with artificial media in the *in vitro* challenge trial that may affect the regulation of immune response. Additionally, the heat-killed pathogen is injected into the muscle of the abalone *in vivo* and would thus take longer for the haemocytes to be exposed to the pathogen rather than *in vitro*, where the haemocytes are directly exposed to the haemocytes. These results provide additional support for the usefulness of a primary haemocyte system as a suitable a tool for studying the abalone immune response to infection at the genetic level as it is sensitive.

The large error in the transcriptional fold change observed for NFκB expression in the heat killed FITC labelled *V. anguillarum* 5676 treated haemocyte group at 2 hpi may be the result of biological variation between the seeded haemocytes (each biological repeat consisted of haemolymph pooled from six abalone). The magnitude of the error may possibly be reduced by performing additional biological repeats as well as utilising a different analytical approach to quantify the real time data. A single reference gene was used in this study and the Pfaffl method (Pfaffl, 2001) of analysis was employed. It is

possible to use multiple reference genes to obtain a reference factor for quantifying the transcript of interest (Hellemans *et al.,* 2007). However, this approach was not possible during this trial as potential reference genes (18s rRNA, elongation factor alpha and 28s rRNA) were found to be differentially expressed in both the *in vitro* and *in vivo* challenge trials (data not shown).

Recent studies have utilised a primary culture system to assess the transcription levels of immune genes. Farcy *et al.* (2007) utilised primary *H. turberculata* haemocytes to detect the effects of temperature on heat shock proteins HSP70 and HSP90. The authors incubated the primary cultures at different temperatures and found an increase in HSP 70 and 90 mRNA expression levels at 25 and 37°C compared to the control temperature of 17°C (Farcy *et al.,* 2007). Cao *et al.* (2007) used primary *M. gallanoprovincialis* haemocytes to assess seasonal variations in haemocyte responses. The authors isolated haemocytes from oysters during the summer and winter months and assayed various immune parameters, such as catecholamine production (dopamine, noradrenaline and adrenaline), and the effect of interleukin 2 (IL-2) on the protein levels of p105 (a protein kinase). The authors found significant differences between the summer and winter haemocytes with respect to catecholamine levels and found that there was differential protein expression levels of p105 in the summer and winter samples when stimulated with IL-2 (Cao *et al.,* 2007). This study indicated that immune changes can be successfully assayed in an *in vitro* system and indicated that future work using primary *H. midae* haemocyte cultures could be extended to investigating protein expression levels of immune genes.

Presently, laboratories are utilising insect cell culture to detect whether anti-microbial genes are regulated by NFκB homologues from marine invertebrates. Huang *et al.* (2009) cloned LvDorsal (NFκB homologue) from *Litopenaeus vannamei* into an expression vector and determined its ability to initiate transcription of anti-microbial genes utilising *Drosophila schneider* 2 (S2) cells. Reporter plasmids containing the 5' flanking region of anti-microbial genes from *L. vannamei* and the full length LvDorsal expression vector were transfected into S2 cells and using a luciferase reporter assay. It was observed that LvDorsal increased the expression of the reporter plasmids via the promoters from the anti-microbial peptides (Huang *et al.*, 2009). The *Drosophila* S2 cell line has been utilised in two other studies. Ho and Song (2009) assessed the mRNA expression levels of anti-microbial peptides in *P. monodon* by transfecting these homologues into S2 cells and Huang *et al.* (2009) transfected a relish homologue (NFκB type I homologue) from *P. monodon* into S2 cells and assessed its ability to regulate transcription via promoters from *P. monodon* anti-microbial peptides.

4.6 CONCLUSION AND FUTURE WORK

The NFκB family of transcription factors are key regulatory genes, which are involved in important processes such as apoptosis, cell division, inflammation and the immune response (Jiang and Wu, 2007). In invertebrate innate immunity, various homologues of NFκB are involved in up-regulating the expression of genes encoding anti-microbial peptides upon infection with a pathogen. In *Drosophila* the NFκB homologue Dorsal is involved in up-regulating anti-microbial peptide genes in response to Gram-positive bacterial and fungal infections (Irving *et al.,* 2004). In marine invertebrates, little is known regarding the mechanistic functions of the immune system; however, class II NFκB homologues have been isolated from *H. diversicolor supertexta* (Jiang and Wu, 2007), *L. vannamei* (Huang *et al*., 2009), *C. gigas* (Montagnani *et al.*, 2004) and the horseshoe crab (Fan *et al.*, 2008). It was found that all homologues were up-regulated either at an mRNA level or at a protein level in response to Gram-negative and Gram-positive bacterial infection.

This study has shown that expression of an *H. midae* NFκB homologue is regulated in haemocytes, *in vitro* and to a lesser extent *in vivo,* upon exposure with the heat killed pathogen *V. anguillarum* 5676. This indicates that this gene may be involved in the immune response of *H. midae* with respect to a Gram-negative bacterial infection, and thus, is a candidate as a biomarker of stress. Haemocytes were successfully maintained *in vitro* for eight days and were partially characterised using various staining techniques. The ability to

successfully conduct challenge trials using *in vitro* abalone haemocytes suggests that this would be an ideal system for studying the immune system of *H. midae* at the genetic and biochemical level.

Two fragments of an NFκB homologue from *H. midae* were PCR amplified over the course of this study; however, it remains unclear whether these amplicons are portions of the same homologue. Future work may include the use of 3' RACE to amplify the 3' region of the RHD amplicon isolated in this study. This method was successfully employed by Jiang and Wu (2007) and Huang *et al.* (2009) to obtain additional sequence information for NFκB homologues from *H. diversicolor supertexta* and *P. monodon,* respectively. Sequencing will determine whether the RHD fragment and the 3' fragment belong to the same homologue. If it is not part of the same homologue, it would be interesting to identify the types of NFκB present in *H. midae* and to determine whether there is a similar arrangement to *Drosophila* which possesses two class II NFκB homologues, Dif and Dorsal (Irving *et al.,* 2004).

Further research is required to determine the relevance of the *H. midae* NFκB homologue as a biomarker of stress. This study demonstrated up-regulation of the NFκB homologue *in vivo* upon exposure to a heat killed Gram-negative pathogen. The response to live and dead Gram-negative bacteria, Gram-positive bacteria, fungi and yeast should be investigated. Montagnani *et al.* (2004) infected *C. gigas* with *E. coli*, *Micrococcus luteus* or a combination of four *Vibrio* strains (*V. anguillarum*, *V. metshnikovii*, *V. tubiashii* and *Vibrio* sp. S322). Various challenge trials with these different infecting agents were performed in order to

determine the regulation of *cg-rel,* an NFκB type II homologue. The authors observed that cg-rel mRNA was not regulated, but the protein expression levels were up-regulated in response to all of the infecting agents at various time points (Montagnani *et al.,* 2004). Jiang and Wu (2007) exposed *H. diversicolor supertexta* to *E. coli* LPS in a nine hour challenge trial with three hour interval time points to determine the regulation of ab-rel. The authors observed that NFκB transcriptional fold change levels increased at 9 hpi. Wang *et al.* (2008) monitored the transcriptional regulation of an NFκB homologue in *H. diversicolor* infected with a cocktail of both live Gram-negative and Gram-positive bacteria and observed that the homologue was upregulated after 36 hpi.

Along with mRNA expression data, protein expression levels should also be investigated for a more thorough understanding of the regulation of the *H. midae* NFκB upon infection. Protein expression levels can be monitored by western blotting and protein ELISAs using antibodies specific to the *H. midae* NFκB homologue.

Flow cytometry can be utilised to confirm the haemocyte types observed in this study. Flow cytometry is able to distinguish cells at both a size and a morphological level (e.g. granule size, nucleus size and cytoplasmic content). This technique analyses each cell individually and plots the data on a scatter plot (Donaghy *et al.,* 2009). Travers *et al.* (2008) performed flow cytometry on *H. turberculata* haemocytes. The authors observed that the haemocytes were composed of two groups, blast-like cells (10% of the population) and large halinocytes (90% of the population). These findings were corroborated with staining

techniques used to identify the cell types (Travers *et al*., 2008). Donaghy *et al*. (2009) found that *H. discus discus* haemocytes consisted of 10 % blast-like cells and 90% halinocytes in the population using flow cytometry and confirmed these results with corresponding staining of the haemocytes (Donaghy *et al*., 2009).

Flow cytometry can also be used to monitor the effect of stress on the *H. midae* haemocyte population. Flow cytometry, a method that can differentiate cell types, may be useful for investigating how the haemocyte population is distributed in response to infection and how this distribution affects physiological responses and the regulation of immune related genes. Parisi *et al.* (2008) observed that different stressors affected haemocyte sub-populations in the mussel *M. galloprovincialis.* Halinocytes and blast-like cells varied in population percentage over the time course of infection when mussels were exposed to Gram-positive and Gram-negative bacteria and their heat killed counterparts (Parisi *et al.,* 2008).

This study provides the first step to gaining a more in-depth understanding of the *H. midae* immune response. Our current knowledge regarding the abalone immune system is limited and largely reliant on data obtained from bivalves that have been more extensively studied (Hooper *et al.,* 2007). Therefore, further insight into the abalone immune system is necessary if genetic tools are to be developed for detection of pathogenic stress within farmed abalone.

REFERENCES

Aladaileh, S., Nair, S. V., and Raftos, D. A. (2007). Induction of phenoloxidase and other immunological activities in Sydney rock oysters challenged with microbial pathogen-associate molecular patterns. Fish and Shellfish Immunology 23, 1196-1208.

Ausubel, F., Brent, R., Kingston, R., Moore, D., Seidman, J., Smith, J., and Struhl, K. (1989). Current Protocols in Molecular Biology, Volume One; New York: Greene Publishing Associates and Wiley-Interscience. ISBN: 0-471-50338-X

Bachère, E. (2003). Anti-infectious immune effectors in marine invertebrates: potential tools for disease control in larviculture. Aquaculture 227, 427-438.

Bettencourt, R., Dando, P., Collins, P., Costa, V., Allam, B., and Santos, R. (2009). Innate immunity in the deep sea hydrothermal vent mussel Bathymodiolus azoricus. Comparative Biochemistry and Physiology 152, 278-289.

Bosch, T. C., Augustin, R., Anton-Erxleben, F., Fraune, S., Hemmrich, G., Zill, H., Rosenstiel, P., Jacobs, G., Schreiber, S., Leippe, M., Stanisak, M., Grotzinger, J., Jung, S., Podschun, R., Bartels, J., Harder, J., and Schroder, J-M. (2009). Uncovering the evolutionary history of innate immunity: The simple metazoan Hydra uses epithelial cells for host defence. Developmental and Comparative Immunology 33, 559-569.

Bosisio, D., Marazzi, I., Agresti, S., Shimizu, N., Bianchi, M., and Natoli, G. (2006). A Hyper-dynamic equilibrium between promoter bound and nucleoplasmic dimmers controls NF-κB dependent gene activity. The European Molecular Biology Organization Journal 25, 798-810.

Branch, G., Griffith, C., Branch, M., and Beckely, L. (1994). Two Oceans: A guide to the marine life of Southern Africa 1 ed. (Cape Town: David Phillip Publishers).

Bugge, D. M., Hlégaret, H., Wikfors, G. H., and Allam, B. (2007). Oxidative burst in hard clam (Mercenaria mercenaria) haemocytes. Fish and Shellfish Immunology 23, 188-196.

Busse, M. S., Arnold, C. P., Towb, P., Katrivesis, J., and Wasserman, S. A. (2007). A kappaB sequence code for pathway-specific innate immune responses. The EMBO journal 26, 3826-35.

Butt, D., and Raftos, D. (2008). Phenoloxidase-associated cellular defence in the Sydney rock oyster, Saccostrea glomerata, provides resistance against QX disease infections. Developmental and Comparative Immunology 32, 299-306.

Caamaño, J., and Hunter, C. (2002). NF-κB Family of Transcription Factors: Central Regulators of Innate and Adaptive Immune Functions. Clinical Microbiology Reviews, 414-149.

Camino Ordas, M., Ordas, A., Beloso, C., & Figueras, A. (2000). Immune parameters in carpet shell clams naturally infected with Perkinsus atlanticus. Fish and Shellfish Immunology, *10*, 597-609. DOI: 10.1006/fsim.2000.0274.

Canesi, L., Betti, M., Ciacci, C., Lorusso, L. C., Gallo, G., and Pruzzo, C. (2005). Interactions between Mytilus haemocytes and different strains of Escherichia coli and Vibrio cholerae O1 El Tor: role of kinase-mediated signalling. Cellular Microbiology 5, 667-674.

Cao, A., Novas, J., Ramoos-Martinez, J., and Barcia, R. (2007). Seasonal variations in haemocyte response in the mussel Mytilus galloprovincialis Lmk. Aquaculture 263, 310 - 319.

Charoensapsri, W., Amparyup, P., Hirono, I., Aoki, T., and Tassanakajon, A. (2009). Gene silencing of a prophenoloxidase activating enzyme in the shrimp, Penaeus monodon, increases susceptibility to Vibrio harveyi infection. Developmental and Comparative Immunology 33, 811-820.

Chen, H., Mai, K., Zhang, W., Liufu, Z., Xu, W., and Tan, B. (2005). Effects of dietary pyridoxine on immune responses in abalone, Haliotis discus hannai Ino. Fish and Shellfish Immunology 19, 241-252.

Cheng, W., Hsiao, I., Hsu, C., and Chen, J. (2004). Change in water temperature on the immune response of Taiwan abalone Haliotis diversicolor supertexta and its susceptibility to Vibrio parahaemolyticus. Fish and Shellfish Immunology 17, 235-243.

Cima, F., Matozzo, V., Marin, M., and Ballarin, L. (2000). Haemocytes of the clam Tapes phillippinarum (Adams & Reeve, 1850): morphofunctional characterisation. Fish and Shellfish Immunology 10, 677-693.

Costa, A. M., Buglione, C. C., Bezerra, F. L., Martins, P. C., and Barracco, M. A. (2009). Immune assessment of farm-reared Penaeus vannamei shrimp naturally infected by IMNV in NE Brazil. Aquaculture 291, 141-146.

Donaghy, L., Lambert, C., Choi, K., and Soudant, P. (2009). Hemocytes of the carpet shell clam (Ruditapes decussatus) and the Manila clam (Ruditapes philippinarum): Current knowledge and future prospects. Aquaculture. DOI: 10.1016/j.fsi.2009.10.006

Fan, Z. H., Wang, X. W., Lu, J., Ho, B., and Ding, J. L. (2008). Elucidating the Function of an Ancient NF-kB p100 Homologue, CrRelish, in Antibacterial Defense. Immunity and Infection 76, 664-670.

Farcy, E., Serpentini, A., Fiévet, B., and Lebel, J. (2007). Identification of cDNAs encoding HSP70 and HSP90 in the abalone Haliotis tuberculata: Transcriptional induction in response to thermal stress in hemocyte primary culture. Comparative Biochemistry and Physiology 146, 540 - 550.

Gagnaire, B., Thomas-Guyon, H., and Renault, T. (2004). In vitro effects of cadmium and mercury on Pacific oyster, Crassostrea gigas (Thunberg), haemocytes. Fish and Shellfish Immunology 16, 501-512.

Gopalakrishnan, S., Thilagam, H., Huang, W., and Wang, K. (2009). Immunomodulation in the marine gastropod Haliotis diversicolor exposed to benzo(a)pyrene. Chemosphere, DOI: 10.1016/j.chemosphere.2008.12.027

Gueguen, Y., Cadoret, J., Flament, D., Barreau-roumiguie, C., Girardot, A., Garnier, J., Hoareau, A., Bachère, E., and Escoubas, J. (2003). Immune gene discovery by expressed sequence tags generated from hemocytes of the bacteria-challenged oyster, Crassostrea gigas. Gene 303, 139-145.

Hellemans, J., Mortier, G., De Paepe, A., Speleman, F., and Vandesompele, J. (2007). qBase relative quantification framework and software for management and automated analysis of real-time quantitative PCR data. Genome biology 8, R19.

Ho, S., and Song, Y. (2009). Cloning of penaeidin gene promoter in tiger shrimp (Penaeus monodon). Fish and Shellfish Immunology 27, 73-7.

Hooper, C., Day, R., Slocombe, R., Handlinger, J., and Benkendorff, K. (2007). Stress and immune responses in abalone: limitations in current knowledge and investigative methods based on other models. Fish and Shellfish Immunology 22, 363-379.

Huang, X. Yin, Z-X., Jia, X-T., Liang, J. P., Ai, H. S., Yang, L-S.,Liu, X., Wang, P-H., Weng, S-P., Yu, X.P., and He, J. (2009). Identification and functional study of a shrimp Dorsal homologue. Developmental and Comparative Immunology. DOI: 10.1016/j.dci.2009.08.009

Iakovleva, N. V., Gorbushin, A. M., and Storey, K. B. (2006). Modulation of mitogen-activated protein kinases (MAPK) activity in response to different immune stimuli in haemocytes of the common periwinkle Littorina littorea. Fish and Shellfish Immunology 21, 315-324.

Irving, P., Troxler, L., and Hetru, C. (2004). Is innate enough? The innate immune response in Drosophila. Comptes Rendus Biologies 327, 557-570.

Jiang, Y., Zhan, W., Wang, S., and Xing, J. (2006). Development of primary shrimp haemocyte cultures of Penaeus chinensis to study white spot syndrome virus (WSSV) infection. Aquaculture 253, 114-119.

Jiang, Y., and Wu, X. (2007). Characterization of a Rel\NF-kB homologue in a gastropod abalone, Haliotis diversicolor supertexta. Developmental and Comparative Immunology 31, 121-131.

Khush, R. S., Leulier, F., and Lemaitre, B. (2001). Drosophila immunity:two paths to NF-κB. Trends in Immunology 22, 260-264.

Kurata, S., Ariki, S., and Kawabata, S. (2006). Recognition of pathogens and activation of immune responses in Drosophila and horseshoe crab innate immunity. Immunobiology 211, 237-249.

Lebel, J., Giard, W., Favrel, P., and Boucaud-camou, E. (1996). Effects of different vertebrate growth factors on primary cultures of hemocytes from the gastropod mollusc, Haliotis tuberculata. Biology of the cell 86, 67-72.

Loker, E., Adema, C., Zhang, S., and Kelper, T. (2004). Invertebrate immune systems-not homogonous, not simple, not well understood. Immunological Reviews 198, 10-24.

Malham, S., Lacoste, A., Gelebart, F., Cueff, A., and Poulet, S. (2003). Evidence for a Direct Link Between Stress and Immunity in the Mollusc Haliotis tuberculata. Journal of Experimental Zoology 295A, 136-144.

Marmaras, V. J., and Lampropoulou, M. (2009). Regulators and signalling in insect haemocyte immunity. Cellular Signalling 21, 186-195.

Martello, L., Friedman, C., and Tjeerdema, R. (2003). Combined effects if pentachlorophenol and salinity stress on phagocytic and chemotatic function in two species of abalone. Aquatic Toxicology 49, 213-225.

Mason, N., Artis, D., and Hunter, C. (2004). New lessons from old pathogens: what parasitic infections have taught us about the role of nuclear factor-κB in the regulation of immunity. Immunological Reviews 201, 48-56.

Matozzo, V., Marin, M. G., Cima, F., and Ballarin, L. (2008). First evidence of cell division in circulating haemocytes from the Manila clam Tapes philippinarum. Cell Biology International. DOI: 10.1016/j.cellbi.2008.03.008

Meng, X., Khanuja, B., and Ip, Y. (1999). Toll receptor-mediated Drosophila immune response requires Dif, and NF-κB factor. Genes and Development 13, 792-797.

Montagnani, C., Kappler, C., Reichhart, J., and Escoubas, J. (2004). Cg-Rel, the first Rel/NF-κB homolog characterized in a mollusk, the Pacific oyster Crassostrea gigas. FEBS Letters 561, 75-82.

Mortensen, S., and Glette, J. (1996). Phagocytic activity of scallop (Pecten maximus) haemocytes maintained in vitro. Fish and Shellfish Immunology 6, 111-121.

Nikapitiya, C., Zoysa, M. D., and Lee, J. (2008). Molecular characterization and gene expression analysis of a pattern recognition protein from disk abalone, Haliotis discus discus. Fish and Shellfish Immunology 25, 638-647.

Novas, A., Barcia, R., and Ramoos-Martinez, J. (2007). Nitric oxide production by haemocytes from Mytilus galloprovincialis shows seasonal variations. Fish and Shellfish Immunology 23, 886-891.

Ordas, M., Ordas, A., Beloso, C., and Figueras, A. (2000). Immune parameters in carpet shell clams naturally infected with Perkinsus atlanticus. Fish and Shellfish Immunology 10, 597-609.

Parisi, M., Li, H., Jouvet, L. B., Dyrynda, E. A., Parrinello, N., Cammarata, M., and Roch, P. (2008). Differential involvement of mussel hemocyte sub-populations in the clearance of bacteria. Fish and Shellfish Immunology 25, 834-840.

Perkins, N. (2000). The Rel/ NF-κB family: friend and foe. Trends in Biochemical Sciences 25, 434-440.

Pfaffl, M. W. (2001). A new mathematical model for relative quantification in real-time RT-PCR. Nucleic acids research 29, 2002-2007

Proudfoot, L. (2006). Population structure, growth and recruitment of two exploited infralittoral molluscs (Haliotis midae and Turbo sarmaticus) along the South East Coast, South Africa, MSc Thesis, Rhodes University Press.

Reddy-Lopata, K., Auerswald, L., and Cook, P. (2006). Ammonia toxicity and its affect on the growth of the South African abalone Haliotis midae Linnaeus. Aquaculture 261, 678-687.

Schröder, M. (2008). Endoplasmic reticulum stress responses. Cellular and Molecular Life Sciences 65, 862 - 894.

Suja, C. P., and Dharmaraj, S. (2005). In vitro culture of mantle tissue of the abalone Haliotis varia Linneaeus. Tissue and Cell 27, 1-10.

Ten Doeschate, K., and Coyne, V. (2008). Improved growth rate in farmed Haliotis midae through probiotic treatment. Aquaculture 284, 174-179.

Tincu, J., and Taylor, S. (2004). Antimicrobial peptides from Marine Invertebrates. Antimicrobial Agents and Chemotherapy 48, 3645-3654.

Travers, M., da Silva, P., le Goıc, N., Marie, D., Donval, A., Huchette, S., Koken, M., and Paillard, C. (2008). Morphologic, cytometric and functional characterisation of abalone (Haliotis tuberculata) haemocytes. Fish and Shellfish Immunology 24, 400-411.

Troell, M., Robertson-Andersson, D., Anderson, R. J., Bolton, J., Maneveldt, G., Halling, C., and Probyn, T. (2006). Abalone farming in South Africa: An overview with perspectives on kelp resources, abalone feed, potential for on-farm seaweed production and socio-economic importance. Aquaculture 257, 266 - 281.

Wang, K., Ren, H., Xu, D., Cai, L., and Yang, M. (2008). Identification of the up-regulated expression genes in hemocytes of variously colored abalone (Haliotis diversicolor Reeve, 1846) challenged with bacteria. Developmental and Comparative Immunology 32, 1326-1347.

Wootton, E. C., and Pipe, R. K. (2003). Structural and functional characterisation of the blood cells of the bivalve mollusc, Scrobicularia plana. Fish and Shellfish Immunology 15, 249-262.

Wootton, E., Dyrynda, E., and Ratcliffe, N. (2003). Bivalve immunity: comparisons between the marine mussel (Mytilus edulis), the edible cockle (Cerastoderma edule) and the razor-shell (Ensis siliqua). Fish and Shellfish Immunology 15, 195-210.

APPENDIX A

SOLUTIONS AND MEDIA

MEDIA AND SOLUTIONS

A.1 General media 119

A.1.1 Luria Broth (LB) 119

A.1.2 Tryptone Soy Broth (TSB) 119

A.1.3 Sea salts 119

A.1.4 Phosphate Buffered Saline (PBS) 120

A.1.5 Luria Agar (LA) 120

A.1.6 Tryptone Soy Agar (TSA) 120

A.1.7 Ampicillin stock solution 121

A.2 Physiological assay solutions 121

A.2.1 L-DOPA 121

A.2.2 Na-alginate 121

A.2.3 MTT stock solution (5mg/ml) 121

A.2.4 Acidic isopropanol 122

A.2.5 Alsever's solution 122

A.2.6 FITC Labelling of bacteria 122

A.2.6.1 $NaHCO_3$ 122

A.2.6.2 FITC isomer 1 stock solution 122

A.2.7 Modified Hank's Buffered Saline Solution (MHBSS) 123

A.2.8 Ethidium bromide 123

A.2.9 Trypan blue stock solution 123

A.3 RNA isolation solutions 124

A.3.1 Diethylpyrocarbonate water (DEPC water) 124

A.3.2 RNA lysis buffer 124

A.3.3 Sodium acetate 2M stock solution 124

A.3.4 Sodium Citrate 1M stock solution 124
A.3.5 Sodium citrate 5M stock solution 125
A.3.6 10 X MOPS Buffer 125
A.3.7 RNA sample buffer and tracking dye 125
A.3.6 1.2% RNA formaldehyde gel 126
A.4 Haemocyte Culture Solutions 126
A.4.1 Supplementary salt solution 126
A.4.2 Hank's M199 modified media 126
A.4.3 Amphotericin B stock solution 127
A.4.4 Hank's M199 Media with antibiotics 127

A.1.1 LURIA BROTH (LB)

NaCl (Saarchem)	10 g
Tryptone (Saarchem)	10 g
Yeast extract (Saarchem)	5 g
dH_2O to	1 *l*

Autoclave

For LB with ampicillin add 1µl of a 1mg/ml ampicillin stock solution per millilitre of LB after media has been autoclaved.

A.1.2 TRYPTONE SOY BROTH (TSB)

Tryptone Soy Broth (Saarchem)	30 g
NaCl	25 g
dH_2O to	1 *l*

Autoclave

A.1.3 SEA SALTS

NaCl	30 g
$MgCl_2.6H_2O$ (Saarchem)	2.3 g
KCl (Saarchem)	0.3 g
dH_2O to	1 *l*

Autoclave

A.1.4 PHOSPHATE BUFFERED SALINE

NaCl	8 g
KCl	0.2 g
Na_2HPO_4 (Saarchem)	1.44 g
dH_2O to	1 *l*

Adjust to pH 7.4 with HCl

Autoclave

A.1.5 LURIA AGAR

NaCl (Saarchem)	10 g
Tryptone (Saarchem)	10 g
Yeast extract (Saarchem)	5 g
Bacteriological Agar (Saarchem)	15 g
dH_2O to	1 *l*

Autoclave

Pour into petri dishes once cooled

For Ampicillin plates, add 1 ml of 1 mg/ml Ampicillin after autoclaving per litre of media

For X-gal agar: add 2 ml of a 20 % (*w/v*) X-gal after autoclaving per litre of media

Store agar at 4°C

A.1.6 TRYPTONE SOY AGAR (TSA)

Tryptone Soy Broth (Saarchem)	38 g
NaCl	25 g
dH_2O to	1 *l*

Autoclave

A.1.7 AMPICILLIN STOCK SOLUTION

Ampicillin (Sigma)	1 mg/ml in dH_2O

Filter sterilise (0.22 µm filter) and aliquot into 1 ml microfuge tubes

Store at -20°C

A.2 PHYSIOLOGICAL ASSAY SOLUTIONS

A.2.1 L-DOPA

L-DOPA (Sigma)	30 mg
dH_2O to	10 ml

Vortex vigorously for 5 minutes

Filter Sterilise (0.22µm filter) and cover container with tin foil as solution is light sensitive

Make fresh for each assay

A.2.2 NA-ALGINATE

Sodium Alginate (Sigma)	2.5 mg
dH_2O	5 ml

Heat to dissolve Na Alginate

Filter sterilise (0.22µm filter)

A.2.3 MTT STOCK SOLUTION (5MG/ML)

MTT (Sigma)	50 mg
1 X PBS to	10 ml

Filter Sterilise (022 µm filter) and store at 4°C.

Cover container with tin foil as the solution is light sensitive

Dilute to 1mg/ml with 1 X PBS when performing the serum anti-bacterial assay

A.2.4 ACIDIC ISOPROPANOL

0.4 M HCl (Merck)	2 ml
Isopropanol (Saarchem)	50 ml

A.2.5 ALSEVER'S SOLUTION

Glucose (Saarchem)	20.8 g
Na-Citrate (Saarchem)	8 g
EDTA (Sigma)	3.36 g
NaCl	22.4 g
Formaldehyde (37%) (Saarchem)	120 ml
dH_2O to	1 *l*

Adjust to pH 7.5

Autoclave

A.2.6 FITC LABELLING OF BACTERIA

A.2.6.1 $NAHCO_3$

$NaHCO_3$ (Saarchem)	0.1 M in dH_2O

Adjust to pH 9

Autoclave

A.2.6.2 FITC ISOMER 1 STOCK SOLUTION

FITC-1 isomer (Sigma)	1 mg/ml in 1 X PBS

Filter sterilise with a 0.22 µm filter and store at 4°C

Cover container with tin foil as solution is light sensitive.

A.2.7 MODIFIED HANK'S BUFFERED SALINE SOLUTION (MHBSS)

Glucose	10.4 g
NaCl	11.2 g
KH_2PO_4(Saarchem)	0.1 g
$CaCl_2.2H_2O$ (Saarchem)	0.47 g
$MgCl_2.6H_2O$ (Saarchem)	2.8 g
$MgSO_4.7H_2O$ (Saarchem)	3.22 g
dH_2O to	1 *l*

Adjust to pH 7.2 using 0.5 M NaOH

Autoclave

A.2.8 ETHIDIUM BROMIDE

For phagocytosis assay:

Ethidium Bromide (Sigma)	100 µg/ml in 1 X PBS

Autoclave

For agarose gels:

Ethidium bromide	10 mg/ml in sterile dH_2O

Autoclave

Add 2 µl per 50 ml of agarose gel

A.2.9 TRYPAN BLUE STOCK SOLUTION

Trypan Blue (Sigma)	2 % (*w/v*) in 1 X PBS

Filter sterilise (0.22 µm filter)

A.3 RNA ISOLATION SOLUTIONS

A.3.1 DIETHYLPYROCARBONATE WATER (DEPC WATER)

DEPC (Sigma ®)	1 ml
2 X autoclaved dH_2O to	1 *l*

Shake solution vigorously and leave overnight for the DEPC to fully re-suspend into the water

A.3.2 RNA LYSIS BUFFER

Guanidium Isothiocyanate (Sigma ®)	4.7 g
Sodium Citrate (1M, pH)	0.25 ml
Sarkosyl (10% *w/v* in dH_2O) (Saarchem)	0.5 ml
B-mercaptoethanol (Sigma)	70 µl
DEPC-water	9.18 ml

Filter sterilise (0.22 µm filter) before the addition of β-mercaptoethanol

Make fresh for each assay

A.3.3 SODIUM ACETATE 2M STOCK SOLUTION

Sodium acetate trihydrate (Saarchem)	27.21 g
dH_2O to	100 ml

Adjust to pH 4

Autoclave twice

A.3.4 SODIUM CITRATE 1M STOCK SOLUTION

1 M Sodium citrate (Saarchem) in dH_2O

Adjust to pH 4

Autoclave twice

A.3.5 SODIUM CITRATE 5M STOCK SOLUTION

5 M Sodium Citrate in dH_2O

Adjust to pH 5.2

Autoclave twice

A.3.6 10 X MOPS BUFFER

MOPS (Sigma)	20 g
NA Acetate	1 g
EDTA (0.5M, pH8)	10 ml
DEPC-H_2O	470 ml

Adjust to pH 7 with NaOH and filter sterilise (0.22 µm filter).

A 1 X solution of this was used as the running buffer for the RNA formaldehyde gels

A.3.7 RNA SAMPLE BUFFER AND TRACKING DYE

10 X MOPS	300 µl
Formaldehyde (37%)	80 µl
Formamide (Saarchem)	900 µl
Ethidium Bromide (10mg/ml) (Sigma)	2 µl
Dye	220 µl

The dye was made up of the following:

Xylene cyanol (Saarchem)	50 mg
Bromophenol blue (Saarchem)	50 mg

DEPC-H_2O	1 ml

A.3.6 1.2% RNA FORMALDEHYDE GEL

Agarose (Saarchem)	0.72 g
DEPC water	43.92 ml

Heat first until agarose dissolves and cool to 60°C before adding;

10XMOPS pH 7	6 ml
Formaldehyde (37%)	10.08 ml

Pour gel and leave to set

A.4 HAEMOCYTE CULTURE SOLUTIONS

A.4.1 SUPPLEMENTARY SALT SOLUTION

NaCl	102.4 g
KCl	1.8 g
$CaCl_2$	5.1 g
$MgSO_4$	16.7 g
$MgCl_2$	11.8 g

Add dH_2O to 1 *l* and autoclave twice

A.4.2 HANK'S M199 MODIFIED MEDIA

M-199 (Gibco)	0.161 g
Supplementary Salt Solution	12.5 ml

Sterile Mili Q water	37.5 ml

Filter sterilise into sterilins using a 0.22 μm filter under the lamina flow hood

A.4.3 AMPHOTERICIN B STOCK SOLUTION

Amphotericin B (Sigma)	1 mg/ml in DMSO

Filter sterilise (0.22 μm) under the lamina flow hood

Dilute to a 0.1 mg/ml working stock solution and store at -20°C

Cover aliquots with tin foil as the solution is light sensitive

A.4.4 HANK'S M199 MEDIA WITH ANTIBIOTICS

Hanks M199 modified media	49.45 ml
Penicillin G/Streptomycin (Invitrogen)	500 μl
Amphotericin B (0.1 mg/ml)	50 μl

Make solution under the lamina flow hood and filter sterilise (0.22 μm filter) solution

Store at 4°C.

APPENDIX B

STANDARD METHODS AND PCR PROFILES

CONTENTS

B.1.1 Mini preparation of plasmid DNA by alkaline lysis ..... ……129

B.1.2. Solutions for plasmid isolation 130

B.2.1. Genomic DNA isolation ..... ……131

B.2.2 Solutions for genomic DNA isolation 132

B 3.1 Standard amplification format and PCR profiles ..... ……133

B.3.2. PCR profiles 134

B.1.1 MINI PREPARATION OF PLASMID DNA BY ALKALINE LYSIS

Plasmid isolation was adapted from the alkaline method as described by Sambrook *et al.* (1989). 5 ml *E. coli* DH5α in LB with ampicillin (Appendix A) cultured for approximately 16 hours at 37°C. Cultures were aliquoted into 2 ml microfuge tubes, centrifuged for 1 minute at 10 000 X *g* and the supernatant removed. This was repeated until all 5 ml of the culture was used and the bacterial cells concentrated in a 2 ml microfuge tube. The cells were resuspended in 0.2 ml solution 1 (Appendix B.1.2.1) and incubated at room temperature for 10 minutes. 0.4 ml of solution 2 (Appendix B.1.2.2) was subsequently added and allowed to incubate on ice for 10 minutes. 0.6 ml ice cold solution 3 (Appendix B.1.2.3) was added to the microfuge tube and incubated for 10 minutes on ice to precipitate the genomic DNA. The resultant mixture was centrifuged for 10 minutes at 12 000 X *g* and the supernatant removed and transferred into clean 1.5 ml microfuge tubes. 1 volume of isopropanol was added to the supernatant containing the plasmid DNA, in order to precipitate the plasmid DNA. The solution was mixed by inversion and incubated for 10 minutes at room temperature. The solution was centrifuged for 5 minutes at 10 000 X *g* and the supernatant removed. The genomic DNA was retained and washed with 70% ethanol by inversion and air dried for 5 minutes to allow the excess ethanol to evaporate. The genomic DNA was re-suspended in 50 µl sterile dH_2O.

B.1.2. SOLUTIONS FOR PLASMID ISOLATION

B.1.2.1. SOLUTION 1 10 X STOCK SOLUTION

Tris-Cl (1 M, pH 8) (Sigma)	25 ml
Glucose (20 % *w/v*)	45.5 ml
EDTA (0.5 M, pH 8)	20 ml
dH_2O	9.5 ml

Autoclave solutions separately and make in a sterile universal container.

B.1.2.2 SOLUTION 2

NaOH (10N) (Saarchem)	2 ml
25 % (*w/v*) Sodium dodecyl sulfate (SDS) (Saarchem)	4 ml
dH_2O	94 ml

Make solution fresh before mini prep

B.1.2.3. SOLUTION 3

K-acetate (Saarchem)	147 g
dH_2O to	250 ml

Adjust to pH 4.8 with glacial acetic acid and make up to a final volume of 500 ml.

Autoclave

B.2.1. GENOMIC DNA ISOLATION

The haemolymph was taken from the pedal sinus of the abalone using a 21 G X 1½″ sterile hypodermic needle (Uniqiao, Wupro Tech.) attached to a sterile 2.5 ml syringe. The blood was centrifuged at 8000 X *g* for 10 minutes to pellet the haemocytes. The serum was discarded and the haemocytes were washed with 1 X PBS. The haemocytes were resuspended in an extraction buffer (Appendix B 2.2.2) and incubated at 37°C for 1 hour. One hundred microlitres of 5 M NaCl (Appendix B 2.2.3) and 80 µl CTAB/NaCl (Appendix B.2.2.4) was added and the solution incubated at 65°C for 10 minutes. An equal volume of chloroform:isoamyl (24:1) was added and the samples centrifuged for 5 minutes at 5000 X *g*. The aqueous phase was removed and aliquoted into fresh microfuge tubes where 0.6 volume of isopropanol was added and resultant solution mixed by inversion. The sample was centrifuged for 15 minutes at 5000 X *g*. The supernatant was discarded and the plasmid DNA washed with 70% ethanol and centrifuged for 5 minutes at 5000 X *g*. The plasmid DNA was air dried for 5-10 minutes to allow the excess ethanol to be evaporated and subsequently resuspended in Tris/EDTA buffer (Appendix B2.2.1) with 1 µl of 10 mg/ml (*w/v)* RNase A (Sigma) to degrade RNA in the solution. Genomic DNA was quantitated on a spectrophotometer (NanoDrop® ND-1000 Spectrophotometer, NanoDrop 1000 software version 3.7.1).

B.2.2 SOLUTIONS FOR GENOMIC DNA ISOLATION

B.2.2.1 TRIS/EDTA BUFFER

Tris-Cl (1M, pH 8)	1 ml
EDTA (0.5M, pH 8)	200 µl
dH_2O to	100 ml
Autoclave	

B.2.2.2 EXTRACTION BUFFER

Tris/EDTA buffer	567 µl
10% (*w/v*) SDS	30 µl
20m/ml Proteinkinase K (Sigma)	3 µl

B.2.2.3 SODIUM CHLORIDE 5M

NaCl	29.22 g
dH_2O	100 ml
Autoclave	

B.2.2.4 CTAB/NACL

NaCl	4.1 g
CTAB (Saarchem)	10 g
dH_2O	100 ml
Autoclave	

B 3.1 STANDARD AMPLIFICATION FORMAT AND PCR PROFILES

Amplification reactions used in this study were set up as follows with the only exception of the magnesium ($MgCl_2^{2+}$) concentration differing for each primer set used:

One microlitre of cDNA or RNA was amplified with 0.3 µM of each appropriate primer pair (Table 2) using the XP thermocycler (Bioer). Twenty microlitre reactions were performed using 0.5 U of Supertherm Taq polymerase (Southern Cross Biotechnology), 2 µl 10 X Taq polymerase buffer, $MgCl_2^{2+}$ and equal amounts of all four dNTPs (0.25 µM each).

6 X tracking dye was added to all PCR products and were visualised on 1 X TAE agarose gels (1.2 – 2% *w/v*) with ethidium bromide (0.4µg/ml) (Sambrook *et al.,* 1989) electrophoresed at 100 V in 1X TAE buffer. The Fermentas 100 bp Range O' Ruler (Fermentas) or a standard Lambda DNA with *Pst*I digestion (Sambrook *et al.,* 1989) was used to track molecular sizes of the products. The gels were visualised using a short wavelength UV light box (Biorad GelDoc EQ-system™, Biorad Laboratories) and the images were captured using the Quantity One® Software (Version 1.7, Biorad Laboratories).

3.2.1 RIBOSOMAL FACTOR L28 AMPLIFICATION

One microlitre RNA was used in a subsequent Ribosomal factor L28 PCR amplification to ensure that there was no contamination by genomic DNA before subsequent cDNA synthesis. A standard PCR reaction was setup with 3mM $MgCl^{2+}$

	Initial denaturation	95˚C for 5 minutes
35 cycles	Denaturation	95˚C for 30 seconds
	Annealing	60˚C for 30 seconds
	Elongation	72˚C for 30 seconds
	Final elongation	72˚C for 5 minutes

3.2.2 M13 FORWARD AND REVERSE AMPLIFICATION

One microlitre of plasmid DNA (1 ng/µl) was used as template in a standard PCR reaction with 3mM $MgCl^{2+}$ concentration.

	Initial denaturation	95˚C for 5 minutes
35 cycles	Denaturation	95˚C for 30 seconds
	Annealing	55˚C for 30 seconds
	Elongation	72˚C for 40 seconds
	Final elongation	72˚C for 5 minutes

3.2.3 18S RIBOSOMAL RNA AMPLIFICATION FOR GENOMIC DNA CONTAMINATION OF RNA

One microlitre RNA was used in a 18s rRNA amplification to ensure that there was no contamination by genomic DNA before subsequent cDNA synthesis. A standard PCR reaction was setup with 3mM $MgCl^{2+}$

	Initial denaturation	95˚C for 5 minutes
35 cycles	Denaturation	95˚C for 30 seconds
	Annealing	60˚C for 30 seconds
	Elongation	72˚C for 30 seconds
	Final elongation	72˚C for 5 minutes

APPENDIX C

PLASMID MAPS

CONTENTS

C.1 Fermentas PZ5R/T Cloning Vector 137

C.2 PDNR-Lib Clontech 138

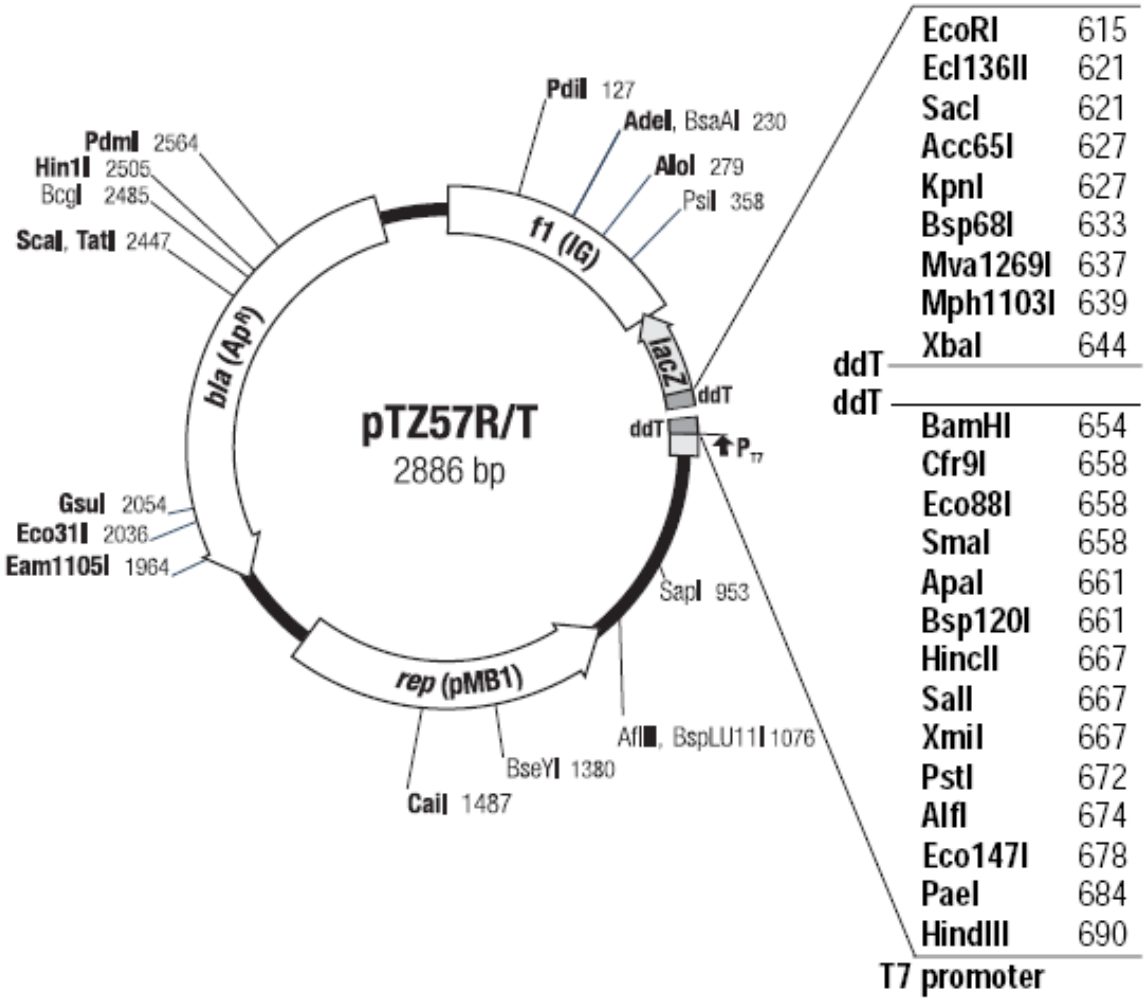

Figure C 1: PTZ57R/T cloning vector used to clone both 5' and 3' amplicons of an NFκB homologue.

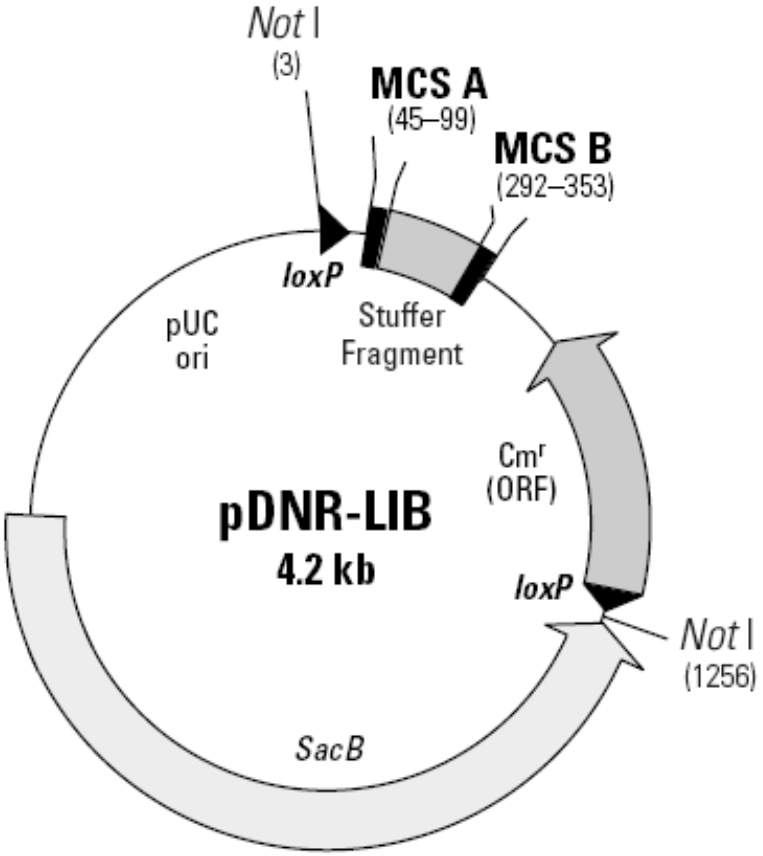

Figure C 2: pDNR-lib used to clone the ribosomal factor L28 by Bronwyn Arendze

APPENDIX D

RNA AND QPCR CONTROLS

CONTENTS

D 1 RNA Controls ..... ……140

D.1.1 RNA integrity 141

D.1.2 gDNA contamintation in RNA for *in vivo* trial 144

D 1.3 gDNA contamination in RNA from *in vitro* challenge trial 145

D 2 qPCR Profiles ..... ……145

D.2.1 qPCR Profiles for *in vivo* trials 146

D 2.2 qPCR Profiles for the *in vitro* challenge trial 149

D 1 RNA CONTROLS

Total RNA integrity was assessed utilising either an RNA formaldehyde gel or the Bioanalyser (2100 Bioanalyser, Agilent Technologies). The images taken for biological repeat 1 and 3 were unfortunately over exposed and clearer images could not be obtained. RNA quantitation for biological repeats 1 and 3 were assessed spectrophotometrically and unequal loading seen in these images may be due to pipeting error and poor exposure used to visualise these images. Throughout the duration of the study, high quality RNA, with no genomic DNA contamination was difficult to isolate. The RNA used in this study represents the highest quality that could be isolated from the challenge trials.

The *H. midae* total RNA profile does not display the 18s rRNA and the 28s rRNA bands separately. This is due to the fact that it appears as a doublet as observed in Figure D 1 and D 2. The electropheregrams (Figure D 4) indicate this too. Quality was assessed by the quantity of total RNA isolated and the presence of the 18s/28s doublet.

The Bioanalyser (Agilent) RNA results for biological repeat 2 indicate the variability of the RNA isolated utilising the same technique and quantity of starting material. The images in Figure D 3 indicate the best total RNA isolated from biological repeat 2.

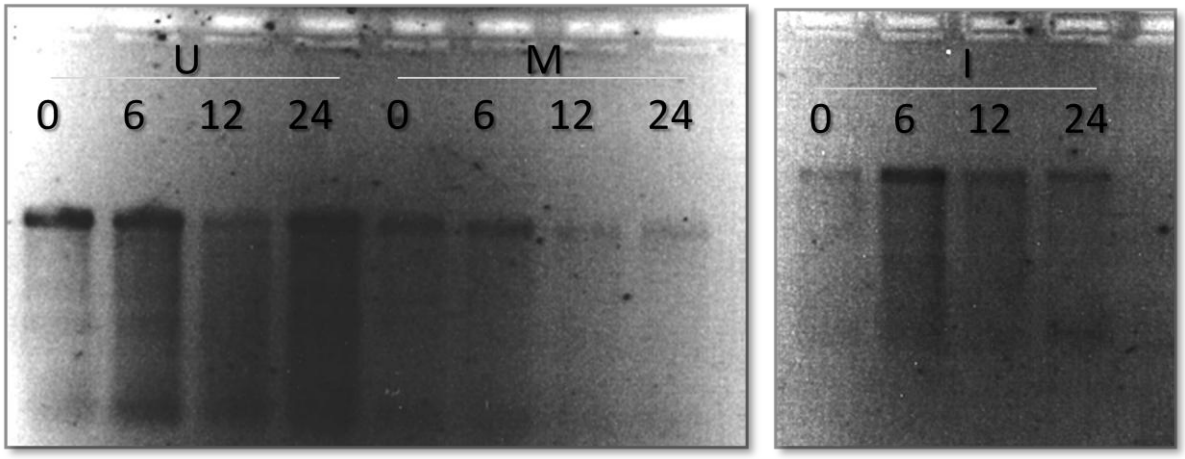

Figure D 1: RNA formaldehyde gel. RNA isolated for biological repeat 1 in the *in vivo* trial at the different time points, 0, 6, 12 and 24 hpi. Abbreviations: U: Unchallenged, M: Mock Infected and I: Infected.

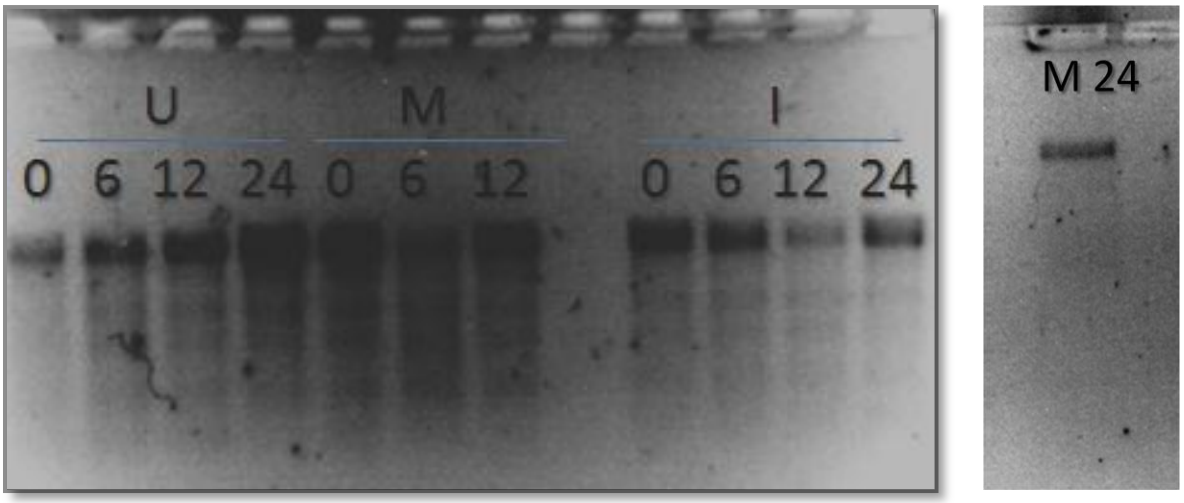

Figure D 2: RNA Formaldehyde gel. RNA isolated in the third biological repeat in the *in vivo* challenge trial at the different time points, 0, 6, 12 and 24 hpi. Abbreviations: U: Unchallenged, M: Mock Infected and I: Infected.

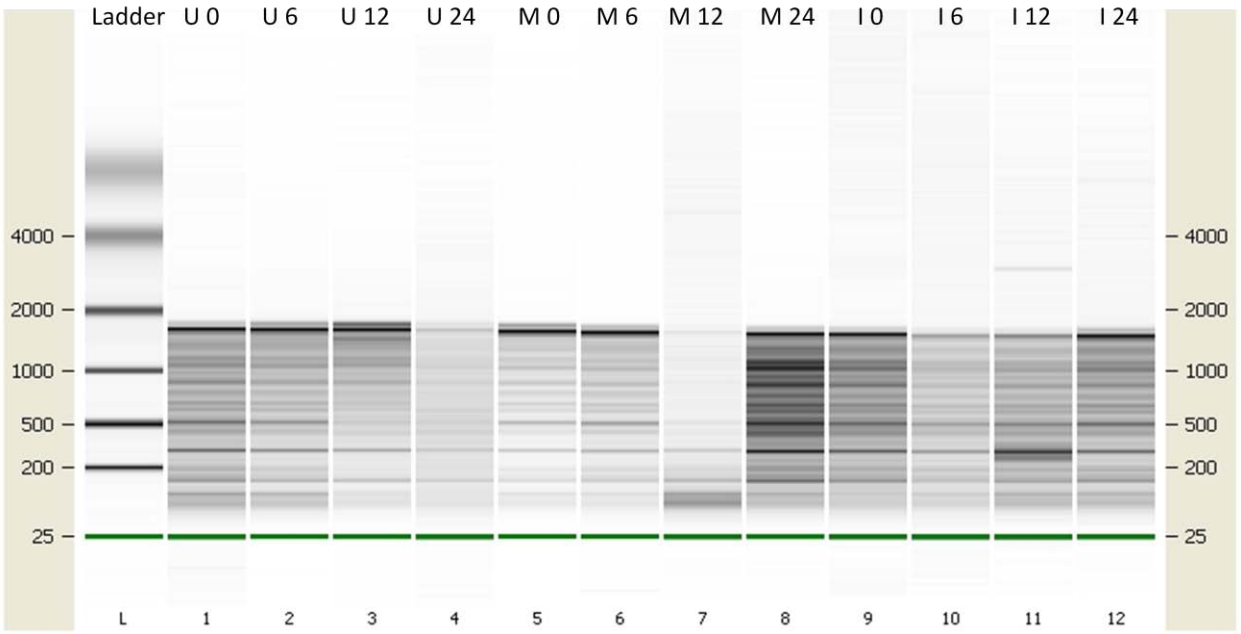

A

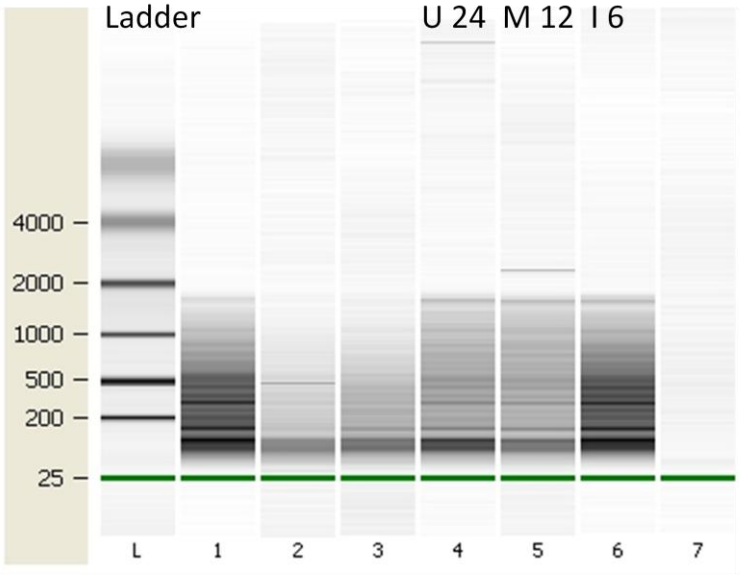

B

Figure D 3: Bioanalyser RNA integrity gel for biological repeat 2. (A) RNA samples isolated from all treatment and time points and (B) the repeat isolation of the samples from (A) that were not of good quality. Abbreviations: U: Unchallenged, M: Mock Infected and I: Infected.

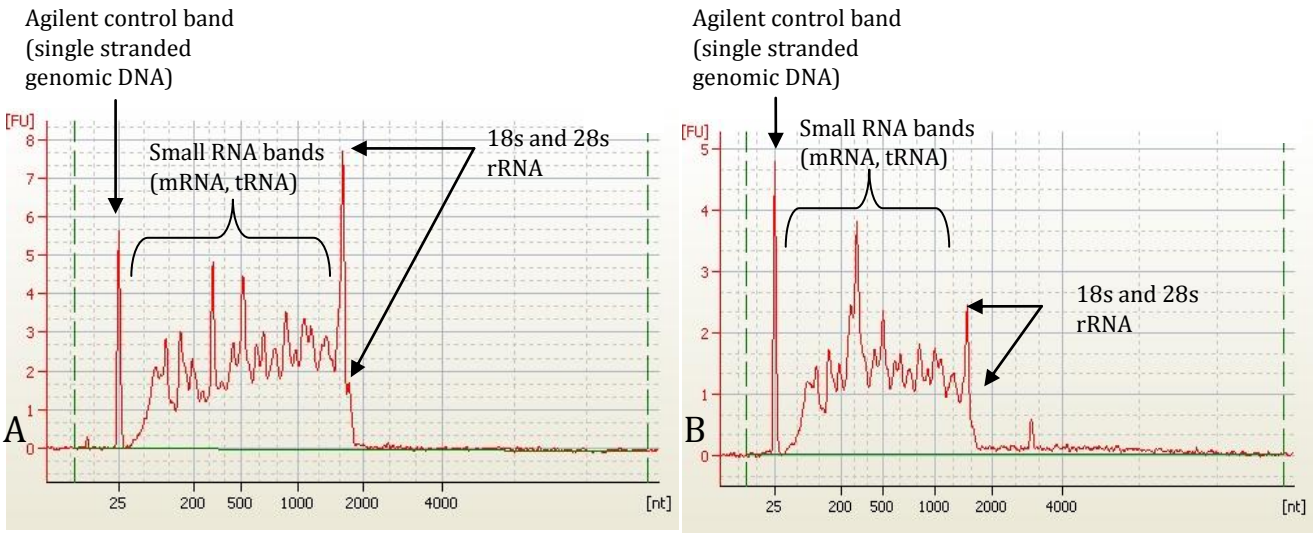

Figure D 4: Electropheregrams of the RNA samples acquired using the bioanalyser. Genomic contamination would appear as broad peaks on the far left hand side of the picture (high molecular weight). (A) Represents a good quality RNA sample (Fig D 3 A, U 0) and (B) represents an acceptable RNA sample used for conversion, as although the 18s/28s doublet is low, the other RNA bands are at the similar fluorescence units (FU) than that of the good sample (Fig D 3 A, I 12).

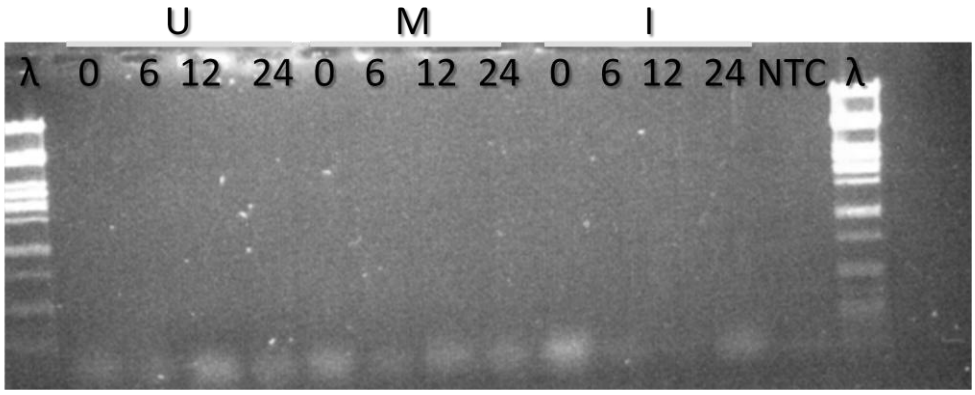

Figure D 5: Ribosomal factor L28 PCR amplification of RNA from biological repeat 1. 1.2% agarose gel indicates no amplification of the product. Some lanes show primer dimers also seen in the no template control (NTC). Abbreviations: U: Unchallenged, M: Mock Infected and I: Infected and λ: Lambda *Pst* I marker. 0, 6, 12 and 24 denote the time points for the challenge trial.

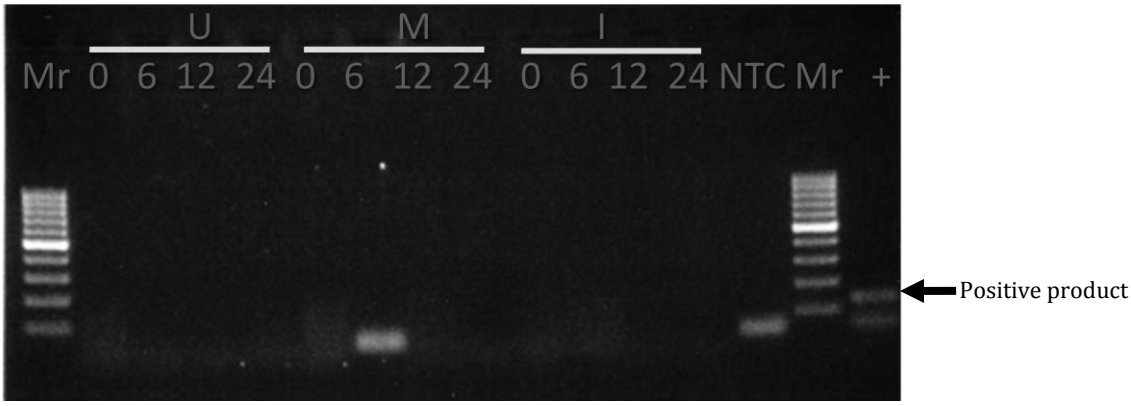

Figure D 6: Ribosomal factor L28 PCR amplification of RNA from biological repeat 3. 1.2% agarose gel indicate no amplification of the product. Some lanes show primer dimers also seen in the no template control (NTC). The positive control (plasmid containing ribosomal factor L28 insert) indicates a 150 bp product not seen in any other sample lanes. Abbreviations: U: Unchallenged, M: Mock Infected and I: Infected and Mr: Fermentas 100 bp Range O' Ruler™ marker. 0, 6, 12 and 24 denote the time points for the challenge trial.

Figure D 7: 18s rRNA Amplification of RNA for biological repeat 1 of the *in vitro* challenge trial. Abbreviations: λ: Lambda *Pst*I digest marker and NTC: no template control. 0, 1, 2, 3 and 6 denote the time points for the challenge trial.

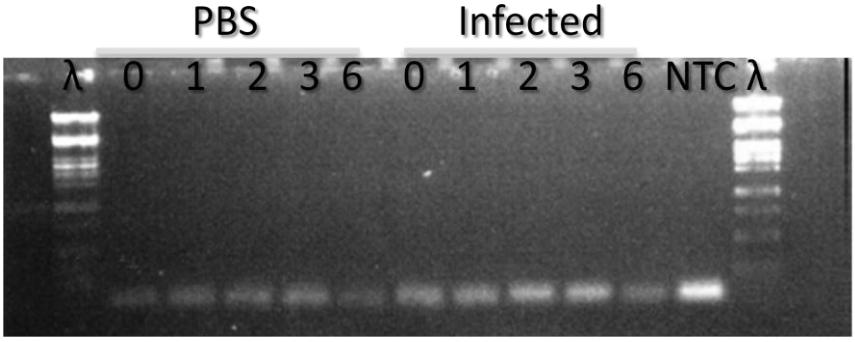

Figure D 8: 18s rRNA amplification of RNA from biological repeat 2 of the *in vitro* challenge trial. There are primer dimers in each sample lane and in the no template control (NTC). Abbreviations: λ: Lambda *Pst*I digest marker and NTC: no template control. 0, 1, 2, 3 and 6 denote the time points for the challenge trial.

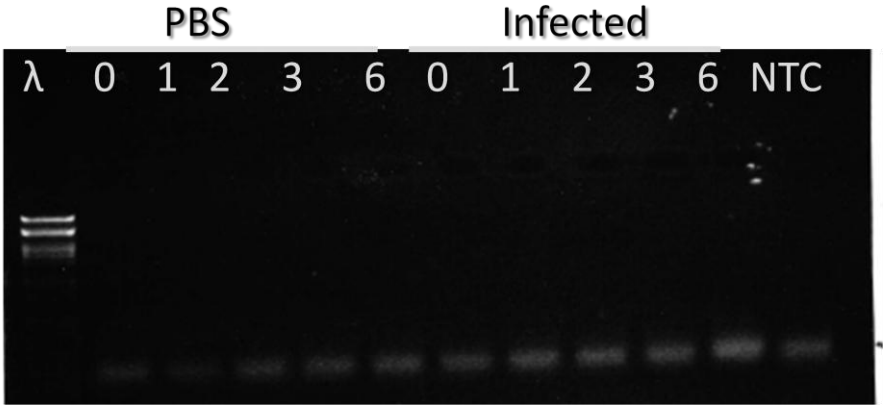

Figure D 9: 18s rRNA amplification of RNA from biological repeat 3 of the *in vitro* challenge trial. There are primer dimers in each sample lane and in the no template control (NTC). Abbreviations: λ: Lambda *Pst*I digest marker and NTC: no template control. 0, 1, 2, 3 and 6 denote the time points for the challenge trial.

qPCR data was assessed using the melt curve and the standard curve obtained in the analysis program (Rotor-Gene™ Series Software version 1.7, Corbett Research). The melt curve identifies that a single product has been successfully amplified from the samples, while the standard curve determines the efficiency of the reaction by plotting the cycle threshold values (Ct) against the concentration of the standard curve samples. Samples that were outliers (standard curve) or not the product of interest (melt curve) were discarded from the analysis.

D.2.1 QPCR PROFILES FOR *IN VIVO* TRIALS

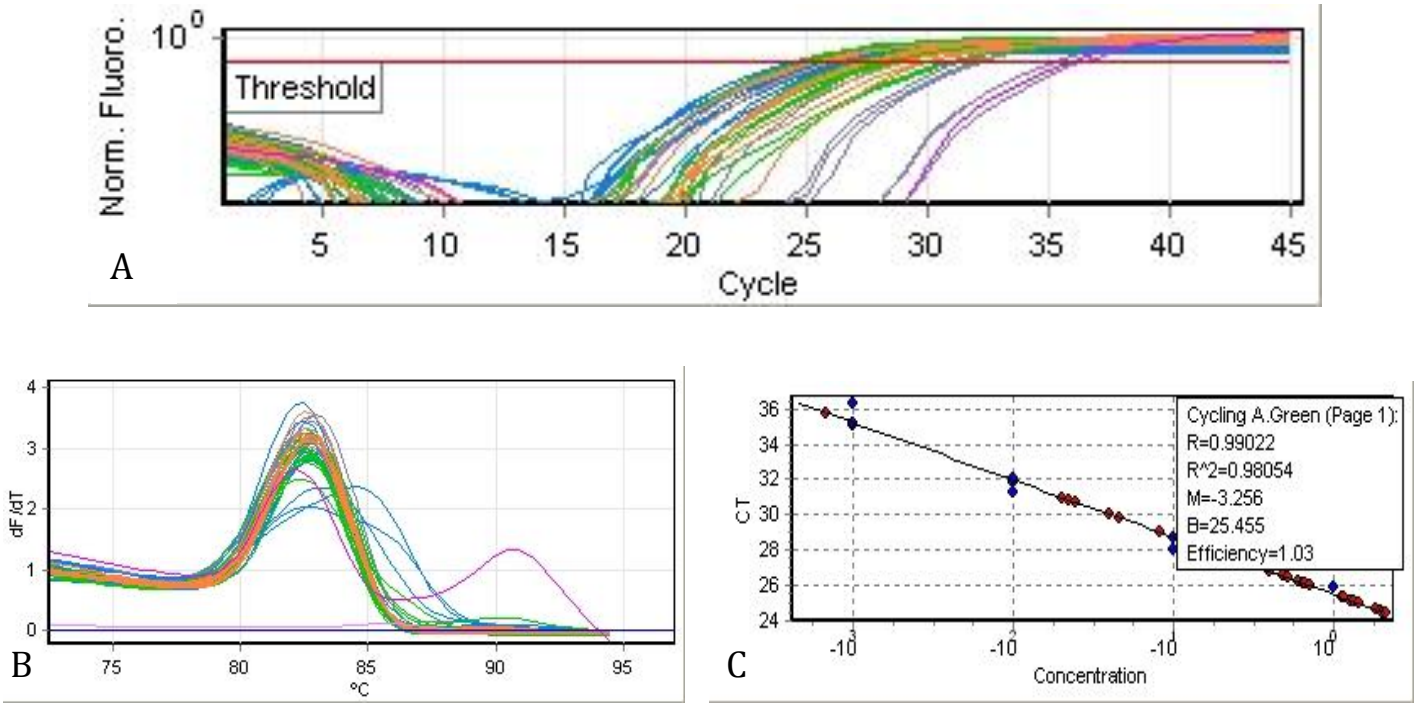

Figure D 10: qPCR profile of the reference gene ribosomal factor L28 for biological repeat 1. (A) the run profile for the gene, (B) the melt curve, note the dark pink curve is the primer dimers in the no template control. (C) The standard curve for the gene and the no template control is the only point (red) on the far left of the curve.

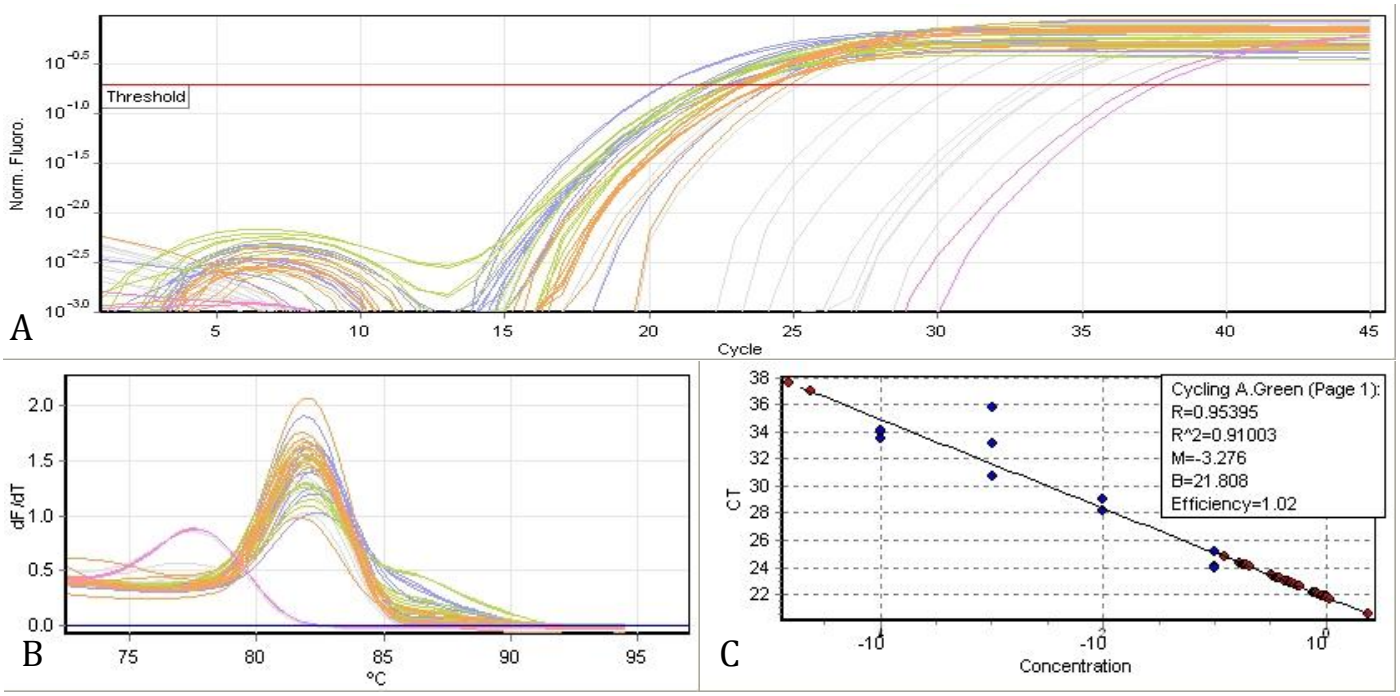

Figure D 11: qPCR profile of the reference gene ribosomal factor L28 for biological repeat 2. (A) The run profile for the gene, (B) the melt curve (pink curves on the left are the no template controls and (C) the standard curve for the gene and the no template control is on the far left of the curve.

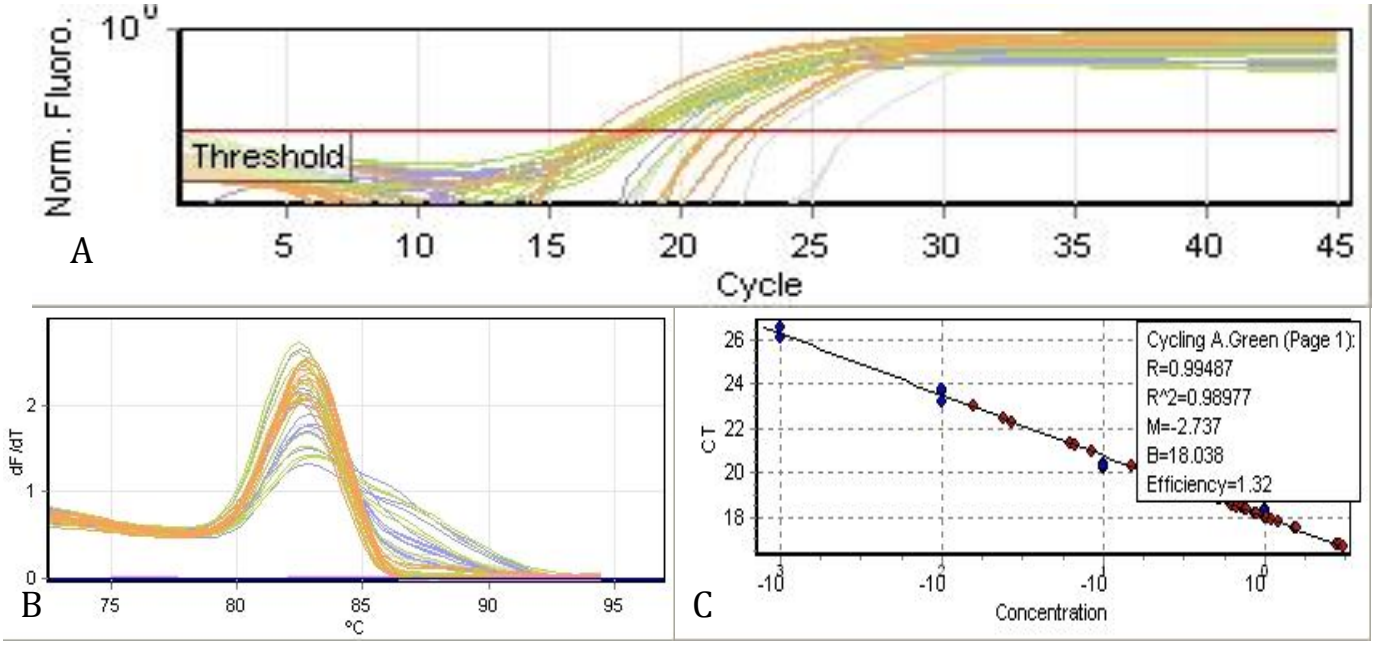

Figure D 12: qPCR profile of the reference gene ribosomal factor L28 for biological repeat 3. (A) The run profile for the gene, (B) the melt curve and (C) the standard curve for the gene

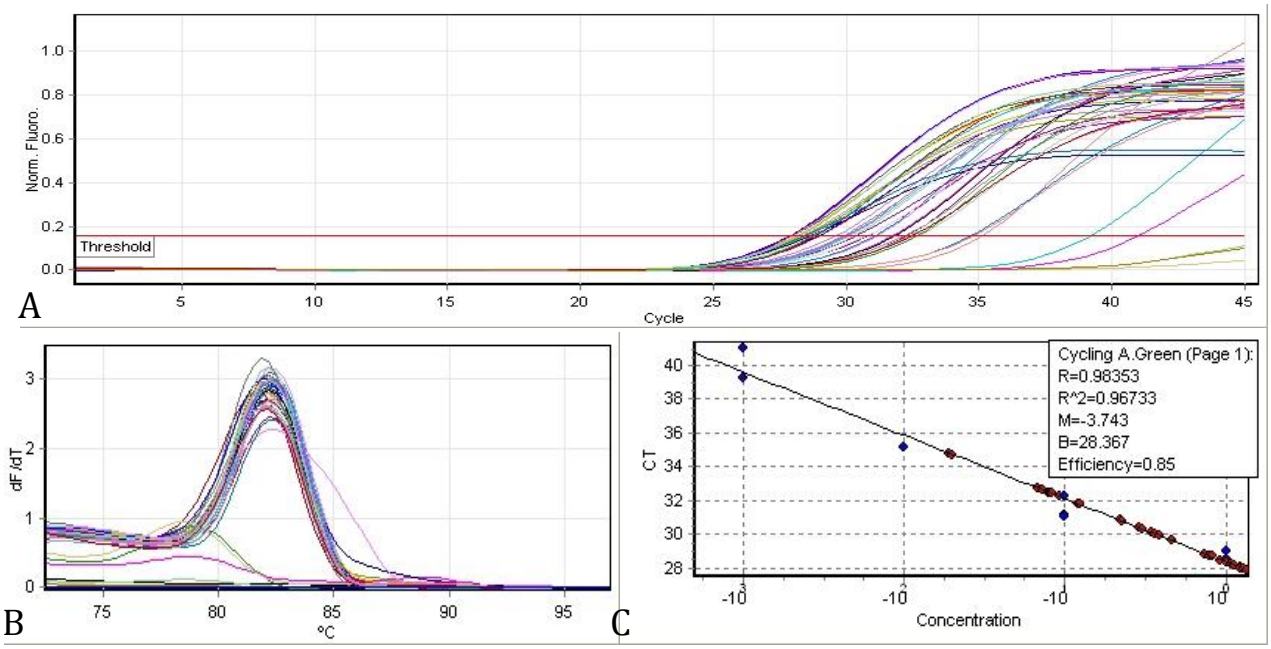

Figure D 13: qPCR profile of the gene of interest (NFκB) for biological repeat 1. (A) The run profile for the gene, (B) the melt curve (pink curve and green curve indicates the no template controls) and (C) the standard curve for the gene

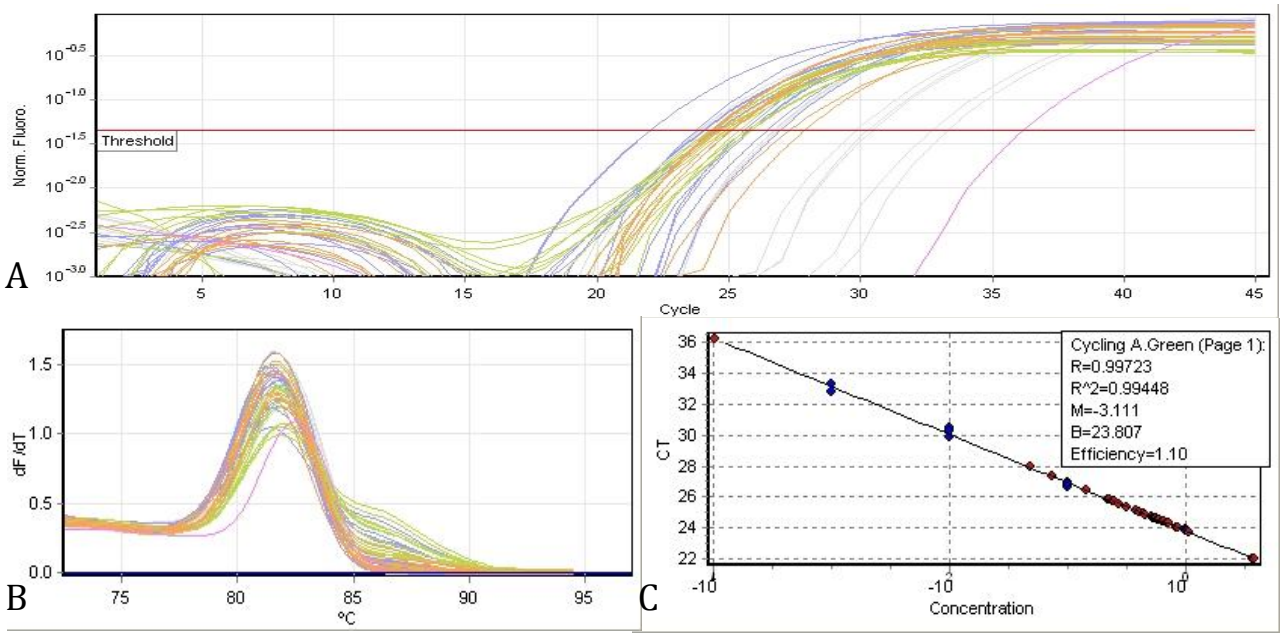

Figure D 14: qPCR profile of NFκB for biological repeat 2. (A) The run profile for the gene, (B) the melt curve and (C) the standard curve for the gene with the no template control on the far left hand side.

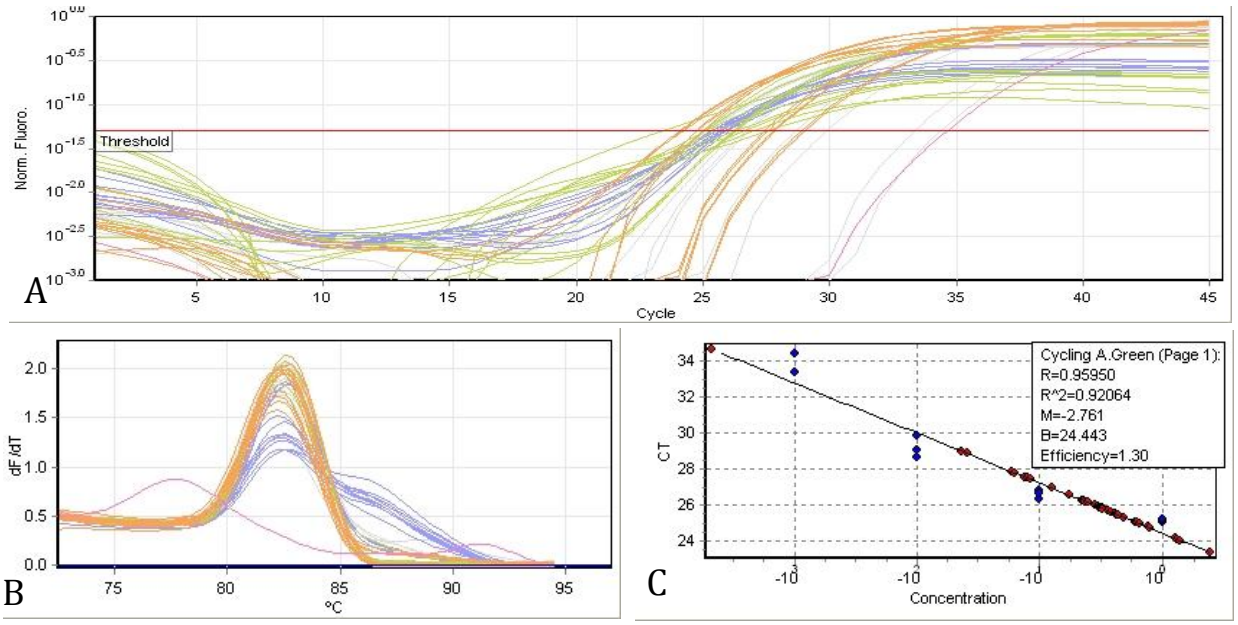

Figure D 15: qPCR profile of NFκB for biological repeat 3. (A) The run profile for the gene, (B) the melt curve (pink curves indicates the no template controls) and (C) the standard curve for the gene with the no template control on the far left hand side

D 2.2 QPCR PROFILES FOR THE *IN VITRO* CHALLENGE TRIAL

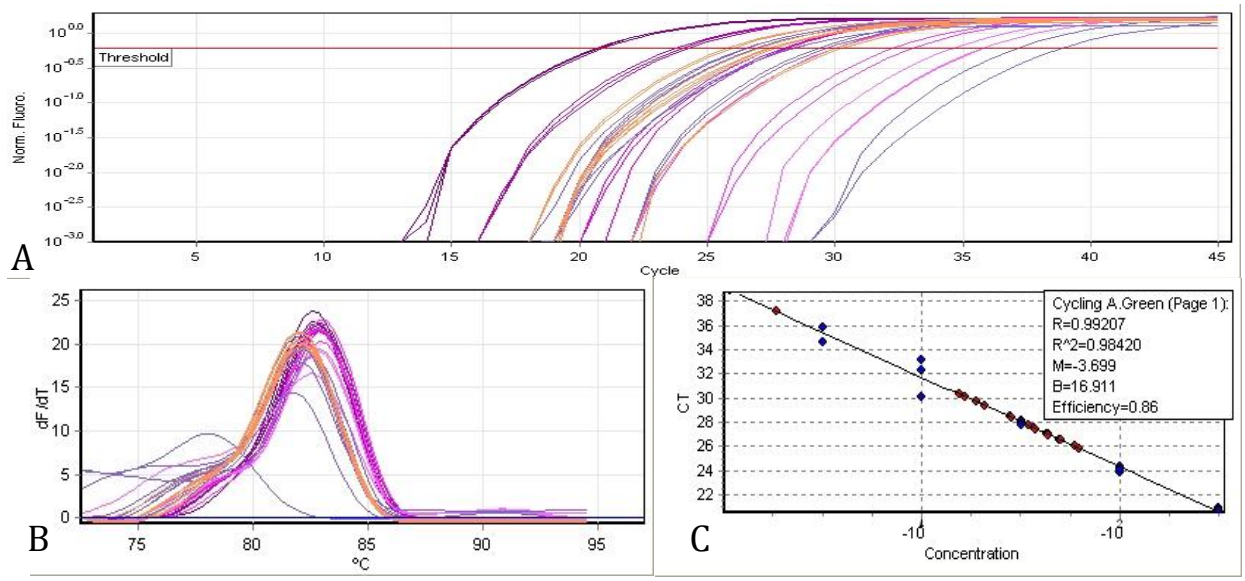

Figure D 16: qPCR profile of the reference gene ribosomal factor L28 for biological repeat 1. (A) The run profile for the gene, (B) the melt curve and (C) the standard curve for the gene with the no template control on the far left hand side. The standard curve is comprised of diluted plasmid containing the L28 insert.

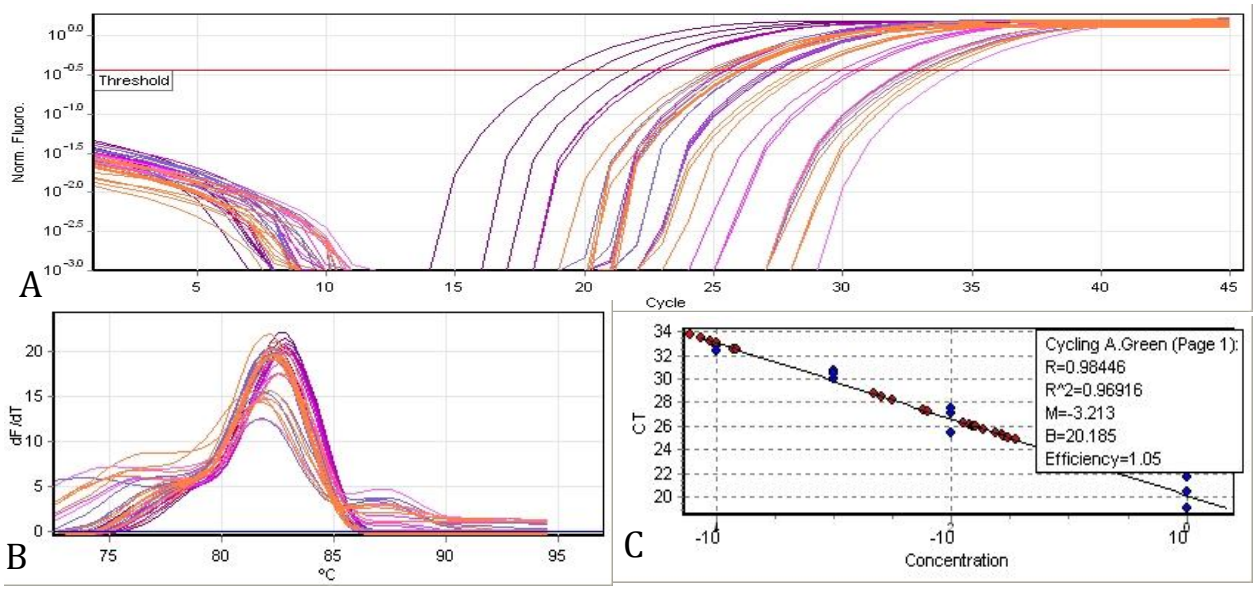

Figure D 17: qPCR profile of the reference gene ribosomal factor L28 for biological repeat 2. (A) The run profile for the gene, (B) the melt curve and (C) the standard curve for the gene.

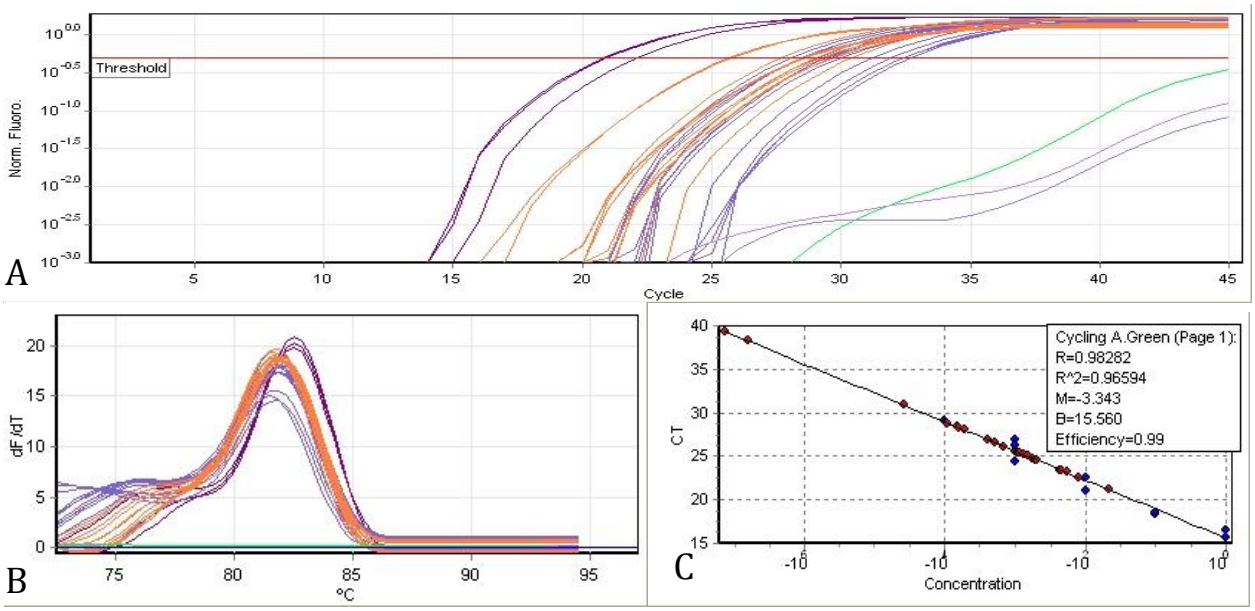

Figure D 18: qPCR profile of the reference gene ribosomal factor L28 for biological repeat 3. (A) The run profile for the gene, (B) the melt curve and (C) the standard curve for the gene.

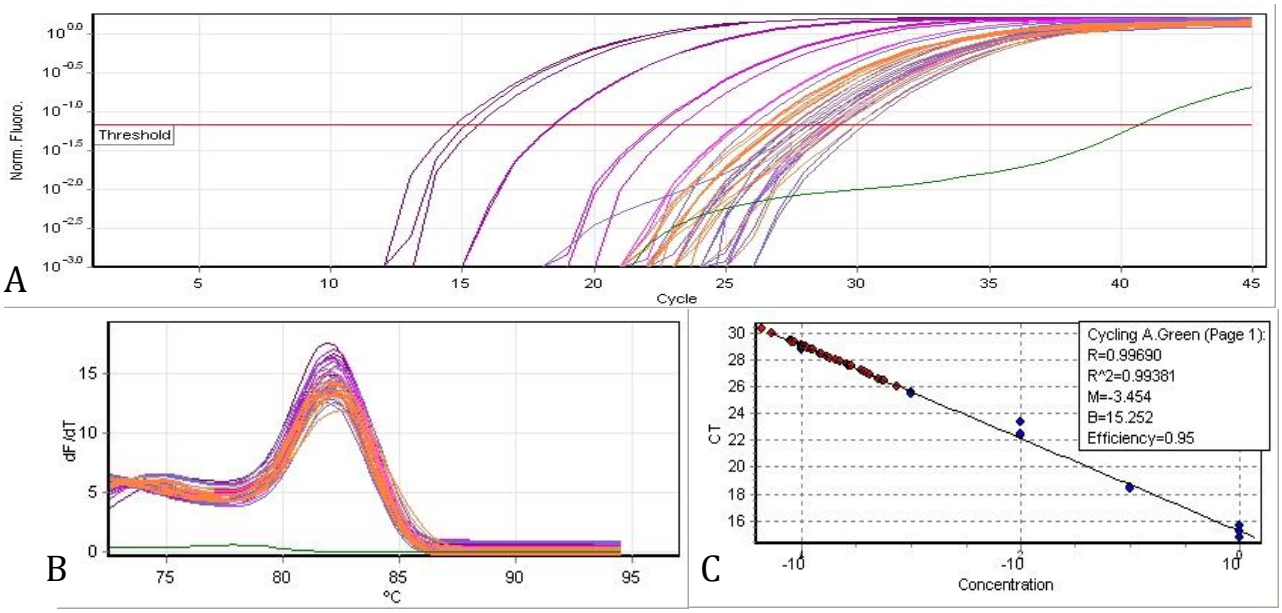

Figure D 19: qPCR profile of the gene of interest NFκB for biological repeat 1. (A) The run profile for the gene (green line indicates no template control), (B) the melt curve and (C) the standard curve for the gene.

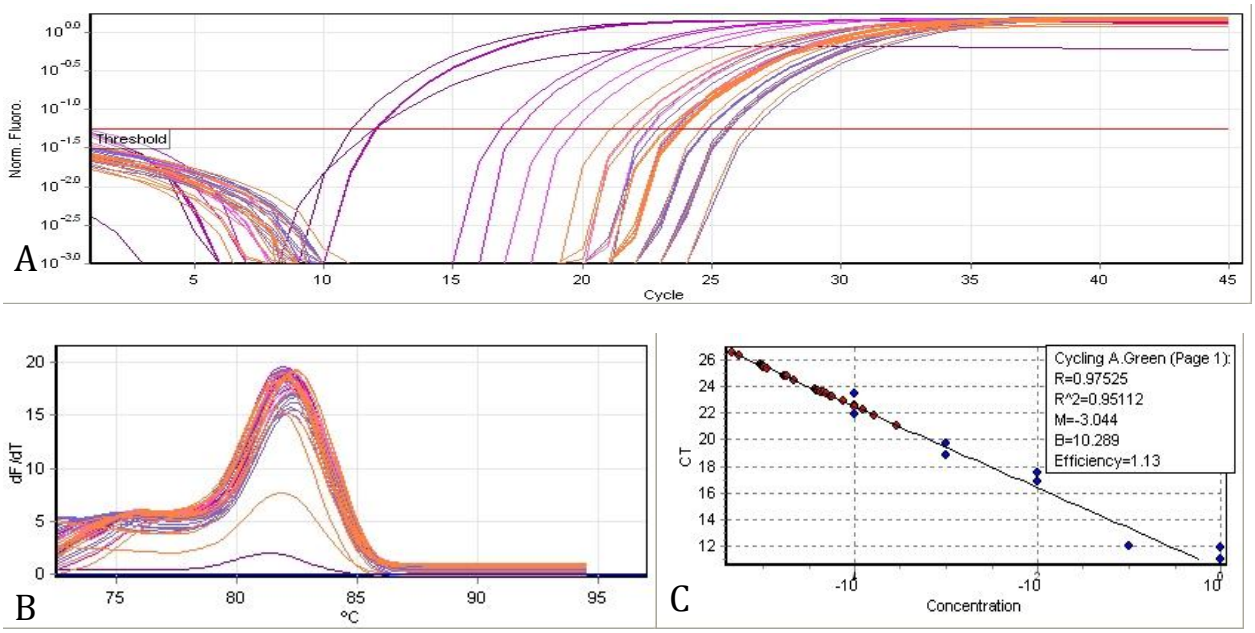

Figure D 20: qPCR profile of the gene of interest NFκB for biological repeat 2. (A) The run profile for the gene (B) the melt curve and (C) the standard curve for the gene.

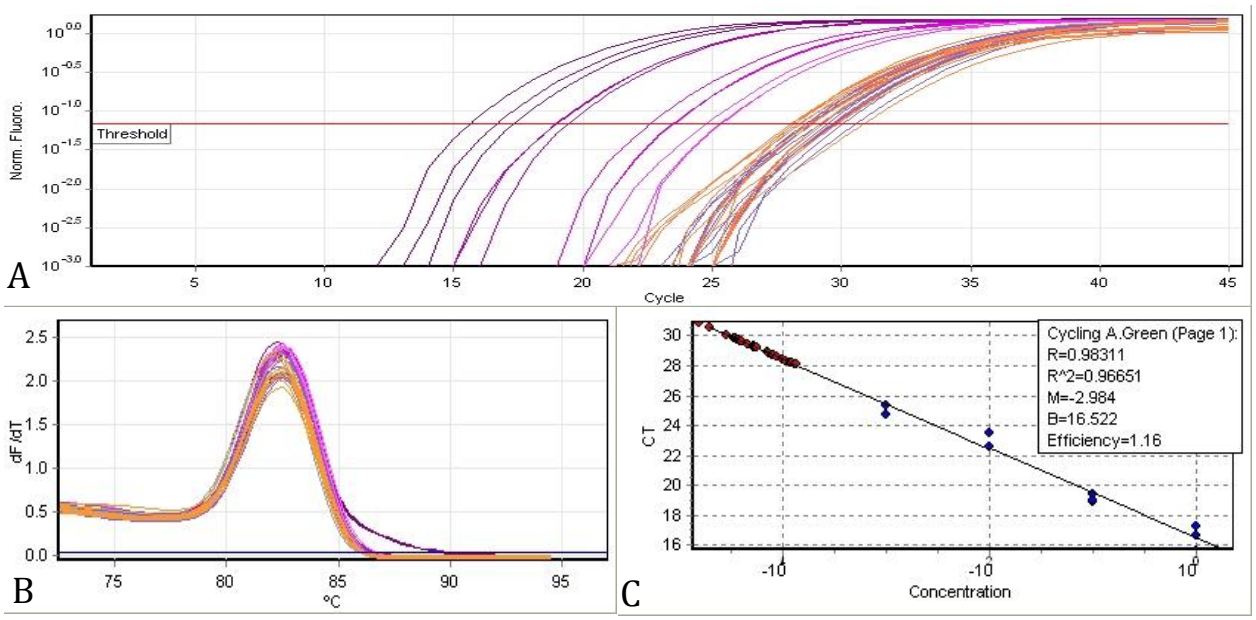

Figure D 21: qPCR profile of the gene of interest NFκB for biological repeat 3. (A) The run profile for the gene (B) the melt curve and (C) the standard curve for the gene.